Atlas-based Automated Surgical Planning for Total Hip Arthroplasty

Otomaru, Itaru

(Degree)
博士（工学）

(Date of Degree)
2012-03-25

(Date of Publication)
2012-04-19

(Resource Type)
doctoral thesis

(Report Number)
甲5486

(URL)
https://hdl.handle.net/20.500.14094/D1005486

Doctoral Dissertation

Atlas-based Automated Surgical Planning for Total Hip Arthroplasty

January, 2012

Graduate School of Engineering, Kobe University

Itaru Otomaru

Contents

List of Figures

List of Tables

Chapter 1

Introduction

In computer assisted surgery, the surgical CAD/CAM paradigm is a common framework [1]. In this paradigm, the CAM systems, that involve intraoperative robotic and computer-guided assistance, ensure accurate execution of preoperative plans constructed using the CAD systems. The firstly developed CAM system in computer assisted orthopaedic surgery (CAOS) is "ROBODOC" proposed by Taylor et al. in 1994 [2]. ROBODOC is a robotic system developed for total hip arthroplasty (THA). THA is an implant surgery, which particularly fits the surgical CAD/CAM paradigm [3]. Given a surgical plan, ROBODOC automatically drills a patient femoral bone so as to position an artificial implant. Since the development of ROBODOC, various CAM systems have been proposed for the past two decades [4, 5, 6, 7, 8, 9]. According to several clinical studies, these CAM systems can achieve higher accuracy in surgery than conventional surgery done by manually operated by surgeons [10, 11]. Therefore, the importance of preoperative planning have been growing.

This study addresses the problem of preoperative planning in THA. Several interactive preoperative planning system have been developed [6, 12, 13, 14]. These systems typically visualize multiplanar images and 3D shape of hip reconstructed from 3D-CT images and provide 3D spatial relations between implants and host bones while quantitative information such as fit-and-fill [15, 16] can be monitored in realtime so as to provide the surgeon with objective information. More recently, biomechanical analysis has been incorporated to evaluate the risk of fracture and implant loosening [17, 18, 19]. Although these quantitative evaluations are useful for improving objectivity and validity of the planning result, user interactions involving trial and error will be still necessary to prepare tentative size selection and positioning as input data for the analysis, which may be time-consuming as well as reduce objectivity [20].

One possibility to solve the problem is to automate the planning process. As previous studies, several automated planning methods have been proposed [21, 22]. The former method [21] targets the planning of the pelvic component (cup) of THA and uses several user-defined constraints based on interviews with experienced surgeons. However, this method can only describe an explicit knowledge which the surgeons can verbalize and cannot describe implicit knowledge. The latter method [22] targets the planning of the femoral component (stem) of THA and uses a reference CT dataset and a preoperative plan on it. However this method uses only a single dataset of preoperative plans as a reference based on the assumption which planning criteria do not change among all cases.

Nowadays, navigated THA is routinely used in some hospitals. Especially in Japan, CT-based

3D preoperative planning is often performed for THA. A large number of the preoperative plans constructed by well-experienced surgeons are accumulated in some of the hospitals. The feedback of these past planning datasets can potentially improve the future planning. Closed-loop surgery to make the best use of past surgical data for future surgery is a recently-emerged paradigm [23]. A typical presentation scheme to realize this paradigm is statistical atlas, which has been intensively applied to solve various problems of medical image analysis [24, 25, 26, 27, 28, 29, 30]. The probabilistic atlas which describes a distribution of a target organs [27] and the statistical shape models (SSMs) which describes statistical shape variation of target shapes [24] are representative examples of statistical atlas. Statistical atlas has been utilized for preoperative planning in several studies. Optimization of prostate biopsy planning is a successful application on surgical planning, in which probabilistic atlas of cancer distributions is utilized [31, 32]. More recently, automated implant fitting was performed for optimizing implant design [33]. In these methods, however, utilized statistical information was on patient anatomy and pathology rather than surgeon's expertise of planning. These have been a few existing studies utilizing the expertise in past preoperative planning datasets. The femoral implant planning in THA was performed using one of the past planning datasets [22] (described in the previous paragraph). As different application, assistance in radiation therapy planning based on retrieval of similar cases from the past planning database is reported [34]. However, statistical representation of the expertise was not utilized in both studies.

The objective of this study is to develop an atlas-based automated 3D planning method for THA. The novel points of this study are as follows:

1. Unlike the single reference dataset-based methods [22, 34], automated planning criteria is based on statistical analysis of a number of past planning datasets constructed by an experienced surgeon.

2. Unlike the previous method which targets the automated planning of cup [21] which uses several user-defined constraints, a simple formulation based on statistical atlas is observed.

Since the artificial joint used in THA consists of femoral implant (stem) and pelvic implant (cup), the automated planning method for stem and cup are developed independently.

This paper consists of seven chapters. The brief overview of each chapter is as follows:

1. **Chapter 1 Introduction**：This chapter.

2. **Chapter 2 Automated planning of femoral implant (stem) based on manually-derived criteria**：In advance of an atlas-based approach, an automated stem planning based on user-defined objective function is described in this chapter.

3. **Chapter 3 Atlas-based approach and validation of automated planning of femoral implant (stem)**: An atlas-based automated stem planning is described in this chapter. The performance between the proposed method and the previous methods described in [22] and Section 2 is compared.

4. **Chapter 4 Atlas-based approach and validation for automated pelvic implant (cup) planning** ：An atlas-based automated cup planning is described in this chapter.

5. **Chapter 5 Applying atlas-based automated cup planning to standard 2D X-ray image** ： The atlas-based cup planning method described in chapter 4 only allows 3D-CT images as input. In this chapter, a preliminary experiment which uses standard 2D X-ray images as input by utilizing a 2D-3D pelvis shape reconstruction method is reported.

6. **Chapter 6 Atlas-based optimization of hip joint function**: This chapter shows a preliminary work for optimizing various hip joint function such as leg length discrepancy and range of motion.

7. **Chapter 7 Conclusion**：This chapter summarizes the achievement, remaining problems, and future directions of this study.

Chapter 2

Automated planning of femoral implant (stem) based on manually-derived criteria

Abstract

This paper describes a 3-dimensional (3D) automated preoperative planning method of femoral component (stem) for total hip arthroplasty (THA). The stem planning is formulated as a optimization problem which determines implant parameters such as size, position, and rotation. An objective function is defined using the fitness between the femoral canal and the stem surface. In addition to the objective function, constraints of position and orientation derived from conventional studies of femoral anatomy is also defined. Since the objective function consists of several parameters, a parameter tuning was performed in advance of the performance evaluation. Optimization of the objective function was performed using the Powell method. The proposed method was applied to 17 cases and the errors of the planning results between the automated planning results and the experienced surgeon's plans were compared. Stem size error was within one size in all cases. Mean positional error and mean orientation error were 3.4 mm and 5.0 deg., respectively. According to a qualitative evaluation performed by an experienced surgeon, 14 cases out of 17 cases were accepted and three cases were rejected. The surgeon commented that the rejected three cases can be accepted after some minor modification. Therefore, the author consider the proposed method would be useful as an automated stem planning method.

2.1 Introduction

Recently, surgical navigation and robotic systems have been developed for total hip arthroplasty (THA) to allow accurate placement of orthopedic implants in preoperatively determined 3-dimensional (3D) position and orientation [8, 6, 5, 35, 36, 10, 37]. Preoperative planning is thus becoming increasingly important because the preoperative plan can be accurately devised using these systems. In preoperative planning of THA, anatomical compatibility of each implant component with the host bone is essential for stable fixation and good clinical results. Recently, computed tomography (CT)-based interactive systems for preoperative 3D planning have been developed to quantitatively visualize the stable fixation. [13, 16]. However, interactive 3D planning is subjective and time-consuming, limiting clinical use.

To solve these problems, the research group including the author has been developing an automated preoperative planning system for THA, to automatically select the optimal size, position, and orientation of each implant. This system calculates the plan of the pelvic implant (cup) and femoral implant (stem) independently [38, 39, 40], then integrates these intermediate solutions considering the difference in limb length and range of motion (ROM) of the hip joint [41]. To develop the automated planning procedure, the author has formulated criteria derived from the plan of an experienced surgeon. The proposed system is hoped to increase the usefulness of surgical navigation systems or surgical robotics systems, as the proposed method realizes the automated preoperative planning based on objective criteria without increasing the workload of the surgeon. The present study considered the automated planning procedure of the stem. In particular, the author used the cementless stem, which is fixed to the host bone by press fitting and postoperative regeneration of the bone texture. The “fit and fill” of the stem in the femoral canal are thus important factors for component stability [42, 43, 35, 44, 36, 45, 15, 46].

In a previous study of my research group, an objective function that describes the “fitness” value of the stem based on the expertise of the surgeon and their planning results is defined. the solution is determined using a one-by-one search at the interval to some extent in each axis [38, 40]. However, this search procedure is inappropriate because this method cannot guarantee optimal stem fitness. In addition, the constraints of position and orientation were not derived from the previous study, which represented appropriate positional relationships of the stem and femur. In contrast, Viceconti et al.

proposed the use of volume registration between the femoral canal and stem for automated placement of the stem [22]. However, the image -matching criteria used in volume registration were not derived from the stem fitness criteria used by an experienced surgeon. Position results for this method may thus be incompatible with the femoral canal of the host bone.

The present study proposes an automated planning procedure of stem placement that satisfies appropriate positional relationships of the stem and femur and guarantees optimality of stem fitness. The definition of "fitness" was as described in previous studies. In addition to this definition, the author proposes new constraints to describe the expertise of the surgeon regarding positional relationships of the stem and femur, and the optimization procedure to maximize fitness. To evaluate performance of the proposed system, applying the proposed method to 17 cases and measuring errors of position, orientation, and size selection between automated planning results and those of an experienced surgeon. In addition, the author adjusted the parameters of the evaluate function from an exhaustive experiment using various parameters and discuss the relationship between parameters and the automated planning results.

2.2 Methods

2.2.1 Overview

A block diagram of the proposed system is shown in Fig. 2.1. As patient information, the author assumes that a 3D-CT image of the hip joint is used for the patient. A 3D model of the femoral canal is reconstructed from CT images, and the femoral coordinate system and anatomical feature points are determined on 3D models. As implant information, the author assumes that 3D shape models of all variations in the femoral stems are given. The output of this system is the set of parameters ($\mathbf{z} = [\mathbf{t}, \mathbf{r}, s]$), for the position $\mathbf{t}$, orientation $\mathbf{r}$, and size s of the stem. In the formulation, the author treats the parameters of size s, position $\mathbf{t}$, and orientation $\mathbf{r}$ independently. First, the author obtains candidates for position $\mathbf{t}$ and orientation $\mathbf{r}$ in each stem size, then the author selects the stem size s.

The position and orientation of the stem are represented in the CT coordinate system. Its origin is defined as the front-left-upper corner, and the *x*, *y* and *z*-axes as the left-right, front-back, and upper-lower directions, respectively.

The femoral coordinate system is shown in Fig. 2.2. In the specification of femoral coordinate

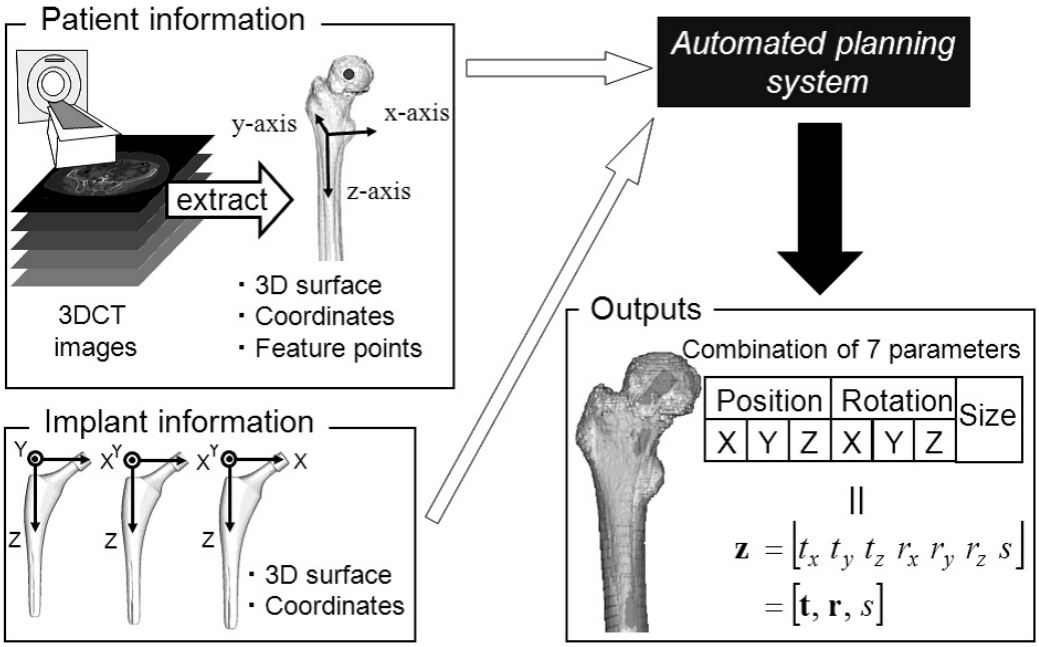

Figure 2.1: Block diagram of the proposed system.

system, the author uses the table-top plane of the femur and the peak of the lesser trochanter. The *z*-axis of the femoral coordinate system is defined as the canal long axis estimated from the 3D model of the femoral canal. The canal long axis is defined as the line connecting two points, which are the gravity center points of two different axial cross-sectional canal shapes. The distance of the two axial plane is 130 mm along the *z*-axis of the CT coordinate system, and the *z*-coordinate of the upper plane is added by 30 mm to that of the lesser trochanter peak. The *x*-axis is orthogonal to the *z*-axis and parallel to the table-top plane. The *y*-axis is defined as the axis orthogonal to both *x* and *z*-axes. The origin is defined as the point of intersection of the *z*-axis and a line perpendicular to the *z*-axis that passes through the peak of the lesser trochanter (Fig. 2.2, sagittal view).

2.2.2 Definition of objective function of stem fitness

The author formulates preoperative planning of the stem as an optimization problem to obtain parameters **z** maximizing the stem fitness evaluate function. The criteria in stem planning are defined as follows:

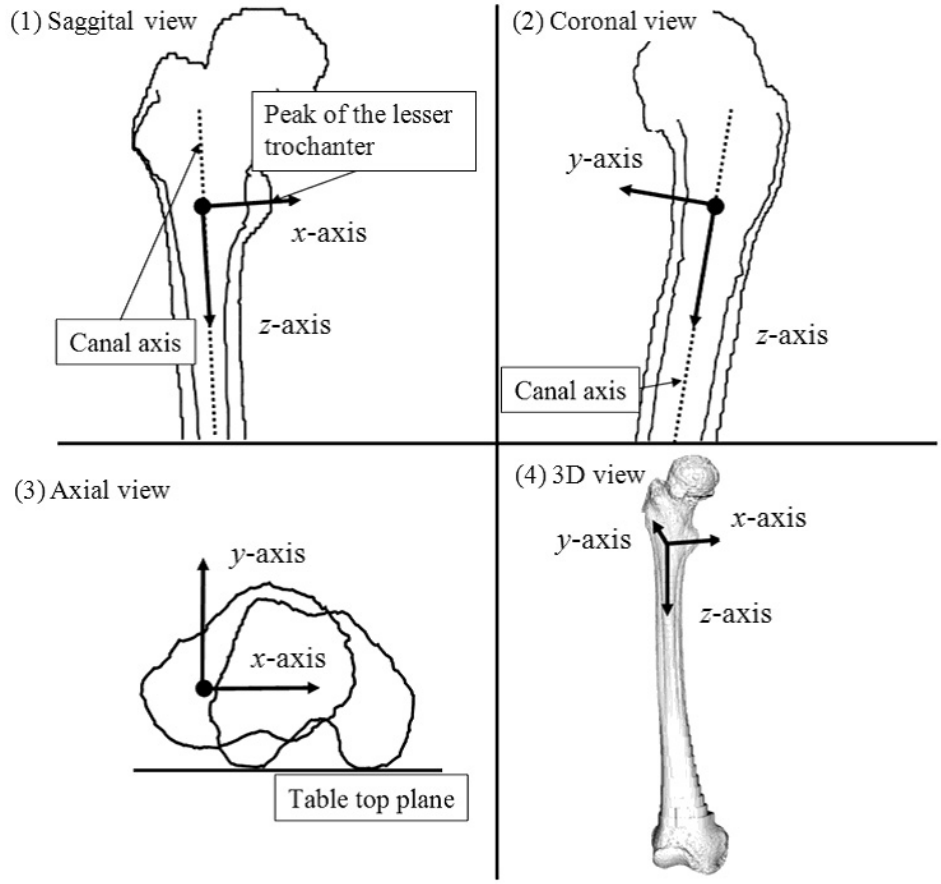

Figure 2.2: Definition of the femoral coordinate system ((1) Sagittal view, (2) Coronal view, (3) Axial view, (4) 3D view)).

1. Overlap of the femoral canal and stem surface is prohibited for the entire stem area.
2. Strong contact with the host bone in the specific area of the stem is desirable.
3. Maintain positional and rotational relationships with the femur.
4. Select the largest stem size unless the stem is not overlapped with of the canal.

In the proposed method, the author uses distance from the femoral canal and stem surface to describe these criteria. A distance obtained as a negative value indicates overlap of the femoral canal and stem surface. Conversely, a distance obtained as a positive value indicates a gap between the canal and stem surface. In particular, when the gap is small, the author considers strong fixation to exist. In addition to the consideration of the distance between femoral canal and the stem surface, the author

defines the positional and rotational constraints derived from anatomical compatibility between the host bone and stem.

In the formulation, the position **t** and rotation **r** of the stem are described as the 4 $\times$ 4 rigid transformation matrix **T**. In addition, **t** and **r** are collectively described as a six-parameter vector $\mathbf{q} = [t_x, t_y, t_z, r_x, r_y, r_z]$. The author determines the parameters **T** in stem size s, maximizing the objective function of stem fitness $F(\mathbf{T})$, and then selects the maximum stem size. The derivation of the optimal **T** is defined as the following optimization problem:

$$\begin{aligned} \text{maximize} \quad &: \quad F(\mathbf{T}) = \iint_S f(\pm|C - \mathbf{Tx}|)d\mathbf{S}, \qquad (\mathbf{x} = [x, y, z]) \\ \text{subject to} \quad &: \quad \pm|C - \mathbf{Tx}| \geq 0, \forall \mathbf{x} \\ &\quad\;\; \mathbf{q}_0 - \mathbf{q}_r \leq \mathbf{q} \leq \mathbf{q}_0 + \mathbf{q}_r \end{aligned} \tag{2.1}$$

where S describes the stem surface, and C describes the femoral canal. **x** are the coordinates of the stem surface point, and **Tx** are the coordinates of **x** when position and orientation of the stem are **T**. $|C - \mathbf{Tx}|$ represents the distance between **Tx** and the closest point on C from **Tx**. The sign of the distance represents whether **Tx** is inside or outside of C. When **Tx** is positioned inside (the side of the femoral internal region) of C, this sign is positive. Conversely, when **Tx** is positioned outside (the side of the femoral host bone) of C, the sign is negative. The first expression of the constraints describes the constraints prohibiting overlap of the entire stem area. $\mathbf{q}_0$ is the central position and rotation of the range of limitation, and the range of limitation is described as $\mathbf{q}$.

To define the function f, the author divides the stem surface into three regions. The proximal region of the surface is called zone one, and the distal region is called zone two (Fig. 2.3). Zone one is a specific area in which strong contact with the host bone is required. Neither zone one nor zone two can overlap with the femoral canal. However, other parts of the stem surface are not evaluated. In terms of the objective function, fitness value is maximized when the gap is smaller than the constant value, and if the gap is larger than the constant, fitness value decreases with distance. The objective function is defined as (Fig. 2.4)

$$f(d) = \begin{cases} 1 & (0 \leq d < c_{th}) \\ -\exp\{-\frac{(d-c_{th})^2}{2\sigma^2}\} & (c_{th} \leq d) \end{cases}, \quad (d = \pm|C - \mathbf{Tx}|) \tag{2.2}$$

where c_{th} and σ are the parameters to be adjusted. c_{th} is the threshold of the distance for which the fitness value is maximized, and σ is the parameter of the Gaussian function that describes the decrease

of the fitness if the distance is larger than c_{th}.

2.2.3 Definition of constraints

The positional and rotational constraints used in the stem planning are determined from the height of the stem position and the anteversion angle. The difference of the height between the femoral head center in the preoperative stage and the tip of the stem neck in the postoperative stage should be minimized. The anteversion angle is the angle of the femoral neck with respect to the body of the femur (left side of Fig. 2.6). This angle affects the range of motion (ROM) of the hip joint After surgery, the femoral neck is removed and replaced by the stem neck. Anteversion angle after surgery is thus redefined using the stem neck (right side of the Fig. 2.6). This change also should be minimized.

To define constraint parameters $\mathbf{q}_0$ and $\mathbf{q}_r$ of the Eq. (2.1), the author refers to conventional study of the prediction of height of the femoral head center and anteversion angle. In the prediction of the femoral head center, applying sphere fitting to the deformed femoral head, as in the present study, is not appropriate. The author therefore used height of the femoral neck saddle instead and limited the range to 8.3 mm of height difference from the femoral neck saddle based on a conventional study (Fig. 2.5) [47]. The height constraint is defined based on the femoral coordinate system. Anteversion angle is defined as the angle of the femoral neck axis with respect tothe table-top plane (Fig. 2.6) [48]. Femoral neck axis is defined as the line connecting the femoral head center with the origin of the femoral coordinate system, which is projected onto the *xz*-plane of the femoral coordinate system. The author fixes this angle during the automated planning because the author has already confirmed experimentally that the stem fitness value has no obvious peak along this parameter.

In the proposed method, the initial position $\mathbf{q}_0$ is defined such that the height agrees with that of the stem neck and the anteversion angle agrees with that before surgery. In the definition of coordinate axes, height corresponds to the translation along the *z*-axis, and anteversion angle corresponds to rotation around the *z*-axis. Using the criteria of the range of limitation in each axis around $\mathbf{q}_0$, $\mathbf{q}_r$ is defined as

$$\mathbf{q}_r = [\infty,\ \infty,\ 8.3\text{[mm]},\ \infty,\ \infty,\ 0]^T \tag{2.3}$$

2.2.4 Optimization procedure

Derivation of the candidate in each stem size is performed using the Powell method with initial values sampled within the possible solution space. The author defines the range of initial positions using $\mathbf{q}_0$ as

$$\mathbf{q}_0 - \mathbf{q}_s \leq \mathbf{q}_I \leq \mathbf{q}_0 + \mathbf{q}_s, \quad \mathbf{q}_s = [P_t,\ P_t,\ P_t,\ P_r,\ P_r,\ 0]^T \tag{2.4}$$

where $\mathbf{q}_I$ is the set of initial positions, and P_t and P_r are the constants that describe the range of the initial position. In the proposed method, the author defines these values as $P_t = 8.0$ mm and $P_r = 4.0$ deg. This range lies inside the constraints, and has already been confirmed experimentally to include the appropriate position and sufficient rotation. $\mathbf{q}_I$ takes a discrete positions, which are sampled with a fixed interval within the solution space defined in Eq. (2.4). The interval of the initial position ΔP is the parameter to be adjusted. The solution is obtained for each stem size. When the optimized fitness values in each initial position are less than zero, the author regards this stem size as having no solution. After determining the solution for all stem sizes, the author obtains stem size as the largest of all sizes displaying a solution.

2.3 Experimental results

2.3.1 Experimental procedure

The author applied the proposed method to 17 cases. Firstly, the author adjusted the parameters of the proposed method according to an exhaustive experiment. The author then compared the automated plans obtained using the fine-tuned parameters with the plans proposed by an experienced surgeon. Planning results were evaluated from a surgeon as acceptable or not. The surgeon who evaluated the automated plan and the surgeon who prepared the ground truth plan was different. The parameters of the proposed method are c_{th} and σ in the evaluation function Eq. (2.2), and the sample rate of the initial position is ΔP in Eq. (2.4). According to the preliminary experiment, the parameters in Eqs. (2.2) and (2.4) are independent of each other. Therefore, the author adjusted the parameters of Eqs. (2.2) and (2.4) independently. The evaluation items were the difference of position, orientation, and size between the automated plans and the surgeon's plans. The author compared the position and orientation of the solution for the same size as used in the surgeon's plan, although stem size selected in automated planning differed from stem size selected by the surgeon, as position and orientation change when stem size changes. The values of parameters used in the experiment were as follows:

- $\Delta P = 1.0, 2.0, 4.0, 8.0$ [mm] or [deg.]
- $c_{th} = 0.0, 2.0, 4.0, 6.0, 8.0$ [mm]
- $\sigma = 0.5, 1.0, 2.0, 4.0, 8.0$ [mm]

For the parameter tuning of the four patterns of ΔP, the other parameters were set as $c_{th} = 0.0$, $\sigma = 1.0$. For the parameter tuning of c_{th} and σ, the author used $5 \times 5 = 25$ patterns and $\Delta P = 4.0$.

2.3.2 Experimental conditions

The slice thickness of the 3D-CT images was 2 mm. Field of view (FOV) was 360 mm $\times$ 360 mm. The segmentation of the 3D model of the femoral surface and femoral canal were basically performed with the threshold-based contour definition. The threshold values used to segment the femoral surface and femoral canal were 200 Hounsfield units (HU) and 800 HU, respectively. However, when appropriate segmentation was not possible due to ankylosis of the pelvis and femoral head caused by dysplasia of the hip, the author used the automated segmentation system based on the statistical shape

Figure 2.3: Evaluation areas.

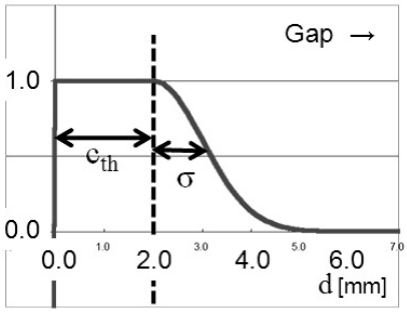

Figure 2.4: Definition of $f(d)$ of stem fitness.

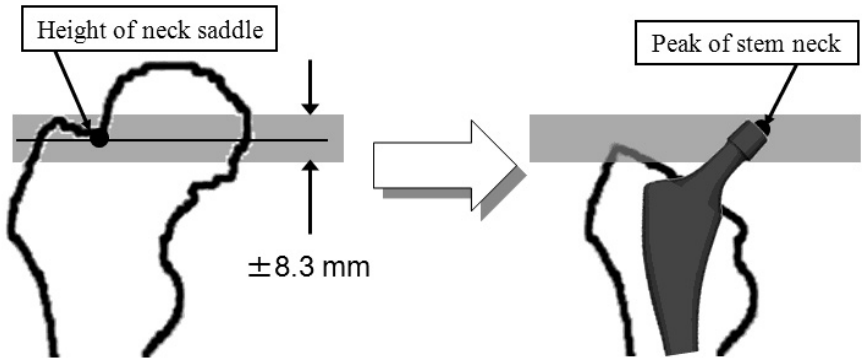

Figure 2.5: Constraints: Limitation of height of the femoral neck saddle and tip of the stem neck.

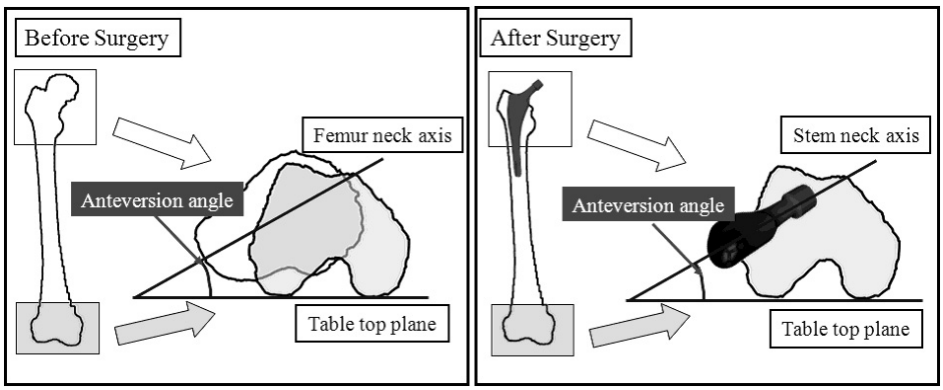

Figure 2.6: Constraints: Agreement of “anteversion angle”.

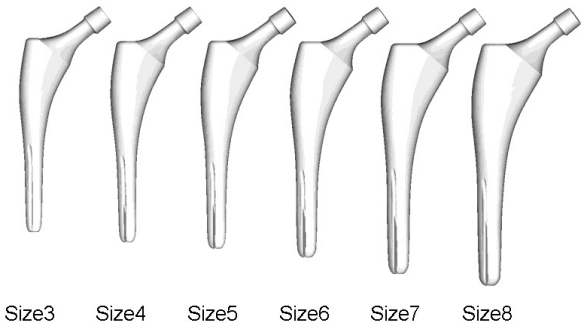

Figure 2.7: Centpillar GB HA Stem (Sizes $3 \sim 8$)

model (SSM) proposed by Okada et al. [49]. The author used Centpillar GB HA Stems (Stryker Orthopaedics, Mahwah, NJ, USA) of sizes 3 to 8 (Fig. 2.7), the preoperative plans made by experienced surgeons using the Stryker CT-Hip System (Stryker Leibinger GmbH & Co. KG, Freiburg, Germany).

2.3.3 Adjustment of parameters

In the parameter adjustment of ΔP, when $\Delta P = 8.0$, the system failed to find a solution for the same stem size as the surgeon's plan in three cases. Conversely, the system succeeded in finding a solution for the same stem size as the surgeon's plan in all cases when $\Delta P = 1.0, 2.0, 4.0$. Table 2.1 shows the time in each ΔP for the calculation of the candidate of the one stem size (including I/O time). The calculation time of $\Delta P = 1.0$ was 1,560 min, far greater than the calculation times of the other sizes. The top left panel of Fig. 2.8 shows the mean error ($\pm$ SD) of position and orientation in each ΔP. Mean errors of position and orientation were approximately the same (approximately 3.4 mm and 5.0 deg., respectively) for ΔP = 1.0 and 2.0. Standard deviations of position and orientation were also approximately the same (approximately 1.6 mm and 2.8 deg., respectively) for ΔP = 1.0 and 2.0. When $\Delta P = 4.0$, mean errors of position and orientation were 3.7 mm and 5.2 deg., respectively, and standard deviations of position and orientation were 2.9 mm and 2.8 deg., respectively. Although mean errors were approximately same as those if ΔP = 1.0 and 2.0, standard deviation of the positional error was larger than those of ΔP = 1.0 and 2.0.

In the parameter adjustment of c_{th} and σ, the calculation time of optimization for the entire stem

size, which was approximately the same in all conditions, was approximately 20 min. The top right panel of Fig. 2.8 shows the number of cases in which the difference in stem size from the surgeon's plan was less than one size. When $c_{th} \leq 2.0$ and $\sigma \leq 2.0$, differences in stem size selection were less than one size in all cases. The bottom of Fig. 2.8 shows mean errors of position in each c_{th} and σ. Mean positional errors increased when $c_{th} \geq 6.0$. On the other hand, the positional error changed little and the error was small when $c_{th} < 6.0$ except for $c_{th} = 0.0$, $\sigma = 0.5$. The smallest positional mean error, 3.7 mm, was attained when $c_{th} = 1.0$ and $\sigma = 1.0$. Mean orientation errors were approximately 5.3 deg. in all conditions. Few changes were seen with changes of parameters.

2.3.4 Results of automated planning with fine-tuned parameters

From the results of the adjustment of parameters, the author sets the parameters as $\Delta P = 2.0$, $c_{th} = 0.0$, and $\sigma = 1.0$. Calculation time in entire stem size was approximately 360 min in each case. Stem size difference was less than one size in all cases. According to the assessment of the surgeon, 14 cases were accepted and three cases were rejected. Figure 2.9 shows mean errors of position and orientation in each coordinate axis of the groups of accepted and rejected cases. Mean positional error was 3.2 mm in accepted cases and 4.0 mm in rejected cases, and mean orientation error was 4.6 deg. in accepted cases and 7.0 deg. in rejected cases. The difference between the accepted cases and the rejected cases was larger in the mean orientation error than the mean positional error. Particularly, the mean orientation error of *z*-axis was large in the rejected cases.

Figs 2.10 and 2.11 show the typical planning results by the experienced surgeon and the proposed method. The planning result of the accepted case is 2.10 and that of the rejected case is 2.11. The color map on the stem surface indicates distance between the stem surface and femoral canal, which was used in the calculation of stem fitness. Yellow and green areas are considered areas of strong stem fitness. In Case 5 (fig. 2.10), positional error of the automated plan was 0.5 mm, and orientation error was 3.4 deg. Conversely, in case 1 (fig. 2.11), positional error was 5.5 mm, and orientation error was 9.2 deg. In case 1 (fig. 2.11), the orientation error of the *z*-axis was particularly different between the automated planning result and the surgeon's plan.

Table 2.1: Result of parameter adjustment: calculation time in each ΔP [min]

	Calculation time [min]
Δ P = 8.0	0.5
Δ P = 4.0	5
Δ P = 2.0	75
Δ P = 1.0	1560

2.4 Discussions

The author has developed an automated planning system to properly determine the size, position, and orientation of each implant by maximizing stem fitness. The author then adjusted parameters of the criteria for the proposed method to apply this method to the Centpillar GB HA stem.

The author discusses the parameter adjustment of ΔP, c_{th}, and σ. ΔP is the sample rate of initial positions in the optimization. For $\Delta P = 8.0$, in three cases, the automated system failed to find a solution for the same stem size as that used in the surgeon's plan. In addition, mean errors were larger than those of the other conditions of ΔP. As a result, ΔP is thought to affect the precision of optimization. ΔP also affects calculation time, as local optimization is performed cyclopaedically in the solution space $\mathbf{q}_I$, which is sampled by ΔP. Considering the calculation time of the results for $\Delta P = 1.0$ and 2.0, $\Delta P = 1.0$ required a calculation time 22 times longer than that for $\Delta P = 2.0$ although the mean errors of position and orientation were approximately same. According to these results, the author considers $\Delta P = 2.0$ as the balanced value of this parameter. c_{th} and σ represent the relationship between distance between the femoral canal and stem surface and stem fitness, respectively. As these parameters increase, latitude of the gap between the stem surface and femoral canal also increases. When $c_{th} \geq 4.0$ or $\sigma \geq 4.0$, the automated system failed to find a solution for the appropriate stem size. Positional error was also large under these conditions. Conversely, although $c_{th} < 4.0$ and $\sigma < 4.0$, positional error was large when $c_{th} = 0.0$ and $\sigma = 0.5$. Positional errors of the rest were almost the same. The results indicate that the ranges of parameters for obtaining reasonable plans are $0.0 \leq c_{th} \leq 4.0$ and $1.0 \leq \sigma \leq 2.0$. The author determined

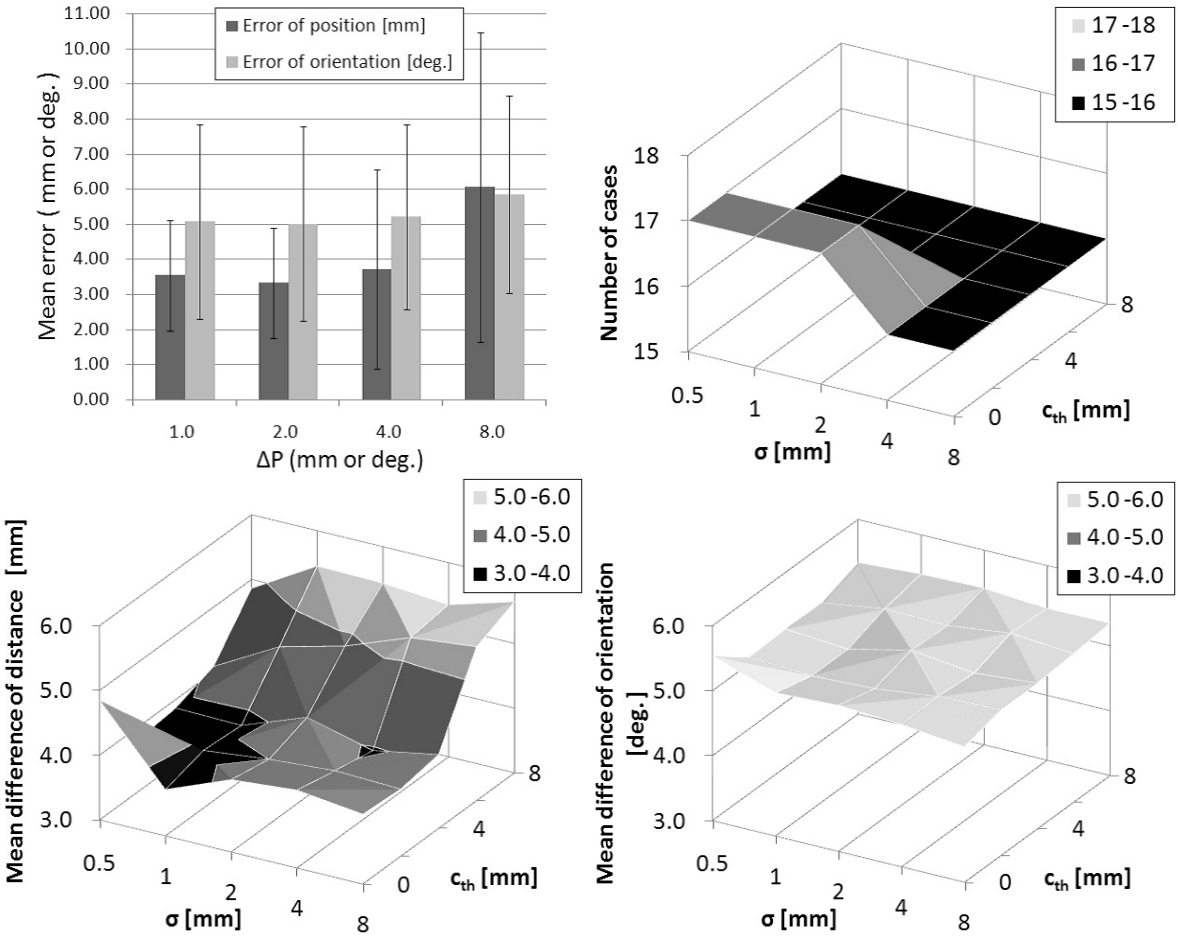

Figure 2.8: Results of parameter adjustment. Top left: mean error ($\pm$SD) of position and orientation in each ΔP. Top right: number of cases in which the difference in size on automated planning is less than 1 size. Bottom left and bottom right: mean difference of position and mean difference of orientation, respectively, for the proposed method.

$c_{th} = 0.0$ and $\sigma = 1.0$ after taking into account the design principle of the stem that strong fixation with no gap is required.

The author discusses the performance of the proposed system based on the automated planning results obtained with the fine-tuned parameters. In stem size selection, the difference between the automated system and the experienced surgeon was less than one size in all cases. This result appears acceptable, as stem selection varies in size to some extent because of limb length adjustments. In addition, the surgeon accepted the automated plan in 14 cases. The remaining three cases were acceptable after slight adjustment by the surgeon. According to these facts, the author consider that

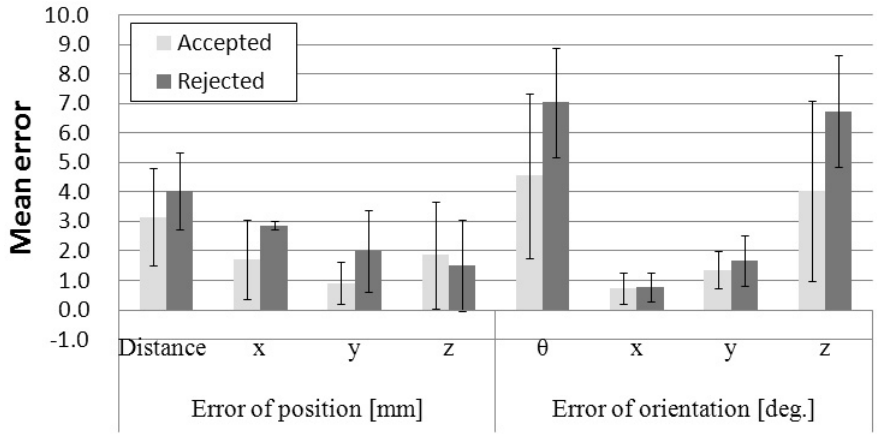

Figure 2.9: Mean error of automated planning with fine-tuned parameters of accepted and rejected cases as assessed by a surgeon.

the proposed method is applicable as an automated preoperative planning system. The remaining problem that appeared in rejected cases was performance of the determination of orientation. The mean error of orientation in cases rejected by the surgeon was 7.0 deg. The author consider that this is due to insufficient description of the surgeon's expertise. In the proposed method, orientation along the *z*-axis, which was assigned with the angle of anteversion, was fixed as the original femoral anteversion by the constraints (described in §2.2.3). However, the surgeon often does not use this criterion in adjusting the angle, considering the fitness in the stem neck area. To overcome this problem, the author will define the fitness in the stem neck and estimation of the orientation of the *z*-axis.

In the proposed fitness function, the small gaps between the stem and canal surfaces are allowable. This criterion is based on the clinical knowledge that the small gaps will be filled due to bone regrowth so that sufficient fixation is attained. Therefore, the author does not consider that these small gaps cause problems. In addition, the author did not precisely adjust the area for contact evaluation within Zone 1 in Fig. 2.3. In my preliminary experiments, the author compared the results of between several patterns of specific areas and the whole area of Zone 1, and significant differences were not observed as long as the Centpillar stem was used. Thus, the author did not precisely adjust the evaluation area.

In general, segmentation requires a great deal of work, since the user must segment manually in all

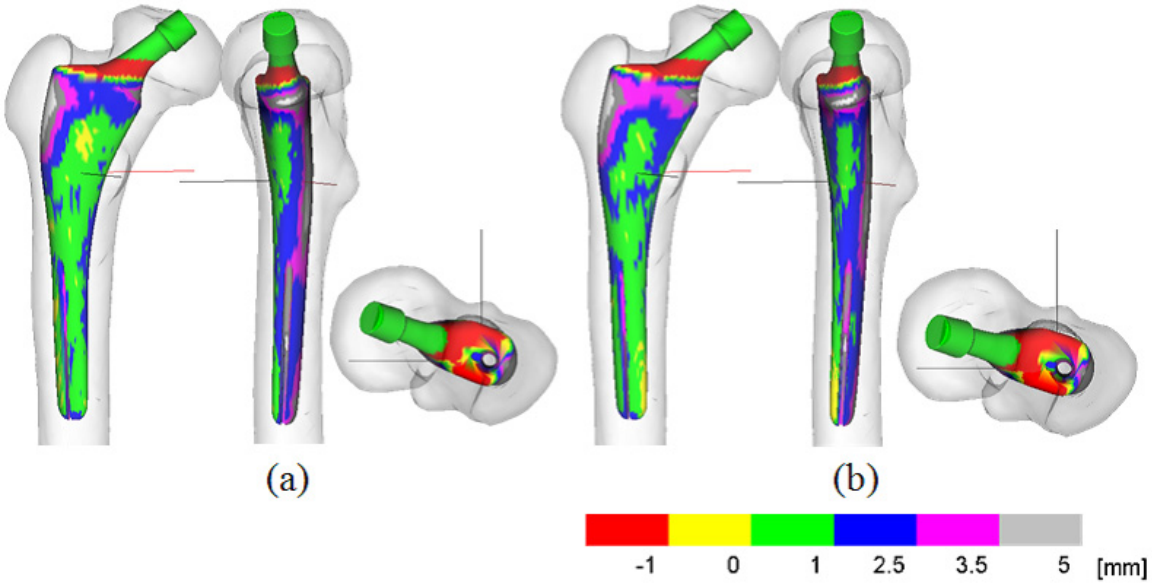

Figure 2.10: Visualization of planning results for an accepted case (Case 5). ((a) Surgeon's plan, (b) Automated plan).

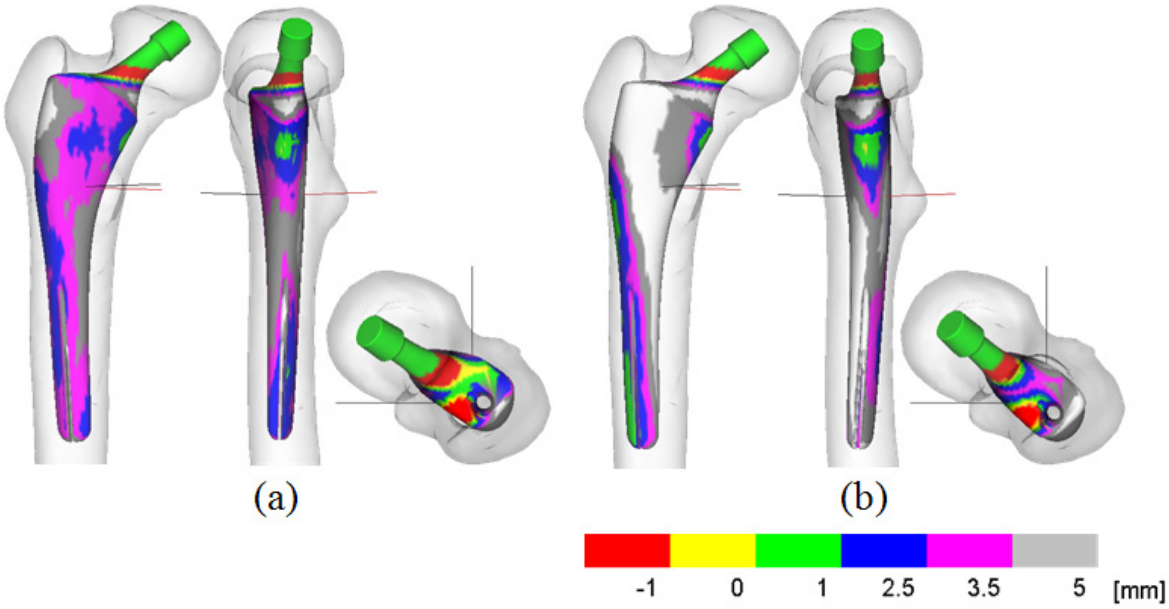

Figure 2.11: Visualization of planning results from a rejected case (Case 1). ((a) Surgeon's plan, (b) Automated plan).

slices of the CT images. About one hour is required for this method for manual segmentation of the femur and femoral canal. In the proposed system, the author employed the automated segmentation procedure of the 3D femur and femoral canal shapes proposed by Okada et al. [49] to overcome this problem. This automated segmentation procedure uses the SSM, which describes the statistical trend of the shape constructed from manually segmented shape models. Using this method, the manual operation time of segmentation decreases to five minutes for obtaining anatomical feature points. Since the segmentation is performed automatically based on several anatomical feature points on the femur, the workload for the surgeon is small. Therefore, the author considers that the segmentation of the femur and femoral canal region is not a serious problem in clinical use.

The proposed method takes approximately 360 minutes for automated planning in the current implementation. The author considers that some parallel computation frameworks may be able to overcome this problem.

2.5 Conclusion

The author has developed an automated planning system of the stem for THA. By executing exhaustive parameter tuning of the objective function, the author succeeded to achieve the planning results which were similar to the experienced surgeon's plans. The author believes that the workload of the surgeon can be reduced in preoperative planning. The proposed system would thus increase the usefulness of various intraoperative surgery systems, such as surgical navigation and robotics systems, One remaining problem is requirement of the parameter tuning of the objective function.

In the future, the author will incorporate criteria of a mechanical analysis and the evaluation function of stem fitness without adjustment of parameters. As a previous study, Reggiani et al.[17] reports a mechanical analysis framework of the stem planning based on a finite element model (FEM) analysis. However, the criteria of preoperative planning to achieve appropriate distributions of stress have not yet been proposed. If these criteria are proposed, reality-based planning with more than only the one criteria of stem fitness will be possible. In addition, to define stem fitness evaluation function without adjustment of the parameter, the author will apply a method based on statistical analysis of the surgeon's plans.

Chapter 3

Atlas-based approach and validation of automated planning of femoral implant (stem)

Abstract

Atlas-based methods for automated preoperative planning of the femoral stem implant in total hip arthroplasty are described. Statistical atlases are constructed from a number of past preoperative plans prepared by experienced surgeons in order to represent the surgeon's expertise of the planning. Two types of atlases are considered. One is a *statistical distance map atlas*, which represents surgeon's preference of the contact pattern between the femoral canal (host bone) and stem (implant) surfaces. The other is an *optimal reference plan*, which is selected as the best representative plan expected to minimize the deviation from the surgeon's preferred contact pattern. These atlases are fitted to the patient data to automatically generate the preoperative plan of the femoral stem. In this paper, the author formulates a general framework of atlas-based implant planning, and then describe the methods for construction and utilization of the two proposed atlases. In the experiments, the author used 40 cases to evaluate the proposed methods and compare them with previous methods by defining the errors as differences between automated and surgeon's plans. By using the proposed methods, the positional and orientation errors were significantly reduced compared with the previous methods and the size error was superior to inter-surgeon variability in size selection using 2D templates on an X-ray image reported in previous work.

3.1 Introduction

The surgical CAD/CAM paradigm is a common framework for computer assisted surgery [1]. In this paradigm, the CAM systems, that involve intraoperative robotic and computer-guided assistance, ensure accurate execution of preoperative plans constructed using the CAD systems. Total hip arthroplasty (THA) is an implant surgery , which particularly fits the surgical CAD/CAM paradigm [3]. In its preoperative planning stage, the sizes of the implants and their 3D positions and orientations relative to the host bones are planned, and then the plan is intraoperatively executed using robotic and computer-guided assistance. The latter CAM systems have been intensively studied for the past two decades [4, 7, 8], and quite a few commercialized systems have been developed [2, 5, 6]. Now that 3D preoperative plans can be executed with high accuracy using the CAM systems, preoperative planning in 3D is regarded as virtually equivalent to performing actual surgery, and thus it becomes highly important once well-developed intraoperative CAM systems are available. Nevertheless, the preoperative planning has not received much attention compared with intraoperative assistance, and its time-consuming and subjective nature is one major obstacle against wide practical use of intraoperative systems for THA.

Preoperative planning for THA using 3D CT data has been mainly implemented as interactive systems [6, 12, 13, 14]. These systems typically visualize 3D spatial relations between implants and host bones while quantitative information such as fit-and-fill [15, 16] can be monitored in realtime so as to provide the surgeon with objective information. More recently, biomechanical analysis has been incorporated to evaluate the risk of fracture and implant loosening [17, 18, 19]. Although these quantitative evaluations are useful for improving objectivity and validity of the planning result, user interactions involving trial and error will be still necessary to prepare tentative size selection and positioning as input data for the analysis, which may be time-consuming as well as reduce objectivity [20]. One possibility to solve the problem is to automate the planning process by formulating it as an explicit optimization problem. In this paper, the author addresses the problem of automating preoperative planning and put my focus on planning of the femoral component, which is called “femoral stem”, in THA.

Nowadays, navigated THA is routinely used in some hospitals. Especially in Japan, CT-based 3D preoperative planning is often performed for THA. A large number of the preoperative plans

constructed by well-experienced surgeons are accumulated in some of the hospitals. The feedback of these past planning datasets can potentially improve the future planning. Closed-loop surgery to make the best use of past surgical data for future surgery is a recently-emerged paradigm [23]. A typical representation scheme to realize this paradigm is statistical atlas, which has been intensively applied to solve various problems of medical image analysis [24, 26, 27, 28, 29, 30]. Optimization of prostate biopsy planning is a successful application on surgical planning, in which probabilistic atlas of cancer distributions is utilized [31, 32]. More recently, automated implant fitting was performed for optimizing implant design [33]. In these methods, however, utilized statistical information was on patient anatomy and pathology rather than surgeon's expertise of planning. There have been a few existing studies utilizing the expertise in past preoperative planning datasets. The femoral implant planning in THA was performed using one of the past planning datasets [22]. As a different application, assistance in radiation therapy planning based on retrieval of similar cases from the past planning database is reported [34]. However, statistical representation of the expertise was not utilized in the both studies. As long as the author knows, statistical information on preoperative planning has not been directly embedded in an atlas representation so as to model not only patient anatomy and pathology but also expertise of the planning, except for preliminary reports of the author's works [50, 51].

In this paper, the author describes an investigation of atlas-based approaches to automated planning of the femoral stem component in THA. To the author's knowledge, there have been two existing methods of automated femoral stem planning using 3D patient data. One is the author's previous method which optimizes a user-defined objective function [52]. The other is a method using a reference CT dataset and a preoperative plan on it [22]. The former method needs adjustment of several parameters involved in the objective function. The latter method uses only a single dataset of preoperative plan as a reference, and how the reference dataset is selected and constructed was not shown in spite that the result will largely depend on the reference. In order to overcome the problems of the existing methods, the author proposes methods which are formulated as optimization problems having the following features.

1. No parameters to be adjusted are involved in the objective function.

2. Constraints derived based on statistical analysis of a number of past planning datasets con-

structed by an experienced surgeon are embedded in the objective function.

In order to realize the above features, the author has developed the following two different methods.

1. The contact pattern between the stem surface and the host bone which the surgeon prefers is statistically modeled and utilized for automated planning.

   Its preliminary report is found in [50].

2. A method for selecting the optimal reference CT and planning dataset from a number of past planning datasets is newly added as an improved version of the method described in [22]

Since experimental validations were insufficient for the existing two methods [52, 22], the author performs a comparative study to clarify the characteristics and performance of the proposed and existing methods.

The structure of this paper is as follows. In Section 3.2, preoperative planning of the femoral stem is formulated as an optimization problem and the two methods are proposed based on this formulation. Section 5.3 describes results of a comparative study which is performed to evaluate performances of the proposed methods. Section 3.4 describes discussions and this study is concluded in Section 3.5.

3.2 Methods

3.2.1 Overview

Problem formulation of the automated planning

Figure 3.1 shows the system overview of automated planning of the femoral stem. Given the patient CT dataset I and the surface models M of a femoral-stem implant design with available sizes, the system selects the proper size of the implant and determines its position and orientation, which are best fit to the patient anatomy. The problem is regarded as

$$\Theta^* = \underset{\Theta}{\operatorname{argmax}}\, f(\Theta; I, M), \tag{3.1}$$

where $f(\Theta; I, M)$ is the objective function and Θ is a vector of the implant parameters to be optimized given by

$$\Theta = \{T, s\}, \tag{3.2}$$

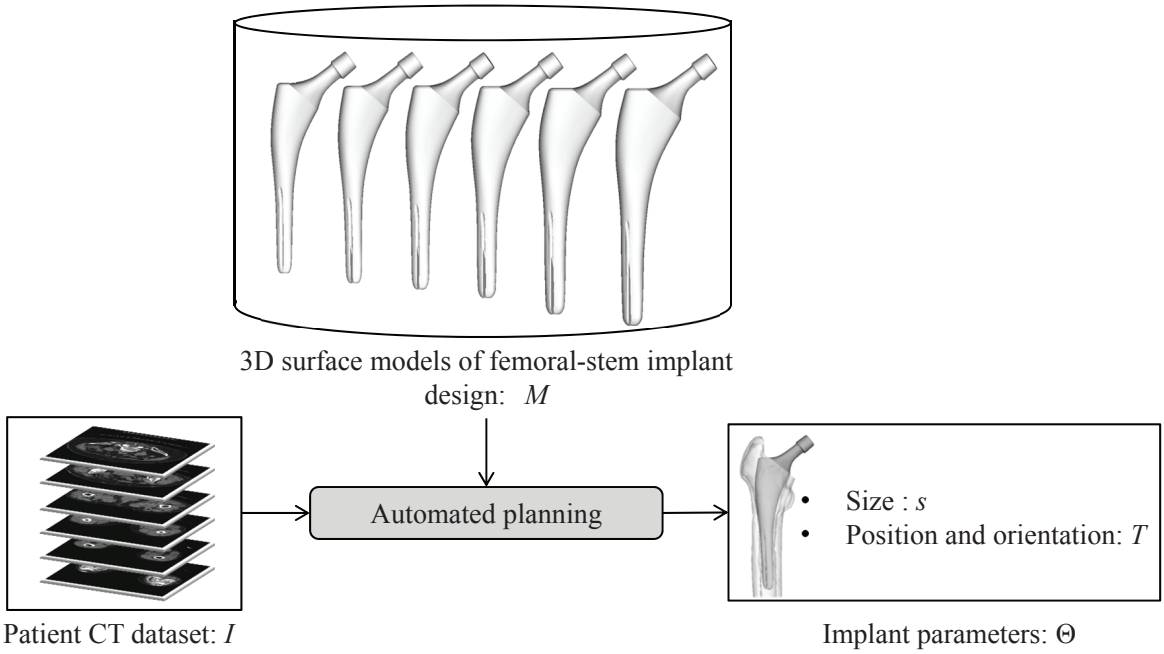

Figure 3.1: Overview of automated planning.

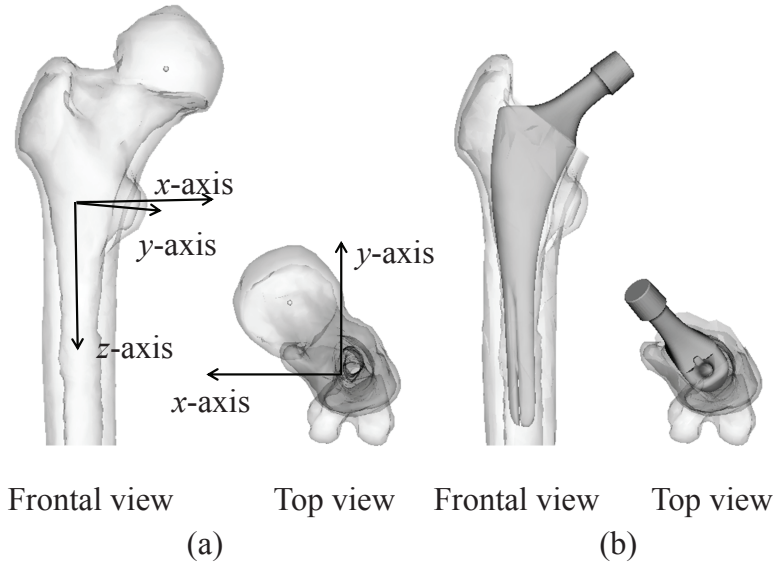

Figure 3.2: Femoral coordinate system and stem implant placement. (a) Definition of femoral coordinate system. (b) Femur whose head and neck are cut by osteotomy and femoral stem placed into the canal.

where T is a 4 $\times$ 4 matrix describing the stem pose (including position and orientation), and s is a numerical indication of the stem size, where the available sizes are finite. In the following, M is not indicated for simplification, and Eq. (3.1) is rewritten by

$$\Theta^* = \underset{\Theta}{\operatorname{argmax}} f(\Theta; I). \tag{3.3}$$

Femoral anatomy and stem implant placement

The author introduces the anatomical coordinate system of the femur (Fig. 3.2(a)), which is defined in [**?**], in order to characterize the stem planning. The coordinate system is determined so that the z-axis corresponds to the femoral shaft axis, the x-axis the direction connecting the two condyle points, and the origin the projection of the lesser trochanter point to the z-axis. The anatomical features needed for determining the coordinate system are localized from CT image using the method proposed in [53, 54], which is briefly described in 3.3.2.

The femoral stem is placed into the femoral canal (Fig. 3.2(b)). During the surgery, the femoral head and neck is cut before stem placement. In the preoperative planning, once the implant parameters Θ have been determined, the osteotomy planes are automatically determined from them. Thus, determination of Θ defines the osteotomy planes, implant size, and positioning.

Basic concept of atlas-based approach

Design of the objective function is a main issue to implement the automated planning system. Two typical criteria in orthopedic implant placement are strong implant-bone fixation and recovery of the original anatomy. In case of the femoral stem placement, the former criterion is related to the stem fit to the femoral canal, and the latter the agreement in the femoral anteversion angle between before and after the surgery, where the anteversion angle corresponds to the rotation angle of the femoral neck axis around the z-axis of the femur coordinate system. Figure 3.3 shows examples of the stem planning prepared by an experienced surgeon. The color maps on the stem surface of the upper row represent the distance maps between the femoral canal and stem surfaces, which reflect the bone-implant fit. They are not uniform over the stem surface and show a similar pattern. The lower row shows agreement in the anteversion angle between the original anatomy and preoperative plan. While the anteversion angle looks almost the same in Cases 1 and 2, there is considerable difference in Case

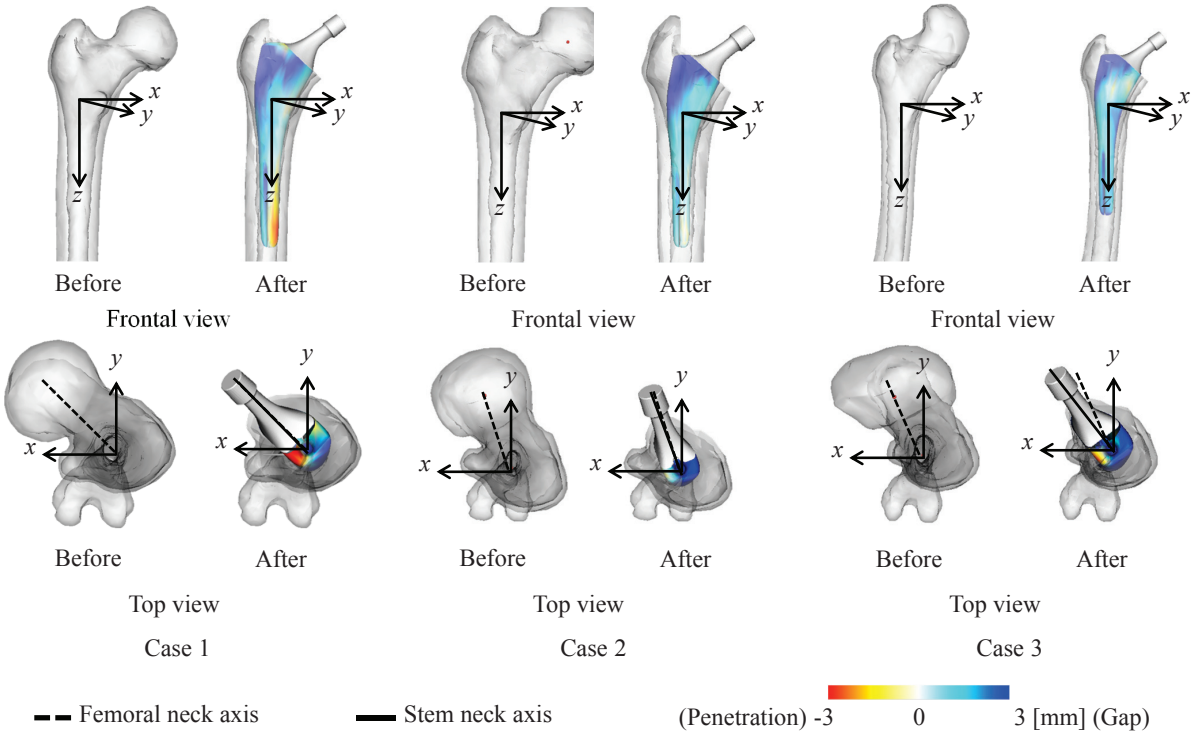

Figure 3.3: Typical examples of stem positioning prepared by experienced surgeon. In each case, x, y, and z-axes represent the femoral coordinate system. Upper: In the frontal view of each figure, color maps on the stem surfaces represent the distribution of distances between the stem and femoral canal surfaces. Red indicates penetration, white contact, and blue gap between stem and femoral canal surfaces. Lower: The anteversion angle before stem positioning is the angle between the xz-plane and the original femoral neck axis. The anteversion angle after stem positioning is the angle between the xz-plane and the stem neck axis. The difference of the anteversion angles before and after stem positioning is indicated.

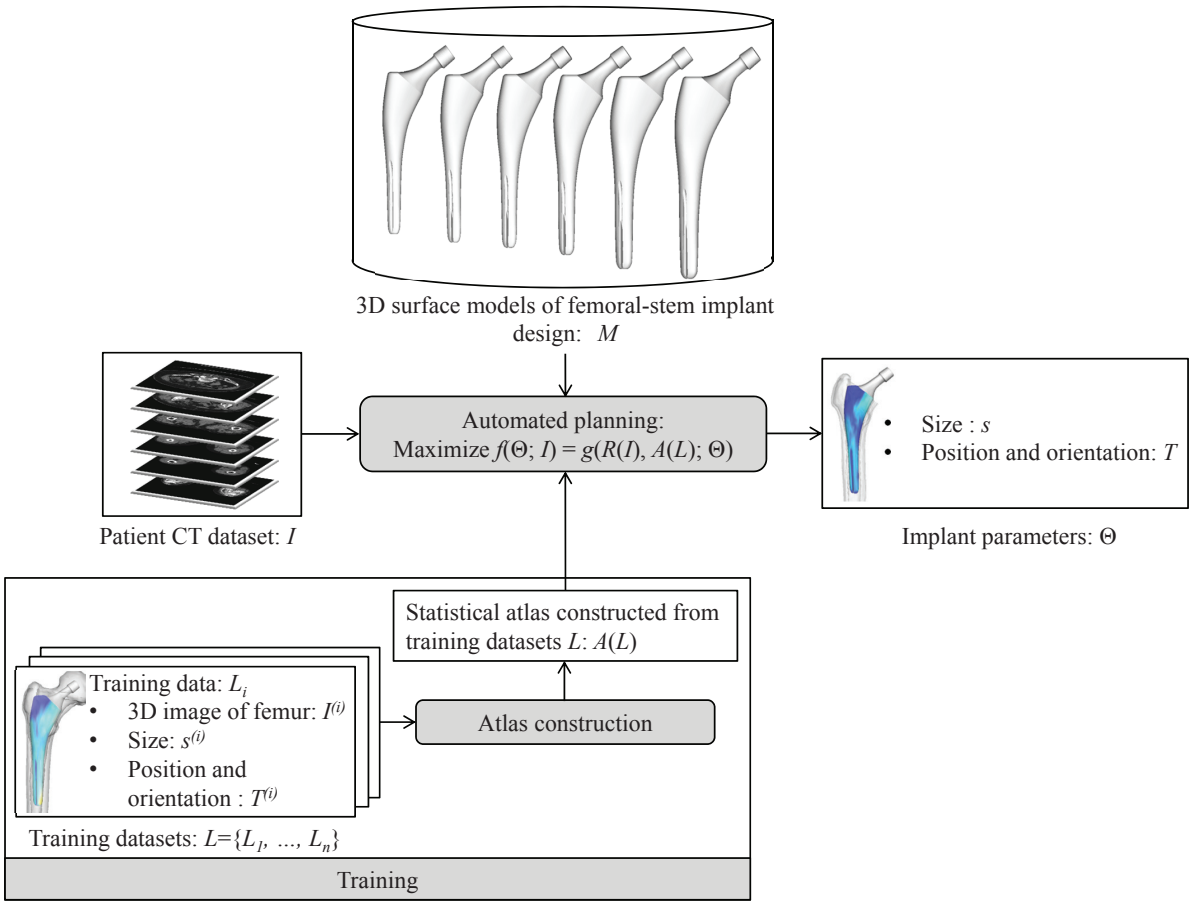

Figure 3.4: Schematic overview of atlas-based automated planning.

3, where there might be a compromise of the two criteria. Typically, balancing different criteria in the objective function may involve trial and error of parameter tuning. Furthermore, the surgeon may use implicit criteria which are not clarified. These balancing and criteria are expected to be embedded in statistical atlas.

Figure 3.4 shows a schematic diagram of the atlas-based approach. In order to derive the objective function, the stem planning datasets which were prepared by the surgeon in past THA surgeries are used as training datasets to construct a statistical atlas of the stem planning. Let $A(L)$ be the statistical atlas constructed from training datasets L which consists of n planning datasets L_i $(i = 1, 2, \cdots, n)$. In this paper, the author defines the objective function as

$$f(\Theta; I) = g(R(I), A(L); \Theta), \tag{3.4}$$

where $R(I)$ is a representation used for atlas matching, which is obtained from patient CT data I, and $g(R(I), A(L); \Theta)$ the similarity measure between $R(I)$ and $A(L)$ given the implant parameter vector Θ. The format of $R(I)$ depends on $A(L)$ and $g(R(I), A(L); \Theta)$.

In this paper, the author proposes two methods to represent atlas $A(L)$ and define the similarity measure $g(R(I), A(L); \Theta)$. One representation scheme of $A(L)$ is a "statistical distance map atlas", which is in the form of the distance map on the stem surface to the canal surface. The other is an "optimal reference plan atlas", which is one set of a raw CT dataset and a positioned stem on it selected as an optimal reference. In the following, the details of the definitions of $A(L)$ and $g(R(I), A(L); \Theta)$ in these two methods are described, followed by the descriptions of the optimization procedure to obtain Θ maximizing the objective function $f(\Theta; I) = g(R(I), A(L); \Theta)$.

3.2.2 Statistical distance map atlas

The distance map on the stem surface, which represents the distribution of the signed distance of bone-implant gap or penetration, is regarded as related to the stem fit [16]. That is, small distance area represent tight contact while large not. The contact pattern that the surgeon prefers is considered to avoid one-sided or unbalanced contact and realize the best-balanced contact. In order to model the bone-implant contact pattern that the surgeon prefers, the average and standard deviation (SD) of the distance maps in the training datasets are calculated and utilized as the atlas $A(L)$. When the statistical distance map atlas is constructed and utilized, the author assumes that the femoral canal

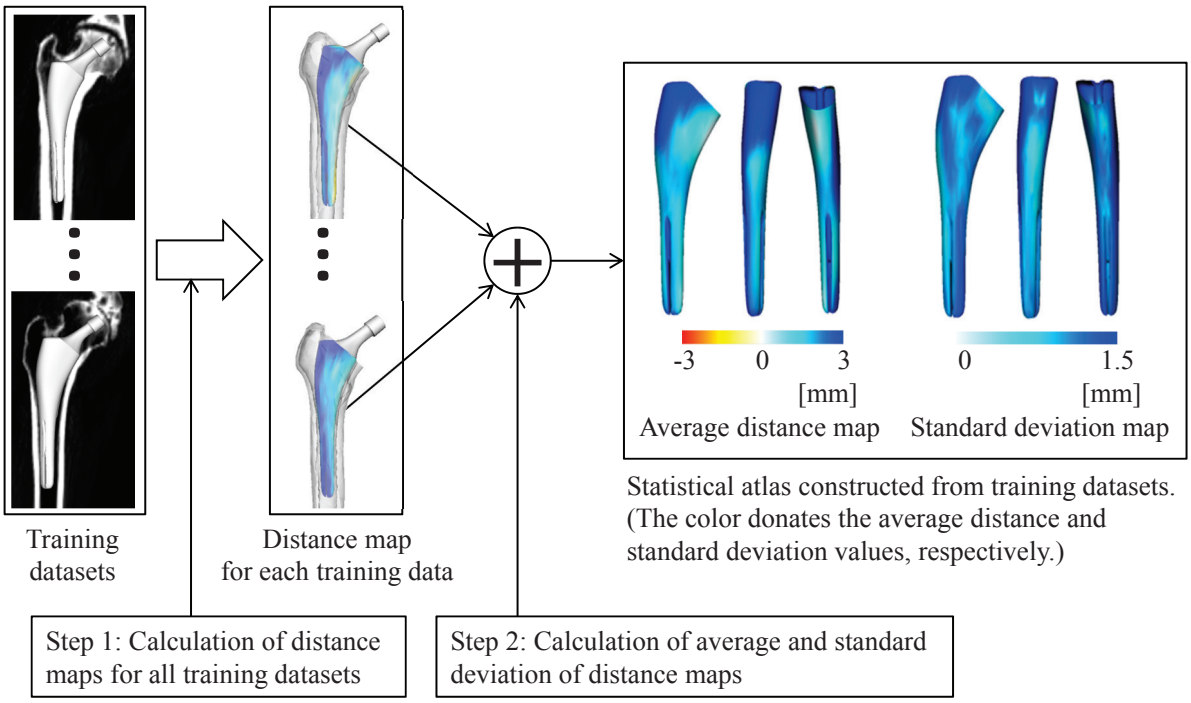

Figure 3.5: Statistical distance map construction.

surface is segmented from CT data. A recently developed automated segmentation method using statistical shape models is used for this purpose [53].

Definition of atlas

A femoral stem design consists of different sizes of the stem, and a specific size is selected for each planning dataset. To integrate the distance maps calculated on the stem surfaces of the different sizes, nonrigid registration among them is performed because the stem shape slightly differs among different sizes. In this study, the author uses a point-based nonrigid registration method [55] for this purpose. After the initialization using the coordinate system attached to each size of the stem (shown in Fig. 3.6(a)), the set of vertex positions $\mathbf{b}_j$ $(j = 1, 2, \cdots, m)$ in the polygon model of one reference stem surface is registered to the stem surface of each size to obtain 3D positions corresponding to $\mathbf{b}_j$ at each size s, which the author denotes by $\mathbf{b}_j(s)$.

Figure 3.5 shows an overview of the construction of the statistical distance map atlas. The author uses the signed distance to represent the distance of the gap between the stem surface and cortical

bone surface of the femoral canal, where the penetration of the stem to the cortical bone tissues is represented by negative distance. Let $d(\mathbf{x}, S)$ be the signed Euclidean distance from 3D position $\mathbf{x}$ to the closest point on surface S. The distance map $D(L_i)$ of the i-th training dataset $L_i (i = 1, 2, \cdots, n)$ is defined as

$$D(L_i) \quad = \quad \{d_{ij} \mid d_{ij} = d(T_i \mathbf{b}_j(s_i), Q_i)\}, \tag{3.5}$$

where d_{ij} denotes the distance value assigned to the j-th vertex $\mathbf{b}_j$ of the stem surface, T_i 4 $\times$ 4 matrix describing the stem position and orientation, s_i the stem size, and Q_i the femoral canal surface segmented from 3D CT data.

The statistical distance map atlas $A(L)$ is given by

$$A(L) = \{D_\mu(L), D_\sigma(L)\}, \tag{3.6}$$

where $D_\mu(L)$ and $D_\sigma(L)$ denote the average distance map and standard deviation map, respectively, defined as

$$D_\mu(L) \quad = \quad \left\{ \mu_j \mid \mu_j = \frac{1}{n} \sum_{i=1}^{n} d_{ij} \right\}, \tag{3.7}$$

$$D_\sigma(L) \quad = \quad \left\{ \sigma_j \mid \sigma_j = \sqrt{\frac{1}{n} \sum_{i=1}^{n} (d_{ij} - \mu_j)^2} \right\}, \tag{3.8}$$

respectively, in which μ_j and σ_j denote the average and standard deviation of the distance at the j-th vertex of the stem surface, respectively.

Similarity measure

The similarity measure for the statistical distance map atlas is defined based on least squares of the difference between the average distance map μ_j and the patient distance map $d(T\mathbf{b}_j(s), Q)$ determined by the implant parameter $\Theta = \{T, s\}$ and the femoral canal surface Q segmented from patient 3D CT data I. By normalizing by the standard deviation map σ_j, the similarity measure $g(R(I), A(L); \Theta)$ for the statistical distance map atlas is defined as

$$g(R(I), A(L); \Theta) = -\sum_{j=1}^{m} \frac{1}{\sigma_j^2} (d(T\mathbf{b}_j(s), Q) - \mu_j)^2. \tag{3.9}$$

3.2.3 Optimal reference plan atlas

Viceconti et al. proposed to use a reference stem plan prepared on a CT dataset [22]. A new patient CT dataset, on which the author wants to prepare the stem plan, is registered with the CT dataset of the referent plan using scaled-rigid registration to obtain the implant parameters. The obtained scale, translation, and rotation parameters combined with the reference stem plan provide the stem size, position, and orientation for the new patient dataset. While one case of the plan, which consists of a CT dataset and the plan on it prepared by the surgeon, is randomly selected from the training datasets in the original method [22], the author proposes the method for selecting the optimal reference plan in this paper.

Definition of atlas

The optimal reference plan is selected by applying a leave-one-out method within training datasets. The suitability as a reference is evaluated for each dataset as follows:

1. Among the training datasets L, one dataset is selected as a tentative reference dataset, which the author denotes by L_k.

2. By using L_k as the reference dataset, the automated planning procedure described in 3.2.3 is applied to CT dataset in each of all the training datasets excepting L_k to obtain the automated planning result.

3. Performance of the tentative reference dataset L_k is evaluated based on comparison between the automated planning results and surgeon's plans for the datasets excepting L_k.

After all the datasets are evaluated as a tentative reference using the above procedure, the dataset which shows the best performance is selected as the optimal reference.

As a performance index, the author uses similarity in the distance map on the stem surface between the automated and surgeon's plans. The performance index for dataset L_i, when dataset L_k is used for reference, is written as

$$p(L_i; L_k) = -\sum_{j=1}^{m} (d(T_{ik}\mathbf{b}_j(s_{ik}), Q_i) - d(T_i'\mathbf{b}_j(s_i'), Q_i))^2 \tag{3.10}$$

where T_{ik} and s_{ik} are automated planning parameters for dataset L_i obtained when L_k is used as the references, T_i' and s_i' surgeon's, Q_i femoral canal surface segmented from CT data in L_i, and $d(\mathbf{x}, S)$

the signed distance from $\mathbf{x}$ to surface S. The optimal reference L_k is selected, which maximizes

$$\sum_{i=0}^{n} p(L_i; L_k). \tag{3.11}$$

Note that the negative sign is added to the deviation from the surgeon's plan in Eq. (3.10) to be explained as a similarity measure and, thus Eq. (3.11) should be maximized.

Similarity measure

The similarity measure for the optimal reference atlas is based on the similarity measure used in intensity-based volume registration between the CT data of the reference plan, I_r, and the patient CT data I on which the author wants to prepare the plan. Normalized cross-correlation is used for this purpose, which is the same as the original method proposed by [22] and thus the similarity measure is given by

$$g(R(I), A(L); \Theta) = C(I, I_r; \Delta T, \Delta s), \tag{3.12}$$

where $C(I, I_r; \Delta T, \Delta s)$ denotes normalized cross correlation of I and the transformed version of I_r by translation and rotation ΔT and scale Δs, and ΔT and Δs are given by

$$\Delta T = T T_r^{-1}, \tag{3.13}$$

and

$$\Delta s = t_s(s)/t_s(s_r), \tag{3.14}$$

in which T and s ($\Theta = \{T, s\}$) denote the implant parameters (translation and rotation T and size s) which the author wants to estimate, T_r and s_r those given as the optimal reference plan, and $t_s(s)$ the conversion table to obtain the actual scale value from the numerical indication of the stem size s. Note that s or s_r denotes just a numerical indication of the stem size as described in 3.2.1 and does not exactly correspond to the actual size. The conversion table is obtained beforehand by scaled registration among different sizes of the stem surfaces. In order to estimate T and s, ΔT and Δs maximizing $C(I, Ir; \Delta T, \Delta s)$ are firstly obtained, and then T and s are calculated using T_r and s_r of the reference plan and Eqs. (3.13) and (3.14).

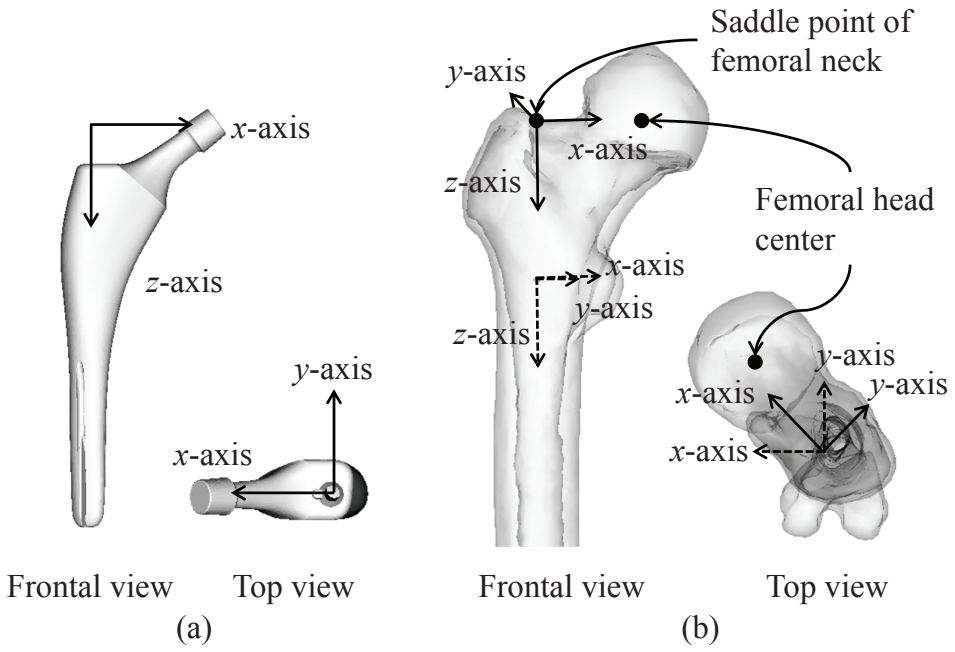

Figure 3.6: Rough alignment of femoral stem to the femur. (a) Coordinate system of femoral stem (provided by implant manufacturer). (b) Alignment of stem coordinate system to femur coordinate system. The coordinate systems denoted in dashed and solid lines correspond to those of the femur and stem, respectively.

3.2.4 Optimization procedure

Powell's Method [56] is utilized to obtain the implant parameters Θ maximizing Eq. (3.4). In order to avoid unwanted local maxima, the author uses multiple initial values. Large uncertainty is typically involved in the translation along the z-axis and rotation around the z-axis in the femoral coordinate system. Therefore, the author uses several initial values for these two degrees of freedom. In order to obtain a reference position and orientation of the stem for positioning the initial values, the author assumes that a method for rough alignment of the stem and femoral coordinate systems is available. By using the reference obtained by the rough alignment, several initial values are set within the predetermined range of the z-coordinates centered at the reference position and the predetermined range of the rotation around the z-axis centered at the reference orientation. The details of initial value setting are described in 3.3.1.

A particular method for the rough alignment of the femoral stem which the author used in this paper is as follows. Fig. 3.6(a) shows the coordinate system of the stem used in this study. Fig. 3.6(b) shows its rough alignment to the femur. As shown in the front view of Fig. 3.6(b), the z-axis of the stem coordinate system is aligned to that of the femoral coordinate system, and then its z-position in the femoral coordinate system is determined so that the xy-plane of the stem coordinate system passes through the saddle point of the femoral neck. As shown in the front view of Fig. 3.6(a), the rotation around the z-axis of the stem coordinate system is determined so that the direction of the x-axis of the stem coordinate system passes through the projection of the femoral head center onto its xy-plane. The anatomical features needed for the alignment are localized from CT image using the segmented femur region and surface obtained by the method proposed in [54, 53], in which the surface nodes are anatomically labeled. The femoral neck saddle is localized as a position where the topology of the segmented femur region in the axial plane changes along the z-direction. The femoral head center is obtained by fitting the sphere to the surface nodes labeled as the femoral head.

3.3 Experimental results

A comparative study was performed to clarify the characteristics and performance of the proposed and existing methods. In this section, firstly experimental conditions are described in 3.3.1, and then methods for automated segmentation of the femoral canal and localization of anatomical landmarks are briefly described in 3.3.2. Experimental methods and results are described in 3.3.3 and 3.3.4, respectively.

3.3.1 Experimental conditions

To evaluate the methods, the author used 40 planning datasets of the osteoarthritis patients, which had been actually used for computer-navigated THA surgery at Osaka University Hospital. Each dataset consisted of 3D CT data and the stem plan prepared on it by the surgeons. The slice thickness and reconstruction pitch of CT data were 2.0 mm. The field of view was 360 $\times$ 360 mm^2 and the matrix size was 512 $\times$ 512. Regarding the stem design, CentPillar GB HA stem system (Stryker Orthopaedics, Mahwah, NJ, USA), which is a so-called anatomical stem and designed based on the anatomical shape of the femoral canal, was used. Six different sizes from three to eight were used for

planning. The stem planning by the surgeon was performed using commercially available interactive THA planning software, Stryker CT-Hip System (Stryker Leibinger GmbH, Freiburg, Germany). Although planning was not performed by a single surgeon, the surgeons who prepared the plans belonged to the same team and the criteria for the planning were regarded as the same.

Regarding the optimization procedure, initial values of T were determined in the following way. Let $\mathbf{p}_0$ and $\mathbf{r}_0$ be the reference position and orientation determined by the rough alignment described in 3.2.4. Given the $\mathbf{p}_0$ and $\mathbf{r}_0$ as the center of the initial value range, nine values were considered for translation along the z-axis from -16.0 mm to +16.0 mm with 4.0 mm interval. Similarly, nine values for rotation around the z-axis from -16.0 deg. to +16.0 deg. with 4.0 deg. interval. Consequently, $9 \times 9 = 81$ combinations of the initial values were used. These range and interval were determined based on the results of preliminary experiments. The above initial value setting was used in the experiments of all the proposed and existing methods.

3.3.2 Automated segmentation of femoral canal and localization of anatomical landmarks

In order to apply the statistical distance map atlas to the patient data, segmentation of the femoral canal from CT data is necessary. Furthermore, to define the femoral coordinate system (3.2.1) and perform the rough alignment (3.2.4), localization of several anatomical landmarks is necessary. These processing tasks were performed using the femur region and surface model segmented by a method based on hierarchically organized statistical shape models (SSMs) [53]. After initial manual specification of five anatomical landmarks on the pelvis needed for determining the pelvic coordinate system [4], the pelvis-femur integrated SSM is fitted to CT data, and then fitting of the individual femur SSM and pelvis SSM were performed, followed by femoral canal SSM fitting. Excepting the initial manual specification, segmentation of the femoral canal was performed automatically. Because anatomical information can be embedded in SSMs, not only segmentation but also anatomical landmark identification needed for the above tasks was possible. Automatically segmented femoral canals and localized anatomical landmarks in all 40 patient CT datasets were checked by an experienced surgeon. As a result, it was confirmed that reasonable accuracy was achieved in all cases. Therefore, the author used these segmentation results without any manual modification.

3.3.3 Experimental methods

The two proposed methods and two existing methods were applied to the 40 datasets for the comparative study. In the following, the two proposed methods are denoted as follows:

1. **Statistical-DM**: Statistical Distance Map atlas (described in 3.2.2).

2. **Optimal-RP**: Optimal Reference Plan atlas (described in 3.2.3).

The following two existing methods were compared with the proposed methods.

3. **Manual-DM**: Manual Distance Map atlas [52] is the specific areas on the stem surface to be contacted to the canal surface, which are manually selected by an experienced surgeon. In order to estimate the implant parameter, the summation of the distances between the canal surface and the specific areas of stem surface is minimized while the rotation around the z-axis is fixed to the measured anteversion angle.

4. **Random-RP** : Random Reference Plan atlas [22] is summarized in the first paragraph in 3.2.3.

All the four methods estimated the implant parameters $\Theta = \{T, s\}$. The evaluation of the methods was based on the error of the estimated parameters, which was defined as the difference between the parameters estimated by the methods and those of the surgeon's plans. Leave-one-out cross validation was performed using the 40 patient datasets excepting Manual-DM, in which training datasets were not involved. The author also performed paired t-test as a significance test.

Regarding the proposed methods, the effects of the number of the training datasets were also evaluated. The error was evaluated using a variation of leave-five-out cross validation. Ten different combinations of randomly selected five datasets were used as the test datasets. The number of the training datasets was varied from 1 to 35 and training datasets were randomly selected from the remaining datasets for each of the test datasets. The average of the errors was calculated for each number of the training datasets.

3.3.4 Results

Table 3.1 shows the averages and standard deviations (SD) of the size, positional, and orientation errors, including the x, y, and z components on positional and orientation errors. The average errors of the two proposed methods were smaller than the existing methods on all aspects. The average size

Table 3.1: Average error and standard deviation (SD) of planning errors (average $\pm$ SD).

		Proposed methods		Previous methods	
		Statistical-DM	Optimal-RP	Manual-DM	Random-RP
Size error		0.5 ± 0.6	0.6 ± 0.6	0.8 ± 0.6	0.9 ± 0.9
		3.6 ± 2.0	4.0 ± 2.1	5.5 ± 2.2	5.9 ± 3.6
Positional	x	1.2 ± 0.8	1.3 ± 0.8	2.1 ± 1.6	1.5 ± 1.0
error [mm]	y	1.4 ± 0.9	1.2 ± 0.8	2.7 ± 1.8	1.6 ± 1.2
	z	2.6 ± 2.3	3.2 ± 2.5	3.3 ± 2.5	4.7 ± 4.1
		3.5 ± 2.1	3.9 ± 2.2	4.7 ± 2.9	6.3 ± 3.8
Orientation	x	0.7 ± 0.5	0.6 ± 0.6	1.2 ± 0.9	1.0 ± 0.7
error [deg.]	y	0.8 ± 0.7	0.8 ± 0.6	1.6 ± 1.0	1.0 ± 0.7
	z	3.2 ± 2.2	3.7 ± 2.3	3.9 ± 3.0	6.0 ± 4.0

error was 0.5 and 0.6 in the proposed methods, Statistical-DM and Optimal-RP, respectively while 0.8 and 0.9 in the existing methods, Manual-DM and Random-RP, respectively. The average positional error was 3.6 mm and 4.0 mm in Statistical-DM and Optimal-RP, respectively while 5.5 mm and 5.9 mm in Manual-DM and Random-RP, respectively. The average orientation error was 3.5 deg. and 3.9 deg. in Statistical-DM and Optimal-RP, respectively, while 4.7 deg. and 6.3 deg. in Manual-DM and Random-RP, respectively. Among the x, y, and z components, the error in the z component was the largest in both positional and translational errors in all the four methods due to the elongated shapes of the femoral stem and canal along the z-axis.

Figure 3.7 shows detailed results of the size error of the four methods. In Fig. 3.7(a), the histogram of the size error is shown. Out of 40 cases, the size was the same as the surgeon's plan in 21 and 20 cases in Statistical-DM and Optimal-RP, respectively, while 14 and 16 cases in Manual-DM and Random-RP, respectively. In Fig. 3.7(b), the joint frequency distributions of the automated and surgeon's size selections are shown in a matrix form. The inter-class correlation (ICC) value of the automated and surgeon's sizes is also shown for each matrix. ICC values were 0.87 for Statistical-

DM and 0.81 for Optimal-RP which were higher than the previous methods (0.76 for Manual-DM and 0.69 for Random-RP).

Fig. 3.8(a) shows the box plots of the positional error and orientation error, respectively. Fig. 3.8(a) also shows the results of paired t-test. Statistical significance was observed in most pairs consisting of the proposed and existing methods while no significance was observed between the two proposed methods although Statistical-DM was slightly better than Optimal-RP. Especially, significance was observed in all the pairs between Statistical-DM and the existing methods on the positional and orientation errors. Regarding the size error, no significance was observed in any pairs among the four methods.

Figures 3.10 to 3.12 show illustrative cases of the planning results. The three cases shown in Figs. 3.10 to 3.12 are the same cases as those in Fig. 3.3. In these three cases, it is observed that the color-coded distance map appeared similar to the surgeon's plan in the proposed methods while not in the existing methods, especially, Manual-DM. Case 1 is a typical case in which the two proposed methods showed better performance where their distance maps were more similar to the surgeon's than the previous methods. In Case 2, the size differed by one size in Optimal-RP where the distance map showed slight penetration compared with Statistical-DM. In Case 3, the rotation angle around the z-axis in the surgeon's plan was largely different from the anteversion angle of the patient as shown in Fig. 3.3. While Manual-DM, which directly measures the anteversion angle, successfully estimated it but failed to approximate the surgeon's plan, Statistical-DM successfully reproduced the surgeon's plan with relatively small error, in which the distance map was similar to surgeon's one.

Figure 3.13 shows the effects of the number of the training datasets on the size, positional, and orientation errors in the proposed methods. Although the size error in Statistical-DM and the orientation error in Optimal-RP still appeared to be decreasing at the maximum number of training datasets, other errors did not change at large numbers and it could be considered that the convergence was mostly attained. Note that the results in Fig. 3.13 (at n = 35) were different from those in Table 3.1 and Figs. 3.7 and 3.8 because the test and training datasets were different.

The average computation time per one case was roughly 2 minutes in Statistical-DM, 150 minutes in Optimal-RP, 20 minutes in Manual-DM, and 150 minutes in Random-RP on Intel Xeon dual core processor (3.0 GHz and 16 GB main memory). In Optimal-RP and Random-RP, voxel-based scaled rigid registrations using 81 different initial positions were required, which was a main cause of longer

computational time. In contrast, computational cost was smaller in Statistical-DM and Manual-DM because computation was needed only on the stem surface.

3.4 Discussion

3.4.1 Significance of using statistical atlas in femoral stem planning

In this paper, the author has addressed the problem of automated preoperative planning of the femoral stem implant in total hip arthroplasty (THA). The performance of the proposed methods using statistical atlases was compared with the previous methods. The error, which was defined as the difference between the automated and surgeon's plans, was reduced in all of size, position, and orientation by using the proposed method in the leave-one-out cross validation using 40 cases which were actually used in past THA surgery. Especially, the error reduction was statistically significant in position and orientation. Regarding the size error, its reduction was not significant. As shown in Fig. 3.7, however, size selection of the proposed methods was the same as the surgeon's selection in more than half cases among all the cases the author tested. In addition, ICC (intra-class correlation) of the size selection between the surgeon and Statistical-DM was sufficiently high (0.87). It should be noted that this ICC value is higher than inter-surgeon ICC of the size selection using 2D implant templates on an X-ray image (0.77), which is reported in [57]. Even though the datasets were different and the comparison is made between 3D and 2D, the author considers that it would have some clinical significance that automated selection in 3D may outperform surgeon's selection in 2D.

One of noticeable points in the experimental results is that the proposed methods (Statistical-DM and Optimal-RP) showed smaller average error and standard deviation in the orientation error around the z-axis, which corresponds to the anteversion angle of the femur, than Manual-DM (Table 3.1). In Manual-DM, the anteversion angle of the femur was directly measured and used in the planning. As described in 3.2.1, the anteversion angle is one of the important criteria to determine the stem orientation so as to recover the original anatomy. Although the proposed methods do not directly incorporate the constraint of the anteversion angle, they showed better agreement with the surgeon's planning in this regard. These results show that the proposed methods attained better compromise between recovery of the original anatomy (anteversion angle) and bone-implant fixation in a similar way as the surgeon considers.

Another point the author should note is that the proposed methods were designed so as to just mimic the surgeon's stem planning. No biomechanical and physiological aspects were considered in them. The author is currently trying to justify the surgeon's plan by using biomechanical simulations [58].

3.4.2 Utilization as a tool for computational modeling of planning criteria

The basic function of the proposed methods is to model the surgeon's expertise used to prepare the past planning datasets and mimic the surgeon's planning. Their characteristics and performance depend on the training datasets. Different statistical atlases are constructed from different datasets. In this study, the past datasets of planning were not prepared by a single surgeon. However, the surgeons who prepared the plans belonged to the same team and the datasets could be regarded as consistent in the criteria for the planning. Different statistical atlases will be constructed by using planning datasets prepared at a different clinical site. Therefore, the author considers that the proposed methods can be potentially used as a tool for modeling the planning criteria. Different stem plans are obtained using the different atlases for unknown patient CT datasets and can be compared to analyze the difference in the criteria among clinical sites.

3.4.3 Comparison between Statistical-DM and Optimal-RP

One of main differences between the two proposed methods, Statistical-DM and Optimal-RP, is requirement of segmentation of the femoral canal. The segmentation of the outer surface of the femur is needed for the both methods to obtain the anatomical features used for rough alignment of the stem (described in 3.2.4). Additional canal segmentation is required only for Statistical-DM. Generally speaking, segmentation is known as an error-prone process. By using a straightforward extension of a segmentation method using a statistical shape model described in [53], the canal segmentation was automatically performed without any additional manual initialization and post-editing for all the 40 cases used in the experiments. Therefore, the requirement of the femoral canal segmentation is not a considerable problem.

Regarding performance, Statistical-DM reproduces the surgeon's plans slightly better than Optimal-RP, but no statistical significance was observed. However, the performance of Optimal-RP may be potentially improved. Currently, only one reference plan is used for Optimal-RP. However, the per-

formance of Optimal-RP may be improved by using multiple reference plans. To do so, future work is necessary to develop procedures for selecting multiple optimal reference plans in atlas construction and selecting the best-registered reference to the patient CT data in atlas utilization.

Regarding computational cost, Optimal-RP is more expensive because it needs scaled volume registration while Statistical-DM only requires computation on the stem surface. However, GPU-based acceleration may be applied to dramatically reduce the computational cost.

3.4.4 Possible improvements for atlas construction

The methods used for atlas construction in this paper will be potentially replaced by more elaborate methods. In Statistical-DM, nonrigid registration for the stem was performed by registering one selected reference to others, which is known to introduce undesirable bias. This conventional method can be replaced by well-developed methods such as group-wise registration [59] and spherical demons [60] for unbiased atlas construction. Further, PCA can be applied to the distance maps of the training datasets in addition to the average and point-wise standard deviation so as to represent the variability of the distance map. In Optimal-RP, an average atlas (consisting of the average CT image and stem plan) such as a Frechet mean [61] may be computed and used as reference instead of selecting the case which minimizes the deviations from the distance map of surgeon's plan. In addition, the optimal reference does not necessarily need to be single although the author used only one reference. The multiple highest-ranked references may be selected and used in a similar way to the multi-atlas approaches combined with appropriate decision fusion methods [62, 63, 64]. In Statistical-DM as well, multi-atlas approaches can be considered. The training datasets are clustered into multiple groups based on similarity of the distance map [65] and the average distance map is obtained for each group. Another way of clustering the training datasets would be based on the use of the stem size in the surgeon's plan (with allowing overlap), which is applicable to both Statistical-DM and Optimal-RP. Future work will include the above described potential improvements of atlas construction.

3.4.5 Application to other stem designs and implants of other bones

In this paper, only one stem design was used. However, various stem designs are available from different manufacturers. In principle, if 3D surface models of a new stem design are available and a sufficient number of planning datasets are prepared using the new stem by an experienced surgeon, the

proposed statistical atlases can be constructed and utilized for automated planning. The stem designs are mainly classified into two categories; anatomical and straight stems. The stem design which the author used in this paper, CentPillar system (Stryker Orthopaedics), is an anatomical stem, which has a more complex shape so as to fit to the femoral canal shape than a straight stem which has a simpler straight shape. The proposed methods will be still effective for other anatomical stem designs but may be unpredictable for a straight stem. As a preliminary experiment, however, the author has applied Statistical-DM to a straight stem and confirmed to obtain similar performance to an anatomical stem [66].

One limitation of the proposed methods is an implicit assumption that different sizes of the stem shapes are quasi-homothetic. Ideally, the proposed statistical distance map should be constructed individually for each size of the stem. However, the author could not prepare a sufficient number of training datasets for each size. Therefore, nonrigid registration among different sizes of the stem was used to average the distance maps across sizes. A large deviation from homotheticity may result in elimination of significant contact patterns. In Optimal-RP, isotropic scaling is explicitly used. It is essential that different sizes of the stem can be approximated by homothetic transform. As long as the author knows, however, not a few stem designs have quasi-homothetic shapes across sizes.

Another problem in application of the proposed methods to other stem designs is that a sufficient number of datasets of the stem plan are needed to be prepared. Future work will include the development of methods of atlas construction from a small number of the datasets. To do so, the author is planning to develop a procedure for selecting a small number of representative patient CT datasets to be planned. Actually, in case of Optimal-RP, the patient CT dataset selected as the optimal reference by the proposed method will be a good candidate of the representative dataset. Also in Statistical-DM, Fig. 3.13(a) shows that the errors became considerably small when around 10 randomly-selected training datasets were used. Better performance would be expected by appropriately selecting the representative datasets instead of randomly selected datasets.

The proposed methods are potentially applicable to implants of other bones. The formulation described in Equations (3.1) and (3.4) are generally applicable to various types of implants. The author has already applied this formulation to the acetabular cup implant of the pelvic side in THA and obtained promising initial results [51].

3.5 Conclusion

The author has described atlas-based approaches to automated femoral stem planning in THA. Two atlas representations generated from a number of past planning datasets were proposed to model the surgeon's expertise of the stem planning. One is the statistical distance map, which represents the distribution of average and standard deviation of the distances between the stem and the femoral canal surfaces. The other is the optimal reference plan atlas, which is selected as the most representative plan and expected to realized the most similar distance map to the surgeon's. Experimental results show that the proposed atlases were quite effective to reproduce the experienced surgeon's plan.

Future work will include extensions of the proposed methods to other stem designs and other implants. The development of methods is also necessary for atlas construction of a new implant using a small number of representative planning datasets without using a large number of them. Finally, the author is now preparing to start a prospective study for clinical evaluations.

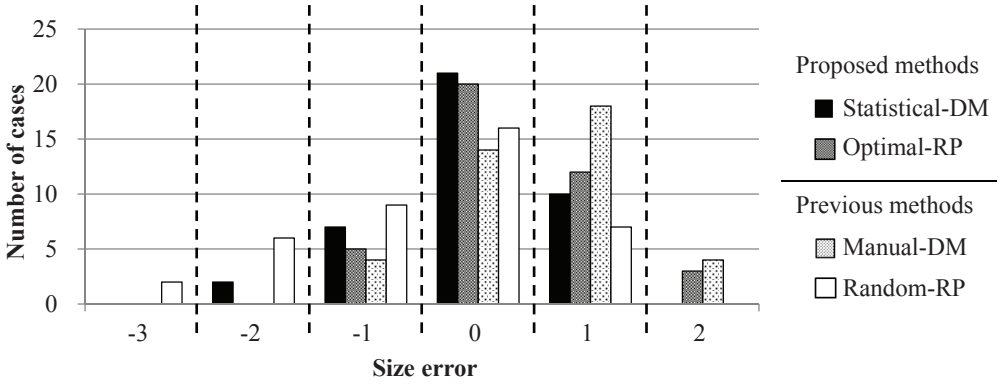

(a)

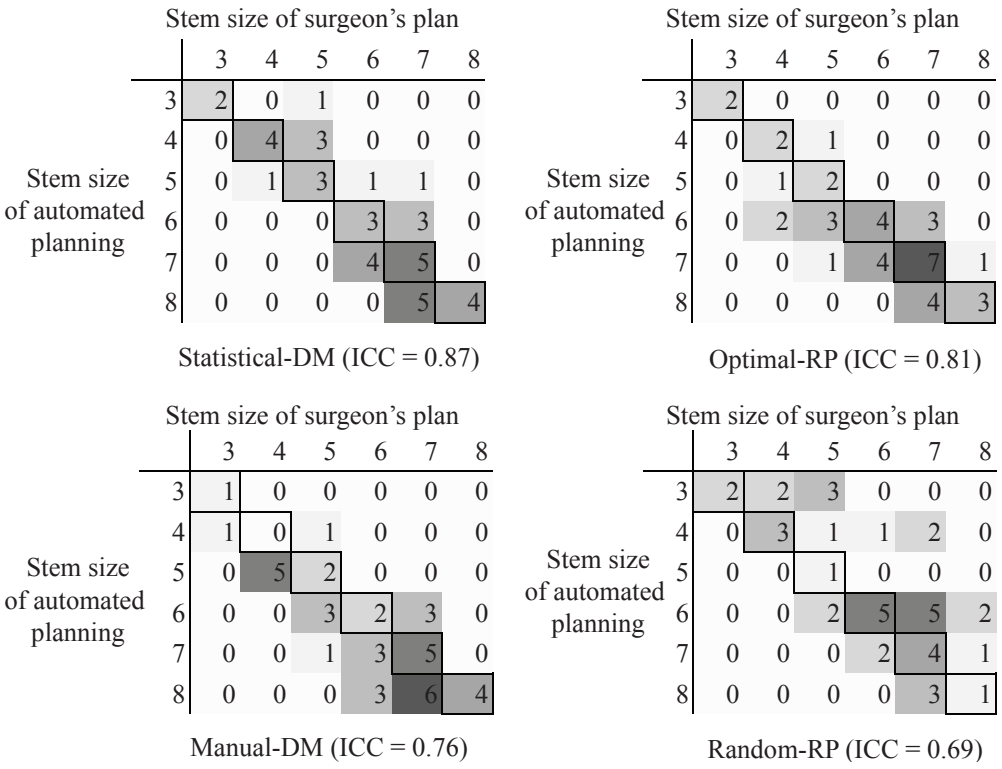

(b)

Figure 3.7: Size error of the femoral stem between automated planning results and surgeon's plans. (a) Histogram of size error. The average error was 0.5 in *Statistical-DM (proposed)*, 0.6 in *Optimal-RP (proposed)*, 0.8 in *Manual-DM (previous)*, and 0.9 in *Random-RP (previous)*. (b) Joint frequency distributions and ICC (inter-class correlation) values of automated planning results and surgeon's plans.

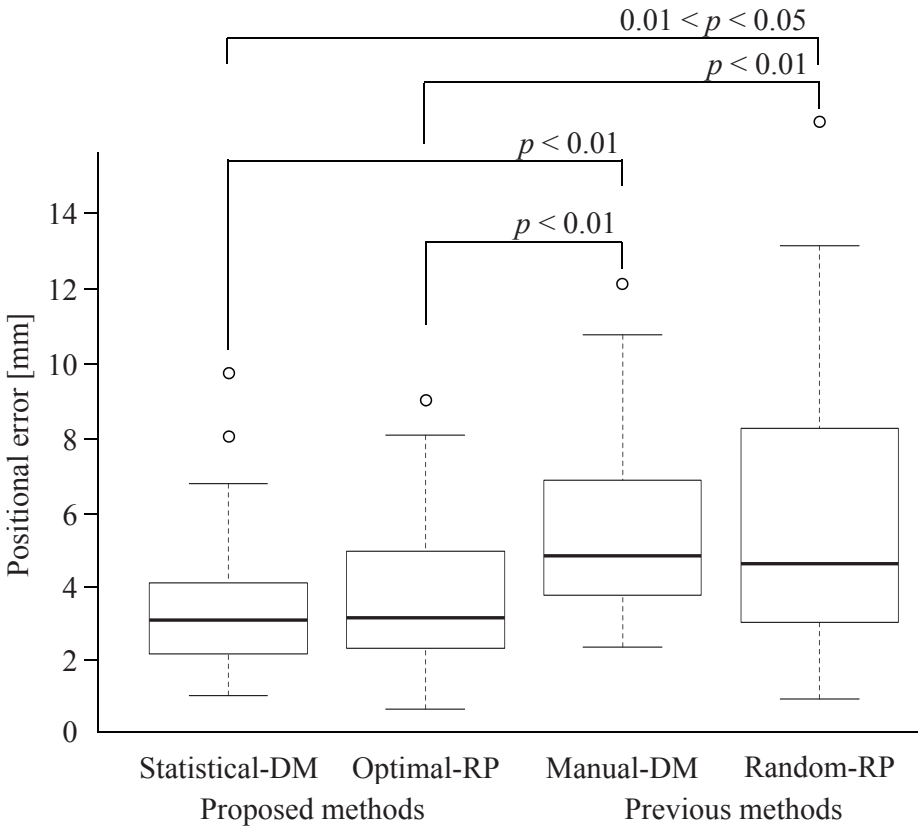

(a) Positional error.

Figure 3.8: Boxplots of positional errors and results of paired t-test. In each box, sample minimum, lower quartile (Q1), median (Q2), upper quartile (Q3), and sample maximum are indicated. Sample minimum and sample maximum are minimum and maximum values after rejection of outliers. Values larger than $(Q3 - Q1) \times 1.5 + Q3$ or smaller than $Q1 - (Q3 - Q1) \times 1.5$ are regarded as outliers. Average error was 3.6 mm in *Statistical-DM*, 4.0 mm in *Optimal-RP*, 5.5 mm in *Manual-DM*, and 5.9 mm in *Random-RP*.

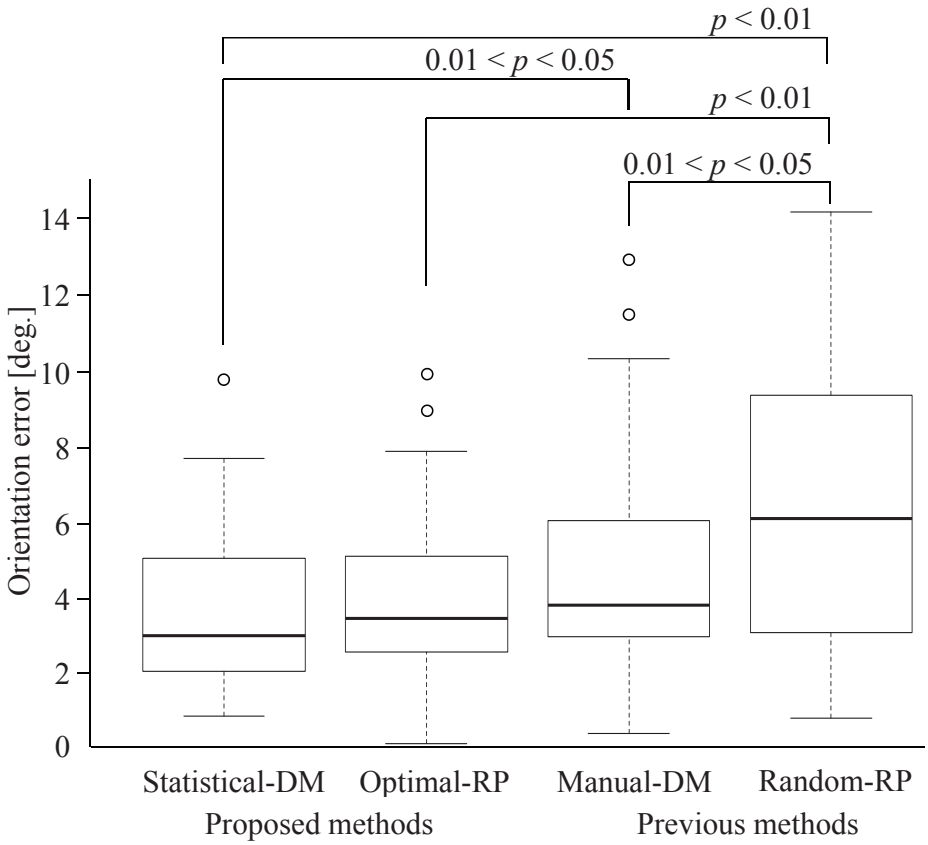

(a) Orientation error.

Figure 3.9: Boxplots of orientation errors and results of paired t-test. In each box, sample minimum, lower quartile (Q1), median (Q2), upper quartile (Q3), and sample maximum are indicated. Sample minimum and sample maximum are minimum and maximum values after rejection of outliers. Values larger than $(Q3 - Q1) \times 1.5 + Q3$ or smaller than $Q1 - (Q3 - Q1) \times 1.5$ are regarded as outliers. Orientation error. Average error was 3.5 deg. in *Statistical-DM*, 3.9 deg. in *Optimal-RP*, 4.7 deg. in *Manual-DM*, and 6.3 deg. in *Random-RP*.

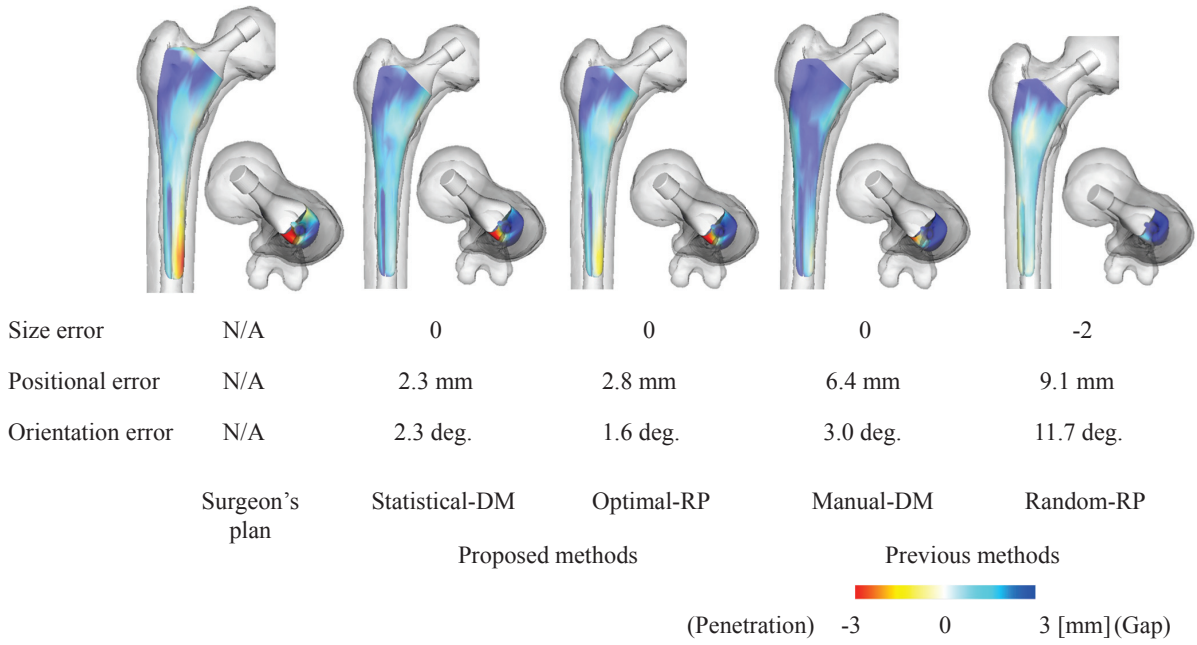

Figure 3.10: Illustrative examples of planning results (Case 1).

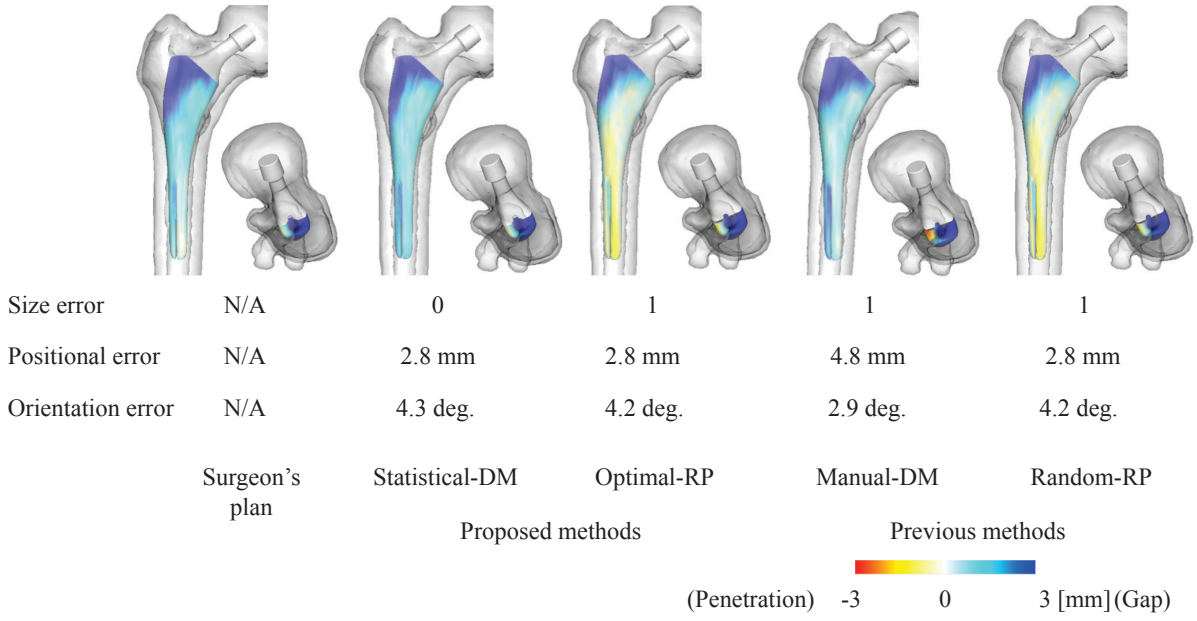

Figure 3.11: Illustrative examples of planning results (Case 2).

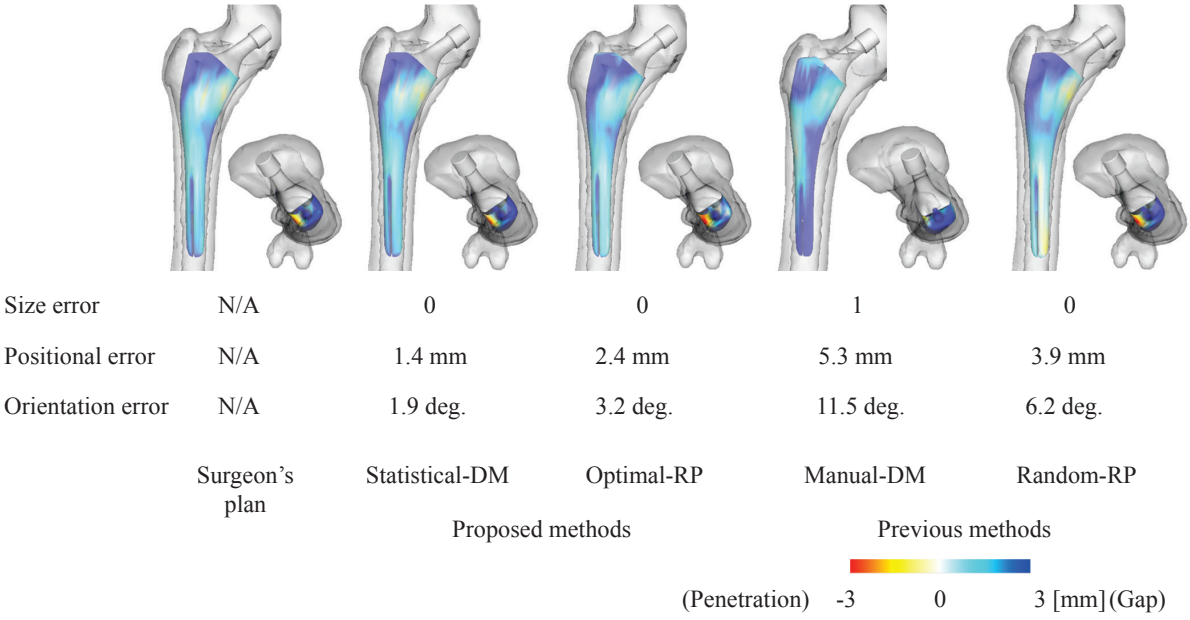

Figure 3.12: Illustrative examples of planning results (Case 3).

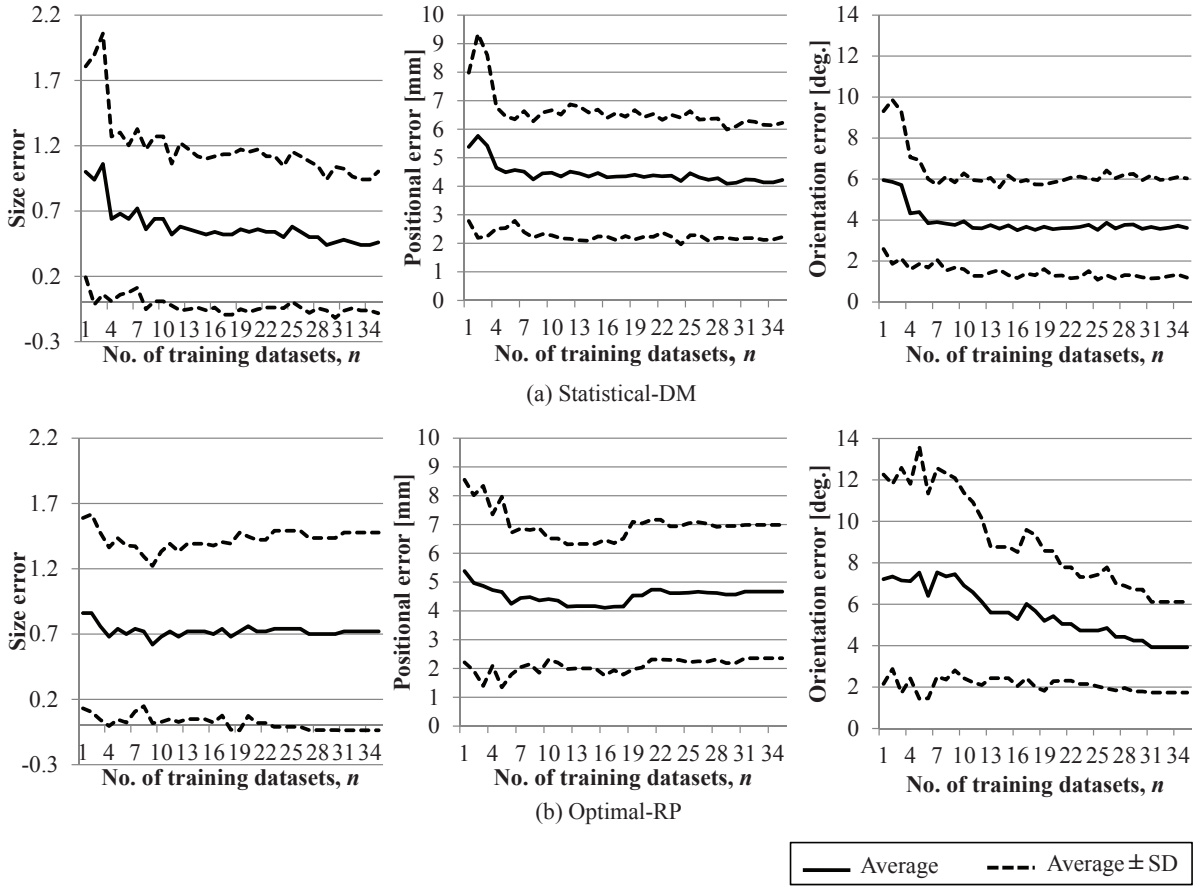

Figure 3.13: Effects of number of training datasets, n, on errors of automated planning. Left: Size error. Middle: Positional error. Right: Orientation error. (a) Statistical-DM. (b) Optimal-RP.

Chapter 4

Atlas-based approach and validation for automated pelvic implant (cup) planning

Abstract

Intraoperative robotic and computer-guided assistances are now commonly used in total hip arthroplasty (THA) for accurate execution of the preoperative plan. Although the preoperative plan to be accurately executed is critical, it is still interactively prepared in a time-consuming and subjective manner. In this paper, atlas-based approach to automated surgical planning of the acetabular cup in THA is described to stabilize its quality as well as reduce its time-consuming nature. Surgeon's expertise is embedded in two types of statistical atlases, which are constructed from training datasets of CT-based 3D plans prepared by experienced surgeons. One is a statistical shape model which encodes global spatial relationships between the patient anatomy and implant. The other is the statistical map of residual bone thickness on the implant surface, which encodes local spatial constraints of the anatomy and implant. Given the 3D pelvis shape of the patient, the author formulates a procedure to determine the best size and position of the acetabular cup which satisfy the constraints derived from the two statistical atlases. The author validated the proposed planning method by retrospective study using the datasets which were actually used in the THA surgery.

4.1 Introduction

Surgical CAD/CAM is one of common frameworks for computer assisted surgery [1], especially, in orthopedic application. The CAM systems, that involve intraoperative robotic and computer-guided assistance, ensure accurate execution of preoperative plans constructed using the CAD systems. In its ultimate form, the surgery can be regarded as virtually completed once preoperative planning is completed. Therefore, the quality of preoperative planning is becoming more critical than ever in this framework [6][13]. Our aim is to automate preoperative planning for total hip arthroplasty (THA) in order to stabilize its quality as well as reduce its time-consuming nature.

Nowadays, navigated THA is routinely used in many hospitals. Especially, for patients with osteoarthritis of the hip caused by congenital hip dysplasia, CT-based 3D preoperative planning is effective due to large deformation of the hip joint. A large number of the 3D preoperative plans prepared by well-experienced surgeons have been accumulated in some of the hospitals. The feedback of these past planning datasets can be utilized for the future planning. Closed-loop surgery to make the best use of past surgical data for future surgery is a recently emerged framework [23]. Atlas-based approach is well-fit to this framework and has been applied to the femoral stem planning [22][50]. One of the simplest forms of such approach is to use one standard 3D plan constructed on CT data as a template [22]. The spatial relations between host bone (femur) and implant (femoral stem) in the template are mapped to each patient by scaled rigid registration between the patient and template. However, the template based on only one dataset is insufficient to deal with inter-patient shape variations. More recently, the statistical map of bone-implant distance on implant surface was generated from a large number of 3D plans to automate femoral stem planning [50].

In this paper, the author develops an atlas-based approach to automated acetabular cup planning. Unlike femoral stem planning, the expertise of cup planning involves more global relations between implant and patient anatomy. Therefore, the author represents statistically-derived constraints of bone-implant relations not only as the form of a statistical map on implant surface but also as a statistical shape model [67] to describe global relations. The author formulates a method for hybrid use of the two statistical atlases to automate cup planning, and evaluate it using planning datasets actually used in navigated THA in comparison with a previous automated cup planning method [68] based on user-specified constraints.

4.2 Methods

4.2.1 Overview

Figure 4.1 shows typical cup planning examples. The position and size of the acetabular cup should be basically determined so as to recover the original anatomy of the acetabulum. Although it is not so difficult to predict the original anatomy for a mildly diseased case (Fig. 4.1(a)), it is somewhat difficult for a severely diseased case due to its large deformation and shift (Fig. 4.1(b)). In both cases, cup size and position should be carefully refined so that residual bone thickness is sufficient on the implant cup surface and no penetration occurs.

Two types of statistical atlases are constructed from a sufficient number of cup plans on CT data prepared by experienced surgeons. One is a combined pelvis and cup statistical shape model (PC-SSM) to roughly predict the cup shape recovering the original anatomy based on global pelvic anatomy [69]. The other is the statistical map of (residual) bone thickness (SM-BT) on the cup surface for subsequent refinement of the cup size and position so as to ensure sufficient residual bone thickness for the host bone which was originally developed to describe the statistical map of bone-implant distance for femoral stem planning [50].

In the proposed automated cup planning, given the pelvis surface model segmented from CT data, the cup position and size are estimated. The cup is modeled as a hemisphere and its diameter and center are regarded as the cup size and position, respectively. The final cup size is determined by selecting the size closest to the estimated diameter among available discrete cup sizes. Because a medical doctor in the research group includes the author determines cup orientation based on femoralanteversion, the author does not address its determination in this paper where only the pelvis is considered.

4.2.2 Construction of planning atlases

The author assumes that N training datasets of cup planning are given. Let P_i and C_i be the 3D shape models of the pelvis and the cup model planned on P_i, respectively, where $i = 1, \cdots, N$. Inter-patient nonrigid registration of P_i and C_i is performed using a point based method. Let $\mathbf{p}_i$ and $\mathbf{c}_i$ be the sets of vertex's position of P_i and C_i, respectively. Then, the author concatenates $\mathbf{p}_i$ and $\mathbf{c}_i$ to obtain the combined pelvis and cup pointset $\mathbf{q}_i$. The combined pelvis and cup statistical shape model (PC-SSM)

is obtained by performing principal component analysis of $\mathbf{q}_i$. PC-SSM $\mathbf{q}$ is defined as

$$\mathbf{q}(\mathbf{b}) = \bar{\mathbf{q}} + \Phi\mathbf{b}, \quad \bar{\mathbf{q}} = \begin{bmatrix} \bar{\mathbf{p}} \\ \\ \bar{\mathbf{c}} \end{bmatrix}, \tag{4.1}$$

where $\bar{\mathbf{q}}$, Φ, and $\mathbf{b}$ are the mean shape vector, the eigenvector matrix, and the shape parameter vector, respectively. $\bar{\mathbf{q}}$ consists of the mean shape vectors of the pelvis and the cup, $\bar{\mathbf{p}}$ and $\bar{\mathbf{c}}$, respectively.

The statistical map of bone thickness (SM-BT) is defined as the distributions of the mean and standard deviation of the residual bone thickness on the cup surface. The residual bone thickness is defined as the remaining thickness of bone tissue when the bone is removed for cup placement. The residual bone thickness is calculated on each cup vertex along each normal direction. If the bone thickness is equal to or smaller than zero, it means that penetration of the cup through the bone occurs. Since the cup surface is not fully covered with the pelvic bone, the target area of SM-BT is defined as the area which are covered with the pelvic bone in 95% cases of the training datasets. Let $\mathbf{v}_{ij}$ be the j-th vertex's position of the cup surface of the i-th training dataset. Let $d(\mathbf{v}_{ij}, P_i)$ be the bone thickness at $\mathbf{v}_{ij}$. If the point $\mathbf{v}_{ij}$ is not covered with the pelvic bone P_i, the bone thickness is not calculated. The distributions of the mean and standard deviation of the bone thickness on the cup surface, U and S, are obtained by the method described in [3] and defined as

$$U = \{\mu_j | \mu_j = \frac{1}{N}\sum_{i=1}^{N} d(\mathbf{v}_{ij}, P_i), \ \ \mathbf{v}_{ij} \in C_i\}, \tag{4.2}$$

$$S = \{\sigma_j | \sigma_j = \sqrt{\frac{1}{N}\sum_{i=1}^{N} (d(\mathbf{v}_{ij}, P_i) - \mu_i)^2}, \ \ \mathbf{v}_{ij} \in C_i\}, \tag{4.3}$$

where μ_j and σ_j represent the mean and standard deviation of the bone thickness at the point $\mathbf{v}_j$, respectively.

4.2.3 Optimization procedure

Two-step optimization is performed for automated cup planning. Let P_a be the patient's 3D pelvis surface model on which the cup is placed. The cup position $\mathbf{t}$ and size s are initially determined by fitting the pelvis part of PC-SSM to P_a, and then they are refined by using SM-BT. When specific parameter $\mathbf{b}$ is given to PC-SSM $\mathbf{q}(\mathbf{b})$ in Eq. (4.1), the pelvis shape $\mathbf{p}(\mathbf{b})$ and the cup shape $\mathbf{c}(\mathbf{b})$ are given by $\bar{\mathbf{p}} + \Phi_{\mathbf{p}}\mathbf{b}$ and $\bar{\mathbf{c}} + \Phi_{\mathbf{c}}\mathbf{b}$, respectively, where $\Phi_{\mathbf{p}}$ and $\Phi_{\mathbf{c}}$ are the submatrices of Φ which correspond to pelvis and cup vertices, respectively. Let the number of vertices of $\mathbf{p}(\mathbf{b})$ and $\mathbf{c}(\mathbf{b})$ be

n and m, respectively. The fitting process of PC-SSM is performed by obtaining $\mathbf{b}$ which minimizes the cost function C_D defined as

$$C_D(\mathbf{b}; \mathbf{p}(\mathbf{b}), P_a) = \sum_{j=1}^{n} d(\mathbf{w}_j(\mathbf{b}), P_a)^2, \tag{4.4}$$

where $\mathbf{w}_j(\mathbf{b})$ and $d(\mathbf{w}_j(\mathbf{b}), P_a)$ are the j-th vertex's position of $\mathbf{p}(\mathbf{b})$ and the shortest distance from $\mathbf{w}_j(\mathbf{b})$ to P_a, respectively. Let $\mathbf{b}_a$ be the shape parameter vector minimizing Eq. (4.4). The author uses Levenberg-Marquardt method for the minimization. Then, initial cup position $\mathbf{t}_a$ and size s_a are determined by fitting a parametric hemisphere model to $\mathbf{c}(\mathbf{b}_a)$. Let $\mathbf{c}'(\mathbf{t}, s)$ be the sets of vertex's position of the parametric hemisphere model which position is $\mathbf{t}$ and size is s.

In the subsequent refinement using SM-BT, the author minimizes the cost function $f(\mathbf{t}, s)$ defined as

$$f(\mathbf{t}, s) = \lambda_1(s - s_a)^2 + \lambda_2(\mathbf{t} - \mathbf{t}_a)^2 + \lambda_3 \frac{1}{m} \sum_{j=1}^{m} \frac{1}{\sigma_j^2} (d(\mathbf{v}'_j(\mathbf{t}, s), P_a) - \mu_i)^2, \tag{4.5}$$

where $\mathbf{v}'_j(\mathbf{t}, s)$ is the j-th vertex's position of $\mathbf{c}'(\mathbf{t}, s)$. The first and second terms ensure that the size and position estimated using PC-SSM should not be far from the initial size and position. The third term ensures that the distribution of the bone thickness on the ongoing cup becomes close to SM-BT. λ_1, λ_2, and λ_3 are the weight parameters balancing the three terms. For the hybrid use of the two atlases, $\lambda_1 = 1.0$, $\lambda_2 = 1.0$, $\lambda_3 = 10.0$ were used while $\lambda_1 = 1.0$, $\lambda_2 = 1.0$, $\lambda_3 = 0.0$ or $\lambda_1 = 0.0$, $\lambda_2 = 0.0$, $\lambda_3 = 1.0$ were used when either atlas was utilized.

4.3 Experimental Results

4.3.1 Experimental conditions

The author compared the proposed method with the previous method described in [68], which is the only one existing method for automated cup planning in 3D to the author's knowledge. In order to investigate effects of the atlases, the author tested the method under three conditions, that is, only PC-SSM, only SM-BT, and the hybrid use of PC-SSM and SM-BT. CT slice thickness and reconstruction pitch were 2 mm. Field of view was 360 mm. The pelvis surface was segmented with the atlas-based automated segmentation method described in [70]. The available cup size variation was 11 sizes from 40 mm to 60 mm. The 3D surface models of pelvis and cups consisted of 3,000 and 353

vertices, respectively. 28 patient datasets including 3D pelvis models and preoperative plans were used for construction of atlases and evaluations. The preoperative plans used for atlas construction and evaluation were made by the experienced surgeons using a commercially available planning system, Stryker CT-Hip System (Stryker Leibinger GmbH, Freiburg, Germany), and applied to the actual navigated THA surgery. The author used the first 10 principal components in PC-SSM fitting to avoid over-fitting [69].

Evaluation was performed by leave-one-out cross validation. Evaluation measures were cup position error, cup size error and the number of cases when the penetration occurred. Error was defined as the difference between the surgeon's and estimated results.

4.3.2 Results

The constructed PC-SSM and SM-BT are shown in Fig. 4.2 and Fig. 4.3, respectively. Fig. 4.2 shows the mean and variations of PC-SSM. Fig. 4.3(a) shows the evaluation area for SM-BT construction. Fig. 4.3(b) and (c) show the distribution of the mean and standard deviation of the bone thickness, respectively. Table. 4.1 shows a summary of the evaluation results. It shows the number of cases when the penetration of the cup occurred, mean positional error, and mean size error. With the previous method, there was no cup penetration, but the mean positional error was the largest among the four conditions, which was 4.3 mm. With the PC-SSM only, the size error was 1.5 mm, which was smaller than the previous method. On the other hand, cup penetration occurred in four cases. With the SM-BT only, the number of cases of penetration was reduced, but the size error was 2.4 mm which was the largest among the four conditions. With the hybrid use of PC-SSM and SM-BT, both positional and size errors were the smallest among the four conditions, which were 3.9 mm and 1.4 mm, respectively. Additionally, only one penetration occurred.

Figure 4.4 shows the planning results of a typical case. With the PC-SSM only, the cup size was same as the surgeon's selection, but there was cup penetration. With the SM-BT only, positional error was the smallest, but larger size was selected. Additionally, there was penetration. On the other hand, with the hybrid use of PC-SSM and SM-BT, the positional and size error was smaller than that of PC-SSM only. Further, there was no penetration.

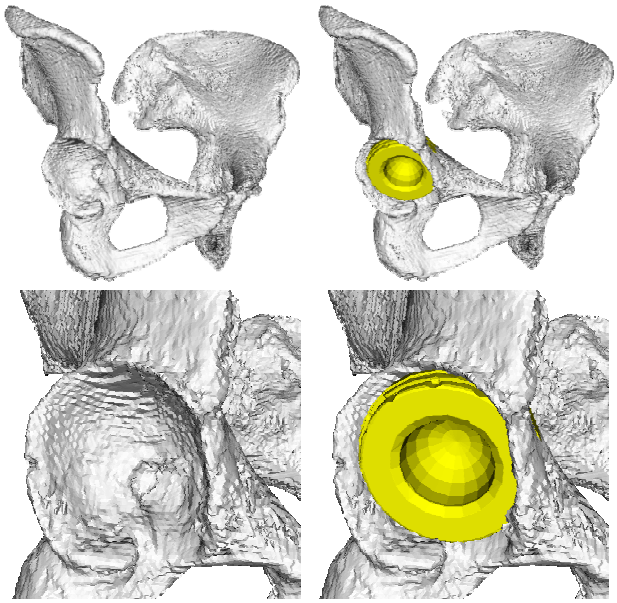

(a) Mildly diseased case.

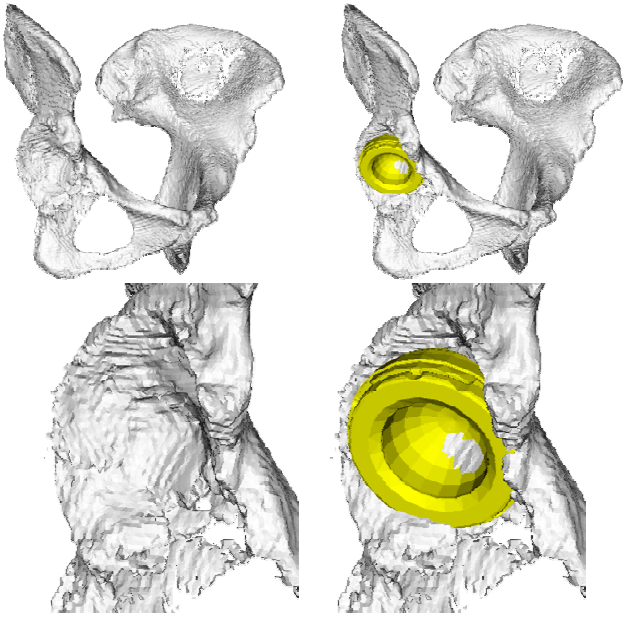

(b) Severely diseased case.

Figure 4.1: Cup planning for mildly and severely diseased pelvises. Cup planning was performed by an experienced surgeon. Left column: Pelvis model. Right column: Cup planning on pelvis model.

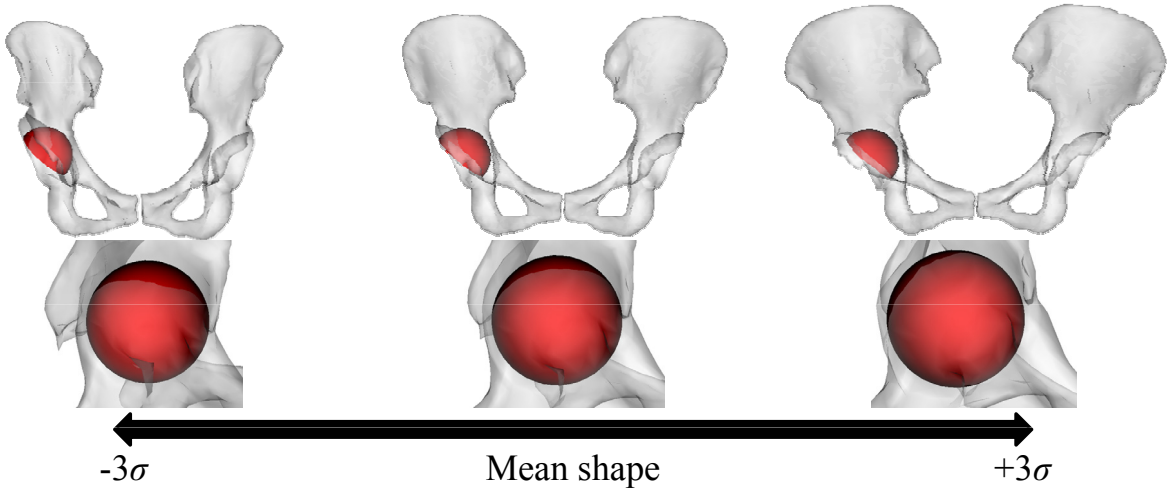

Figure 4.2: Shape variations of combined pelvis and cup statistical shape model (PC-SSM). The first mode is shown.

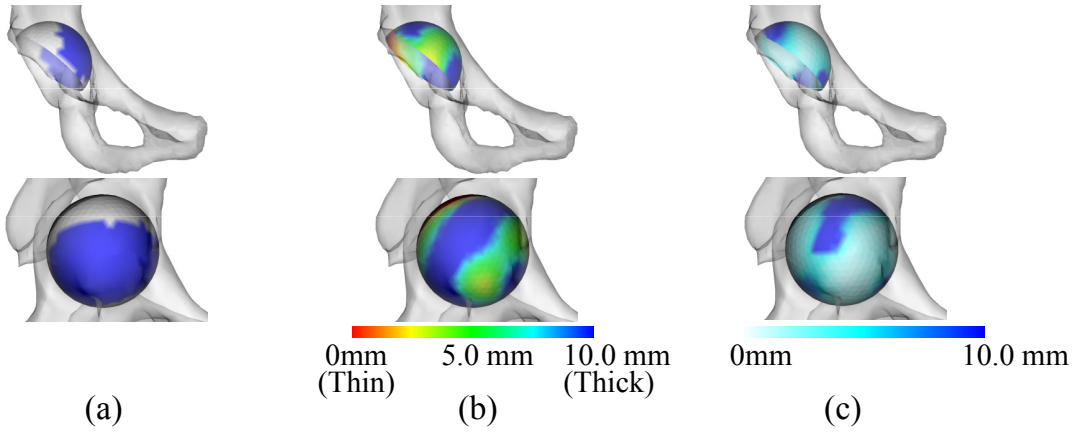

Figure 4.3: Statistical map of residual bone thickness (SM-BT). (a) Blue area indicates the cup coverage over 95 % of datasets. (b) Distribution of mean bone thickness. (c) Distribution of standard deviation of bone thickness. Color bars at bottom of each figure represent the residual bone thickness.

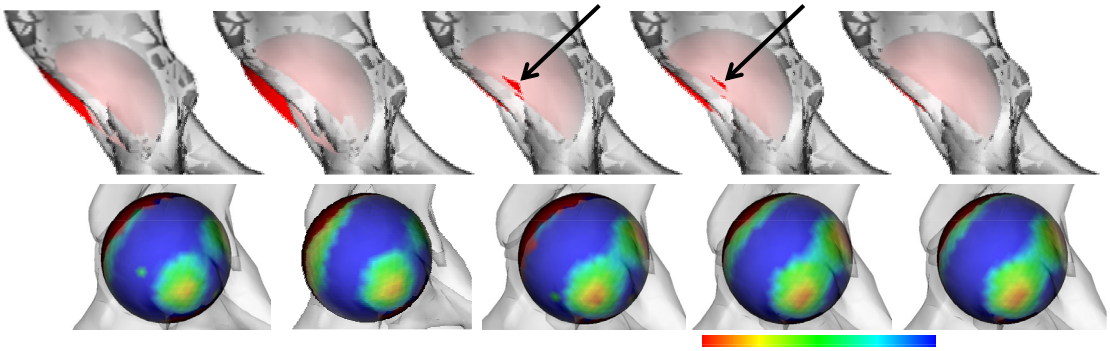

Penetration	No	No	Yes	Yes	No
Positional error	N/A	2.7 mm	3.5 mm	2.5 mm	2.9 mm
Size error	N/A	2 mm	0 mm	2 mm	0 mm
	(a)	(b)	(c)	(d)	(e)

Figure 4.4: Illustrative case of experimental results. (a) Surgeon's plan. (b) Previous method. (c) PC-SSM only. (d) SM-BT only. (e) Hybrid use of PC-SSM and SM-BT. Values below each figure indicate penetration occurred or not (top), positional error [mm] (middle), and size error [mm] (bottom), respectively. Arrows indicate the areas where penetration occurred. Colors on cup surface indicate bone thickness distribution.

Table 4.1: Evaluation results of automated planning.

	Previous	PC-SSM only	SM-BT only	Hybrid use of PC-SSM and SM-BT
Number of cup penetration	0	4	1	1
Mean positional error [mm]	4.3	4.2	4.0	3.9
Mean size error [mm]	2.1	1.5	2.4	1.4

4.4 Discussion and Conclusion

The author proposed a method for hybrid use of the two atlases to automate 3D planning for acetabular cup placement in THA. One is a combined pelvis and cup statistical shape model (PC-SSM) which encodes global spatial relationships between the patient anatomy and implant. The other is a statistical map of residual bone thickness (SM-BT) which encodes local spatial constraints of the anatomy and implant. The proposed method could provide a framework for learning and modeling the planning policy of the surgeon because the two atlases are constructed from training datasets of experienced surgeons. It involves few manual parameter tuning while the previous method has many parameters. According to the experimental results, mean errors in size and position were better for the hybrid use of PC-SSM and SM-BT than the previous method (Table. 4.1). It would be arguable that this improvements is clinically significant or not. Currently, the author has already had some preliminary results to evaluate clinical significance, that is, comparison with inter-surgeon difference. The mean inter-surgeon difference for eight cases was 1.3 mm in size while the mean differences from a surgeon of the proposed and the previous methods were 1.5 mm and 2.0 mm, respectively. These results may show some implication on clinical significance. The author will evaluate the statistical significance of these results as future work.

In the previous method, there was no penetration since it explicitly prohibited the penetration. However, cup penetration occurred in four cases when only PC-SSM was used. The author considers this is because the variation of PC-SSM described by the training datasets is insufficient for fitting of severely diseased cases. On the other hand, with the hybrid use of PC-SSM and SM-BT, the number

of cases of penetration was reduced. The author considers that this is because the cup size and position were determined so as to minimize the difference between the resulting bone thickness and SM-BT which had no penetration. However, the current atlas could not prohibit all of the penetrations completely. The constraint which explicitly prohibits penetrations could be introduced to overcome the problem.

In principle, given a sufficient number of planning datasets that a surgeon planned, the method is applicable to various implants for different bones. As future work, the author is planning to apply the method to the femoral stem.

Chapter 5

Applying atlas-based automated cup planning to standard 2D X-ray image

Abstract

In total hip arthroplasty (THA), intraoperative assistance systems such as computer navigation and surgical robotics have been developed. To input an appropriate preoperative plan to these systems, a 3D-CT based automated preoperative planning method has been proposed. However, the usefulness of this method is limited because preoperative acquisition of 3D-CT images is not available for THA in most hospitals. The aim of this study is to perform 3D automated planning from single standard X-ray radiograph. In this study, the author targets an acetabular component (cup). To achieve the objective, the author integrates a statistical reconstruction method of 3D pelvis shape from a standard X-ray radiograph and a 3D-CT based automated preoperative planning method which have been previously proposed. As evaluation, the author applied the method to six mildly diseased pelvises. Compared to the pelvis shape reconstructed from 3D-CT images, the average reconstruction error was 1.8 mm. Compared to the experienced surgeons' plans, the size and positional errors of cup planning were 1.2 $\pm$0.8, 4.4$\pm$0.7 mm for standard X-ray radiograph, respectively, and 0.5$\pm$0.5, 3.6$\pm$1.8 mm for 3D-CT images, respectively. Because the accuracies of the cup size and position were about same, the proposed method would be useful. However, the errors of 3D pelvis reconstruction from a standard X-ray radiograph caused large cup size errors in some cases. To improve the method, the proposal of an improved method which acquires two X-ray radiographs from different direction would be useful.

5.1 Introduction

In total hip arthroplasty (THA), intraoperative assistance systems such as computer navigation and surgical robotics have been developed. These systems require 3D CT images and 3D preoperative plan. To construct appropriate 3D preoperative plans, usefulness of computer-assisted interactive preoperative planning systems have been confirmed [14]. More recently, an automated preoperative planning method has been proposed [51]. However, preoperative acquisition of 3D CT images is not available for THA in most hospitals. Therefore, usefulness of 3D preoperative planning and intraoperative assistance is limited.

The aim of this study is to perform 3D automated planning from single standard X-ray radiograph. In this study, the author targets an acetabular component (cup). Although one 2D semi-automated method exists from an X-ray radiograph for femoral component (stem) [71], there are no methods which determine 3D cup plan to the author's best knowledge. In this study, the author utilizes a reconstruction method of 3D pelvis surface proposed by Zheng et al. [72]. The author validates the proposed method by comparing errors of shape reconstruction and cup planning.

5.2 Methods

Figure 5.1 shows schematic diagram of the present approach. Given the standard X-ray radiograph of the patient and the training datasets, the 3D anatomy of the patient's pelvis is extracted using an atlas-based 2D-3D reconstruction. The 3D anatomy consists of 3D shape model, anatomical landmarks, and coordinate system. The training datasets in this process are 3D pelvis surface models segmented from 3D-CT images. After 2D-3D reconstruction, given the 3D anatomy, training datasets, and the implant database, an atlas-based automated planning is performed. The training datasets in this process are merger of 3D pelvis surface model and cup planning result prepared by experienced surgeons. After automated planning, the proper size, position and angle are determined.

34 cases were used as training datasets and six cases were used for evaluation. The evaluation data was excluded from training datasets. In all evaluation cases, the Crowe's classification [73] was class I. Each dataset consisted of a standard X-ray radiograph and 3D CT images of the hip and a preoperative plan. Source-image distance of the X-ray radiograph was 1,200 mm and pixel size was 0.1×0.1 mm^2. Voxel size of 3D CT images was $0.7 \times 0.7 \times 2.0$ mm^3 and field of view was 360

$\times$ 360 mm^2. The preoperative plan was constructed by experienced surgeons using a commercially available planning system, Stryker CT-Hip System (Stryker Leibinger GmbH, Freiburg, Germany), and executed in the actual navigated THA surgery at Osaka University Hospital.

Figure 5.2 shows overview the 2D-3D reconstruction of pelvis and the automated planning used in the proposed method. The procedure of the proposed method was as follows:

1. Given the standard X-ray radiograph of the patient's hip, vertices of pelvis's boundaries were estimated.

2. Using estimated boundaries, the 3D pelvis shape model was constructed by fitting the statistical shape model (SSM) of pelvis.

3. Using the pelvis surface model, cup size and position were determined.

In this procedure, step one and two were correspond to Zheng's method [72] and step three was correspond to Otomaru's method [51]. Because the cup orientation was determined based on the femoral anteversion angle in surgeons' planning, the author did not evaluate it.

In the original reconstruction method [72], a scaling parameter of pelvis shape is estimated using a calibration marker. To prevent the effect of scaling parameter estimation on cup planning result, the author assumed that the scaling parameter was known in this study. For evaluation, the author prepared reference data of 3D pelvis shape and cup plan. The reference 3D pelvis shape was extracted from 3D CT images using an automated segmentation proposed by Yokota et al. [53]. The reference cup plan was obtained using Otomaru's method [51] from the reference 3D pelvis shape.

5.3 Results

Table 5.1 shows the reconstruction error of the pelvis shape and the errors of cup planning. The reconstruction error of the pelvis shape is defined as average and standard deviation of distances between each vertices of the reconstructed pelvis shape and the reference pelvis shape. Minimum average reconstruction error was 1.5 mm and maximum reconstruction error was 2.2 mm. Size and positional errors of cup planning were defined as the difference between automated planning result and the surgeons' plan. Average and standard deviation of cup size were 1.2 ± 0.5 for standard X-ray radiograph and 0.5 ± 0.5 for 3D-CT images, respectively. Average and standard deviation of cup size

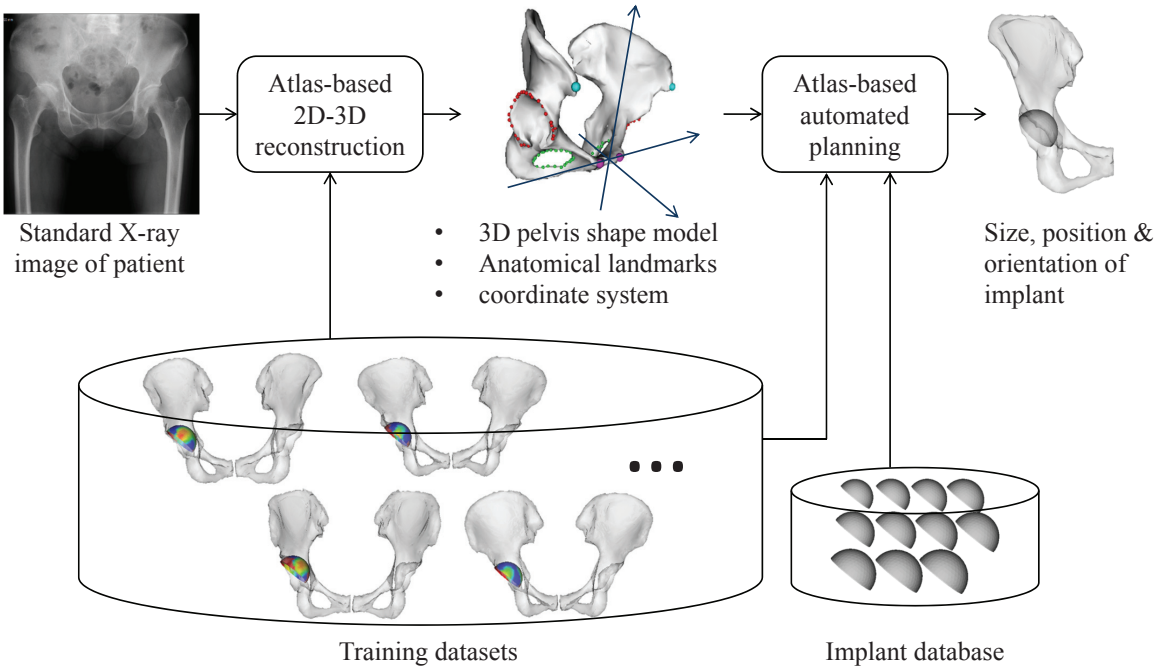

Figure 5.1: Schematic diagram of present approach.

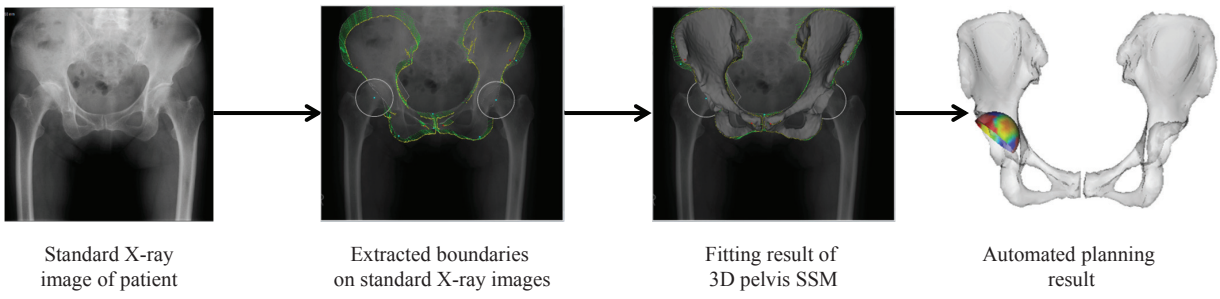

Figure 5.2: Overview of 2D-3D reconstruction of pelvis and automated cup planning.

Table 5.1: Reconstruction error and error of cup planning result of each case.

	Reconstruction error [mm]		Selected Size		Positional error [mm]	
	Average	SD	Standard X-ray radiograph	3D-CT images	Standard X-ray radiograph	3D-CT images
Case 1	1.8	1.4	2.0	1.0	4.5	3.0
Case 2	2.2	1.7	1.0	0.0	3.8	2.2
Case 3	1.6	1.3	1.0	1.0	3.6	1.7
Case 4	1.8	1.5	0.0	1.0	5.1	6.3
Case 5	1.7	1.3	2.0	0.0	4.4	5.2
Case 6	1.5	1.2	1.0	0.0	5.2	3.5
Average			1.2	0.5	4.4	3.6
SD			0.8	0.5	0.7	1.8

were 4.4 ± 0.7 mm for standard X-ray radiograph and 3.6 ± 1.8 mm for 3D-CT images, respectively. Considering the standard deviation of each result, the errors of the X-ray radiograph and the errors of the 3D CT images were about same.

Figure 5.3 shows the results whose cup size error for standard X-ray radiograph was same as that of 3D-CT images. With regards to the reconstruction accuracy of the acetabulum region from the standard X-ray radiograph, the reconstruction results were appropriate (fig. 5.3(c)). With regards to the cup planning results, both standard X-ray radiograph and 3D-CT images were about same as surgeons' plans (fig. 5.3(d)). Fig. 5.4 shows the results whose cup size error for standard X-ray radiograph was larger than that of 3D-CT images. With regards to the reconstruction accuracy of the acetabulum region from the standard X-ray radiograph, the shape errors were large in the regions which arrows indicate in fig. 5.4(c). With regards to the cup planning results, although both standard X-ray radiograph and 3D-CT images positioned cup in same position as the surgeon's plan, the cup size error for standard X-ray radiograph was large (fig. 5.4(d)).

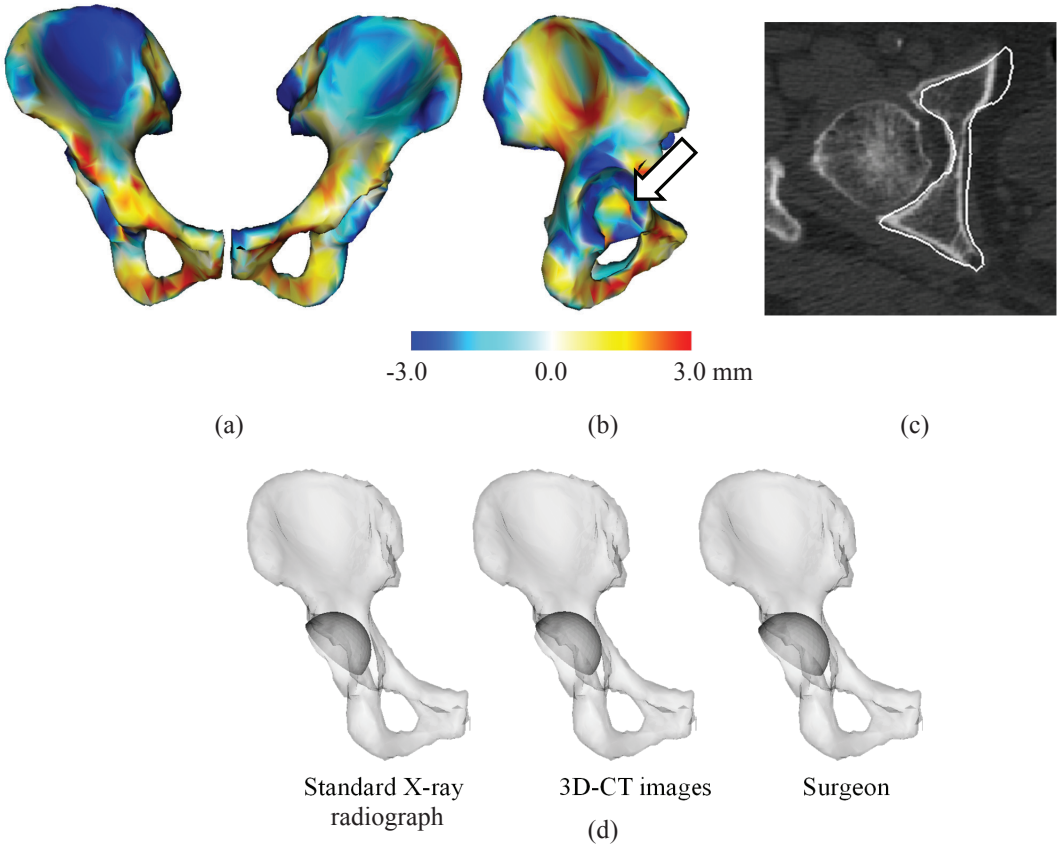

Figure 5.3: Result of 2D-3D reconstruction and automated cup planning of case 3. (a) and (b) show reconstruction errors on 3D pelvis surface. Error values are indicated by color bar. (c) show results of 3D pelvis reconstruction around acetabulum region. White line indicates boundaries of reconstructed surface. (d) shows results of cup planning of each method.

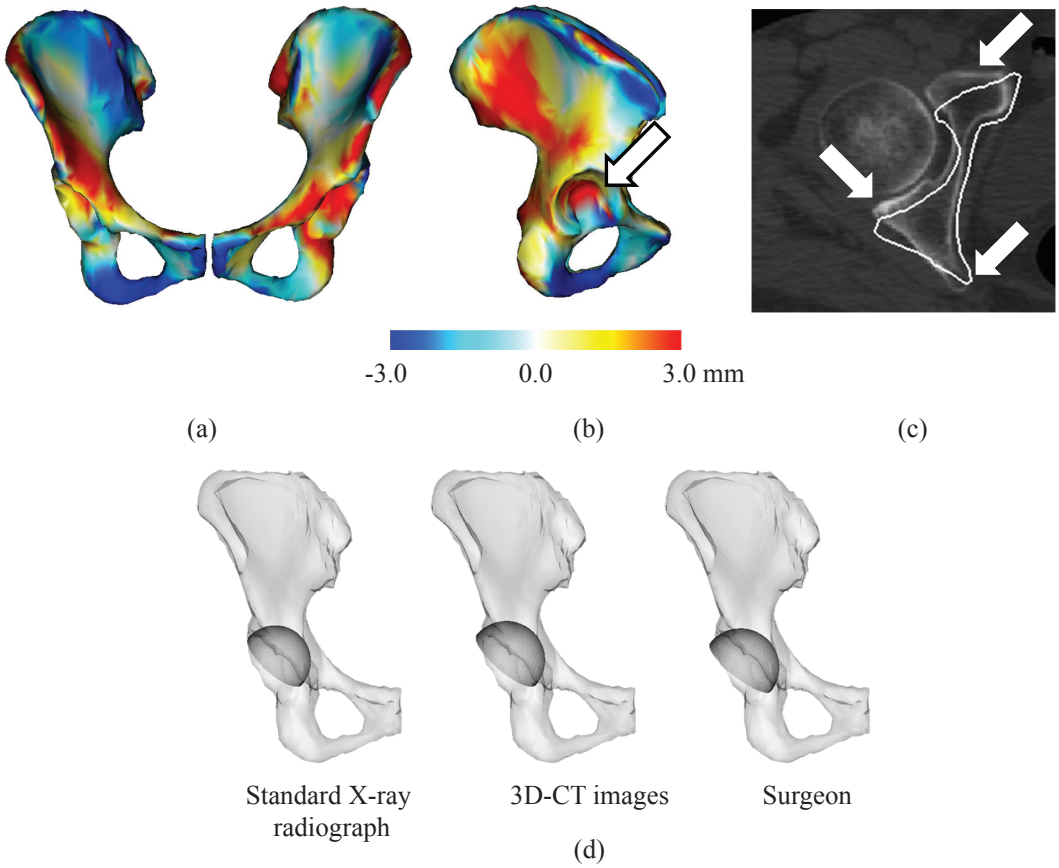

Figure 5.4: Result of 2D-3D reconstruction and automated cup planning of case 5. (a) and (b) show reconstruction errors on 3D pelvis surface. Error values are indicated by color bar. (c) show results of 3D pelvis reconstruction around acetabulum region. White line indicates boundaries of reconstructed surface. (d) shows results of cup planning of each method.

5.4 Discussions and Conclusion

In this study, the author performed an automated 3D cup planning for standard X-ray radiograph using 3D pelvis reconstruction proposed by Zheng et al. [72] and the automated 3D planning proposed by Otomaru et al. [51]. According to the results, the cup size error and positional error were about same as the plans determined using 3D CT images. Therefore, the author considers the proposed method would be useful. Pelvis shape reconstruction was good for the whole pelvis shape. On the other hand, there were shape errors along anterior-posterior direction in acetabular regions in some cases. The author considers that this is the reason of the error of the cup size and position. To solve this problem, the proposal of an improved method which acquires two X-ray radiographs from different direction would be useful.

Current limitations of this study are as follows:

1. The author only targeted mildly diseased cases whose Crowe's classification was class I.

2. The author assumed that the scaling parameter in the pelvis shape reconstruction was known.

The author considers the effect of scale estimation on cup planning would be important. According to the author's preliminary experiment, cup size did not change when scaling parameter changed 5 % larger and smaller from the correct value. As future work, the author will apply the proposed method to severely deformed cases whose Crowe's classification will be more than 1. Additionally, the author will firstly validate the proposed method when the scaling parameter will be misestimated. Then, the author will use a calibration marker under the condition that the scaling parameter will be completely unknown.

Chapter 6

Atlas-based optimization of hip joint function

Abstract

In computer aided surgery (CAS), intraoperative assistance such as surgical navigation systems and robotic systems have been developed. Because these systems ensure accurate execution of preoperative plans, the quality of preoperative planning is becoming more critical than ever. Our aim is to automate preoperative planning for total hip arthroplasy (THA). In THA, a pathologically deformed hip joint is replaced by an artificial hip joint. The artificial hip joint consists of pelvic implant (cup) and femoral implant (stem). The preoperative planning for THA is defined as determinations of size (one parameter), 3D position (three parameters), and 3D angle (three parameters) for cup and stem, respectively. In previous work, the research group including the author proposed Statistical Implant Plan Atlas (SIMPLA)-based automated pre-operative planning method for each implant (cup and stem). The SIMPLA is constructed by performing a statistical analysis of a number of preoperative plans prepared by experienced surgeons. In this paper, the author describes a method for finding an optimal combination of the pelvic side planning and femoral side planning. As a first step, the author extracts combined planning candidates which are fulfill the restrictions defined statistically with surgeon's plans. As a second step, the planning optimization is performed by maximization of scores calculated by an evaluation function which adds up normalized parameter of criteria of hip joint function. In clinical field, cup coverage ratio, leg length discrepancy (LLD), and range-of-motion (ROM) are used for the evaluation of hip joint function. To evaluate the proposed method, the author compared the scores and parameters of hip joint function criteria between the plans of the proposed methods and surgeon's. As the results of our methods showed better or similar scores and parameters compared to surgeon's plans, the proposed methods would be useful.

6.1 Introduction

In computer aided surgery (CAS), intra-operative assistance such as surgical navigation systems and robotic systems for implant replacement of pathologically deformed hip joint have been developed [74, 13, 75]. Because these systems ensure accurate execution of pre-operative planning, the quality of pre-operative planning is becoming more critical than ever. For total hip arthroplasty (THA), pelvic side implant (cup) and femoral side implant (stem) are used as alternative of native hip joint. On computer assisted pre-operative planning systems, surgeons determined the size (one parameter) and 3D positions (three parameters), and 3D angles (three parameters) for each implants with considering various evaluation criteria which indicates the implant compatibility and hip joint function. As some of the criteria has trade-off relationships, finding the best-balanced solution often become time-consuming tasks for surgeons. Therefore automatic optimization of 3D surgical planning is highly desirable.

In the previous works of the research group including the author, automated preoperative planning methods for pelvic implant (cup) and femoral implant (stem) based on surgeon's expertise are reported. These methods optimize the user-defined objective functions or search for a solution which maximizes one of the compatibility criteria by exhaustive search [68, 40]. Even though planning of cup and stem are optimized independently, it is difficult to perform the parameter tuning because of existence of various types of bone deformations and the balances between the criteria. In order to solve the problem, the author has started to propose the Statistical Implant Plan Atlas (SIMPLA)-based automated pre-operative planning methods. The SIMPLA is constructed by performing a statistical analysis of a number of preoperative plans prepared by experienced surgeons. The author already have developed SIMPLA for pelvic implant (cup) and femoral implant (stem) which are inserted into host bone for implant fixation [51, 52].

In this paper, the author describes a method for finding an optimal combination of the pelvic side planning and femoral side planning. As far as the author knows, there are no reports of automated optimization methods of pre-operative planning of the combined implants except ours. The optimization is performed by maximization of a score calculated by an evaluation function which adds up normalized parameter of criteria of hip joint function. As SIMPLA for pelvic implant (cup) often generates so many planning candidates, it is needed to reduce the combined planning candidates

with restrictions which are also statistically determined with surgeon's plans. For criteria of implant compatibility and hip joint function, cup coverage ratio, leg length discrepancy (LLD), and range-of-motion (ROM) are used. As an optimal solution, the size, 3D position, 3D angle, and parameters of criteria of cup and stem are recorded. To evaluate the proposed method, the author compared the scores and parameters of hip joint function criteria between the plans of the proposed methods and surgeon's.

6.2 Methods

The author assume that candidates of pelvic side planning and femoral side planning which include the size, 3D positions, 3D angles of each implant have already been determined using the proposed SIMPLA methods [51, 52]. The pelvis and femur segmentation was performed by a statistical-shape-model (SSM) based automated method [53]. In addition, the coordinate systems of pelvis, femur, and hip joint were assumed to be determined automatically by the bony landmarks of SSM [53].

Figure 6.1 shows the system overview of automated optimization of combined pre-operative planning for pelvic and femoral implants. Our method works in two phases: The first phase is the extraction stage of planning candidates with statistically determined restrictions, which reduces computational time, and the second phase is the optimization stage for determining the best-balanced solution which maximize the evaluation function of combined pre-operative planning. The author describe the evaluation items for optimization in section 2.1, the normalization method of evaluation criteria in section 2.2, and the optimization algorithm in section 2.3.

6.2.1 Evaluation items

As evaluation items, cup coverage ratio (implant compatibility), leg length discrepancy (LLD), and range-of-motion (ROM) (hip joint function) are used in both first phase and second phase. Additionally, the similarity measure for cup-SIMPLA is also used in first phase. Cup coverage ratio is defined as a ratio of bone-contact-area on pelvic side implant (cup) surface, which indicates implant compatibility and stability. Leg length discrepancy (LLD) is defined as the difference of length of right and left upper limbs which are aligned to the longitudinal axis. Range-of-motion (ROM) is defined as an angle of movable range of hip joint for a specific movement (the author treats the internal movement

at flexion 90 degrees). LLD and ROM indicate the hip joint function.

In order to import the tendency of the pre-operative plans prepared by experienced surgeons, the author performs statistical analysis of the evaluation items of them based on normal distribution, which determines the restrictions of each items. The evaluation items are classified into three types for defining proper restrictions:

- Criterion considered to be better in higher value on normal distribution (Cup coverage ratio and ROM).
- Criterion considered to be better in lower value on normal distribution.
- Criterion considered to be better in value on center of normal distribution (LLD).

The defined restrictions are used in the first phase (extraction stage of planning candidates).

6.2.2 Normalization of evaluation criteria

The author formulates a normalization procedure of each criterion in order to treat several evaluation criteria impartially in evaluation function of pre-operative planning. This normalization is based on the Gaussian distribution approximation of criteria which are obtained in the cases of the training datasets (prepared by surgeons). In the second phase of planning, the author uses the normalized scores of evaluation criteria in evaluation function.

6.2.3 Optimization algorithm

In this section, the author describes the automated optimization algorithm of combined pre-operative planning. The best-balanced solution is determined using the following steps.

1. Generate all candidates of combined pre-operative planning. All plans of pelvic side implants (cup) and plans of femoral side implant (stem) are combined and constructed as virtual artificial hip joint.
2. Extract candidates which fulfill the restrictions. In order to reduce the planning candidates, the ones which fulfill the statistically determined restrictions, that are described in section 2.1, are extracted (the first phase of optimization). If no candidate is extracted, the restrictions are relaxed and step 2 is redone.

3. Find a best-balanced solution of evaluation criteria To evaluate each of the planning candidate, the author defines the evaluation function in Eq.(1) with normalized scores of each criterion described in section 2.2.

$$TS_t = \sum_t NS_i \tag{6.1}$$

where TS_t denotes total score (t: numbers of criteria) and NS_i denotes normalized score of i-th evaluation criterion.

The optimization is performed by maximization of the score calculated by the evaluation function (the second phase of optimization). In THA pre-operative planning, NS1:cup coverage ratio, NS2:LLD, and NS3:ROM are used. The combined pre-operative planning which obtains a maximum score is the final solution.

6.2.4 Workflow of proposed methods

The two proposed methods are denoted as follows:

1. AOCP-w/R: Automated Optimization of Combined pre-operative Planning With Restrictions (which uses whole optimization steps (1 to 3), described in 2.3)

2. AOCP-w/oR: Automated Optimization of Combined pre-operative Planning WithOut Restrictions (which uses two optimization steps (1 and 3 (2 is skipped)), described in 2.3)

6.3 Results

The author used eight preoperative datasets of the dysplastic hip patients for experiments. Each dataset consisted of 3D CT data and planning candidates data of pelvic side and femoral side. The slice thickness and reconstruction pitch of CT data were 2.0 mm. The field of view was 360 mm $\times$ 360 mm and the matrix size was 512 $\times$ 512. To evaluate the methods, the author compared the scores and parameters of the criteria in both AOCP-w/R and AOCP-w/oR, and calculate the pelvic implant (cup) positional differences between the automated methods and surgeon's. The proposed methods were implemented on Windows Server 2008, Intel Xenon dual core processor 3.0 GHz and 16 GB main memory.

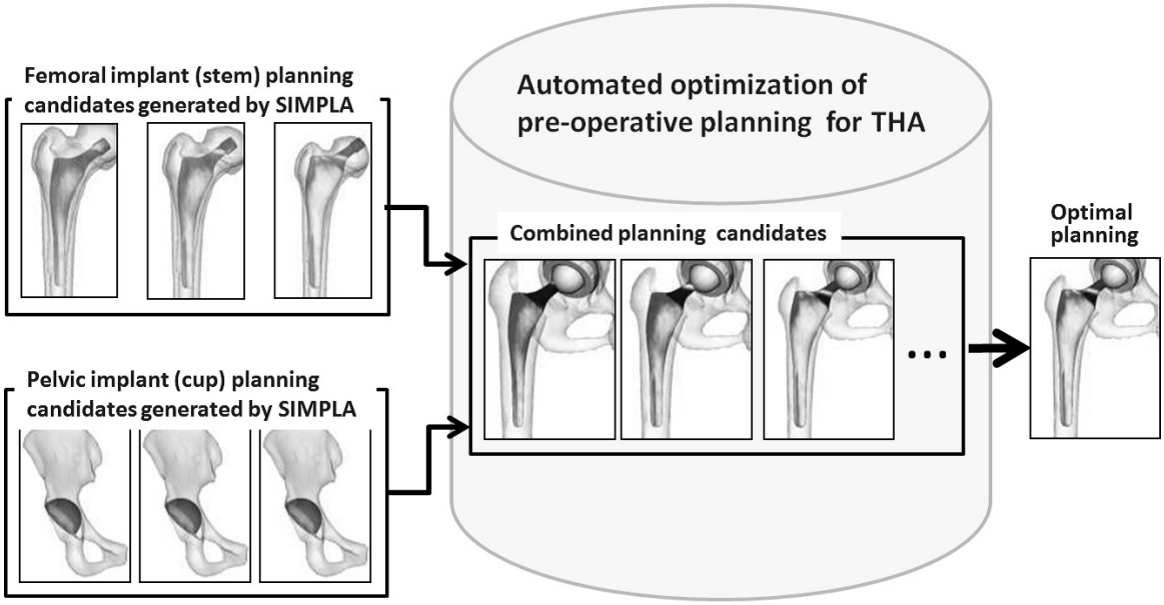

Figure 6.1: Overview of automated optimization of pre-operative planning.

The author obtained optimal results in all cases with both AOCP-w/R and AOCP-w/oR.The average scores and calculated parameters of cup coverage ratio, LLD, and ROM are shown in Fig. 6.2 and Fig. 6.3. For cup coverage ratio and ROM, the scores and parameters of AOCP-w/oR were better than those of AOCP-w/R. For ROM, AOCP-w/R was better than AOCP-w/oR. However, statistical significance was not observed in all the pairs between AOCP-w/R and AOCP-w/oR. Fig. 6.4 shows the average cup positional differences between surgeon's planning and AOCP-w/R or AOCP-w/oR. Significance was not observed between two proposed methods. Figure 6.5, 6.6, 6.7, and 6.8 shows the scores in each case.

The average computation time for one case was about 1.7 hours in AOCP-w/R, 22.5 hours in AOCP-w/oR. The computation time in AOCP-w/R was greatly reduced when compared to AOCP-w/oR.

6.4 Discussion

In most cases, the scores of cup coverage ratio and LLD were comparatively better than surgeon's in both AOCP-w/R and AOCP-w/oR, as shown in Fig. 6.6 and Fig. 6.7. Only in case No. 1, all criteria of

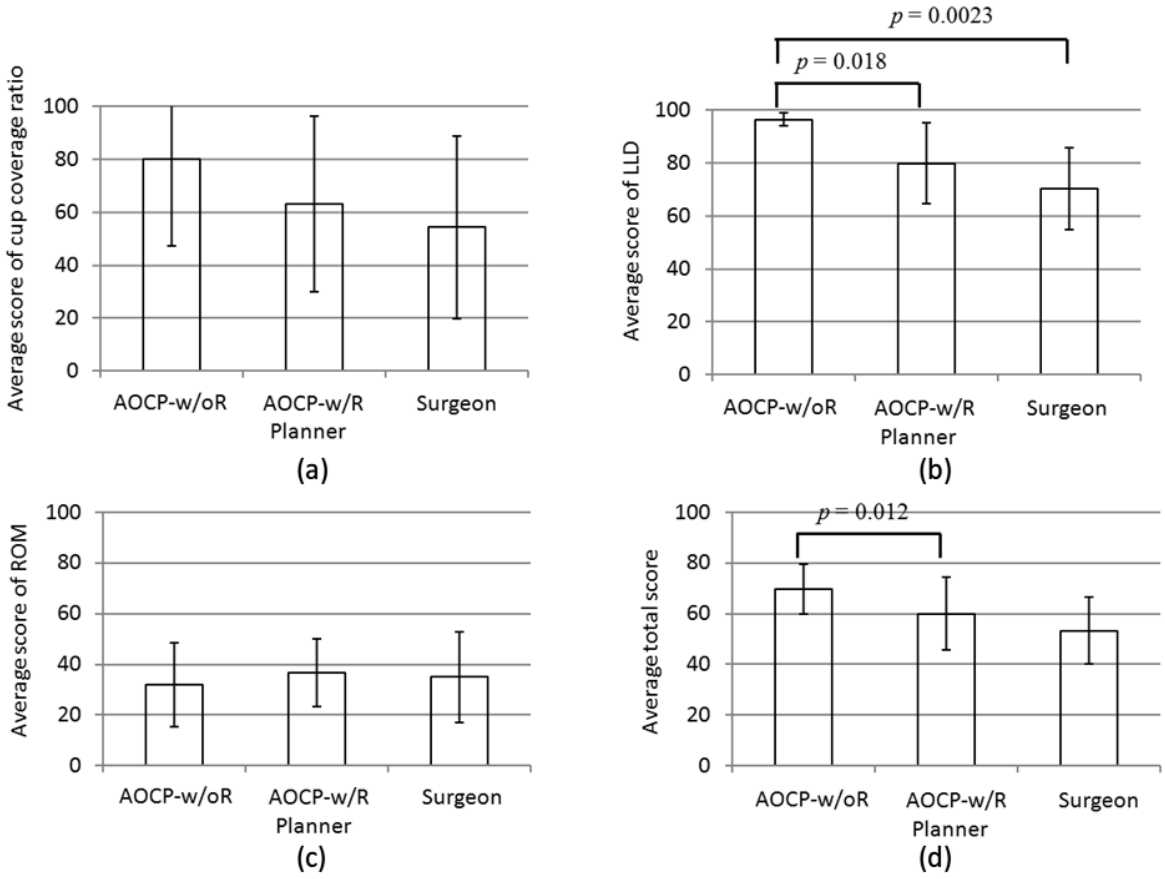

Figure 6.2: Comparison of average score of criteria between results of proposed methods and surgeon's. (a) Score of cup coverage ratio. (b) Score of leg length discrepancy. (c) Score of range of motion. (d) Total score.

the optimal solution of AOCP-w/R scored over 30 points. While the parameter of cup coverage ratio of it was considerably lower than that of AOCP-w/oR method, the parameter of ROM of it secures sufficient score (over 30 points). In case No. 7, the score of cup coverage ratio was almost zero in the results of both AOCP-w/R and AOCP-w/oR and the cup positional differences from surgeon's were over 10 mm. This case was thought to be a statistically irregular case which had severe deformation of host bone for optimizing positions of implants with the statistical approach.

The results of the experiments showed that AOCP-w/oR is better than AOCP-w/R in the aspect of the efficiency, as the optimal solution of AOCP-w/oR scored significantly better in cup coverage ratio and LLD, and similar in ROM to the one of AOCP-w/R. However AOCP-w/oR required the

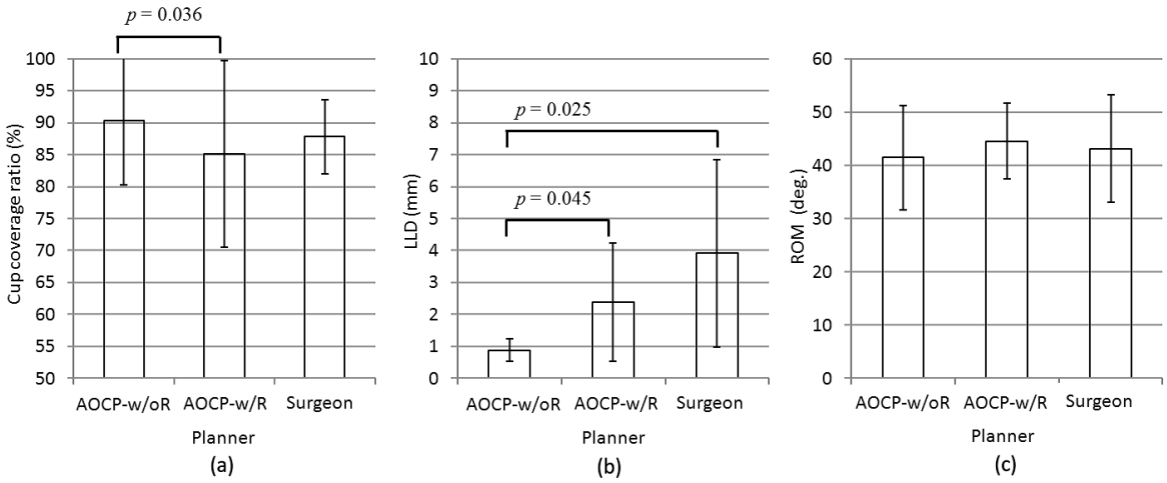

Figure 6.3: Comparison of average parameters of criteria between results of proposed methods and surgeon's. (a) Cup coverage ratio. (b) Leg length discrepancy. (c) Range of motion.

measurement of LLD and ROM, which cause long computation time, in over one thousand or hundred thousand planning candidates and the total computation time often became over 24 hours. In contrast, AOCP-w/R was able to obtain the optimal solution within several hours because of fewer planning candidates which were extracted with the restrictions. Therefore, the author considers AOCP-w/R is suitable for practical uses.

6.5 Conclusions

The author has described an automated optimization method for combining pelvic side planning and femoral side planning with evaluation function which adds up the normalized parameters of implant compatibility and hip joint function by the Gaussian distribution approximation of criteria. The method was evaluated by comparison with results of an automated planning with restrictions (AOCP-w/R) and an automated planning without restrictions (AOCP-w/oR), and an experienced surgeon planning results. Even as preliminary results showed promising data, the author will validate the methods with in many cases.

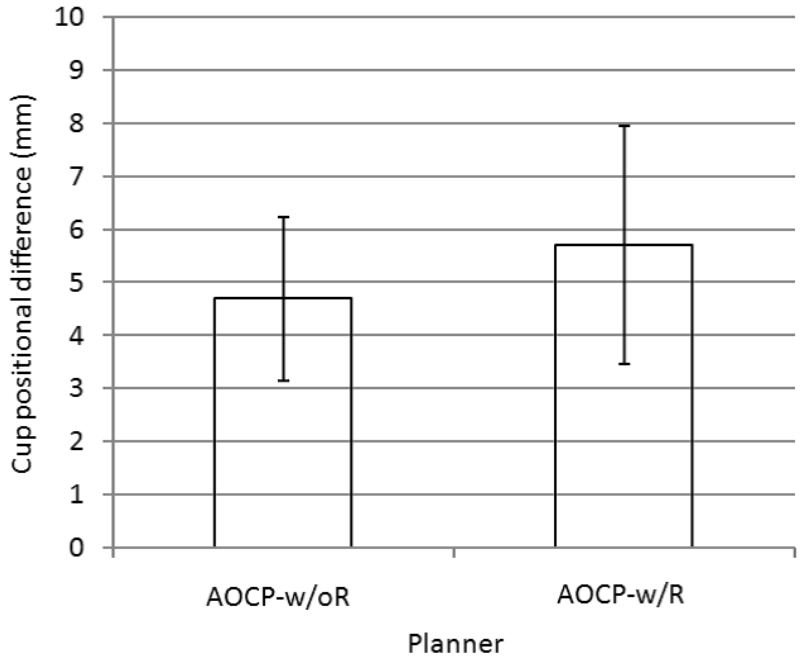

Figure 6.4: Comparison of average cup positional differences from surgeon's between proposed methods.

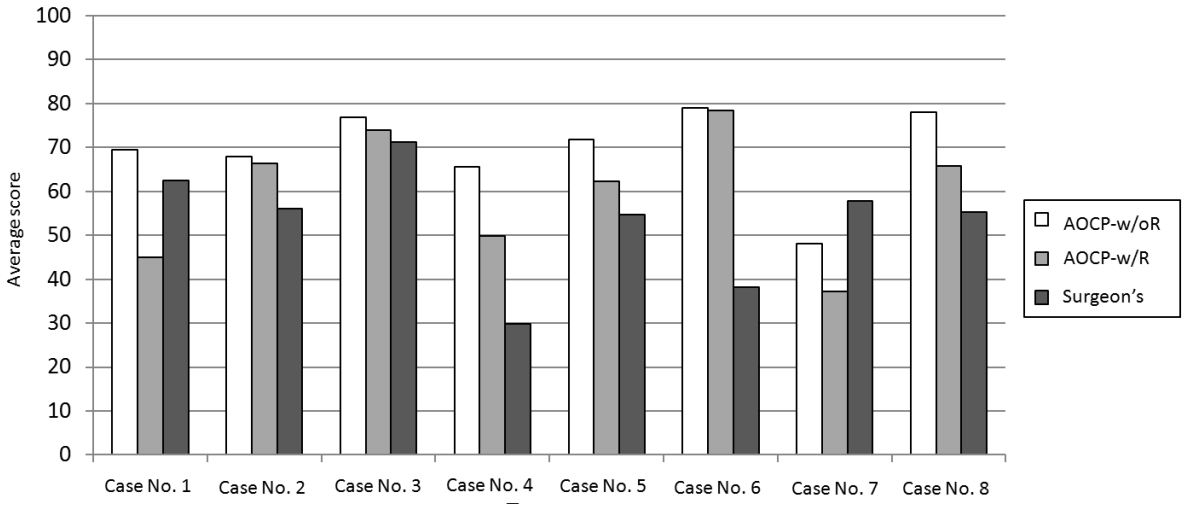

Figure 6.5: Comparison of average score in each case.

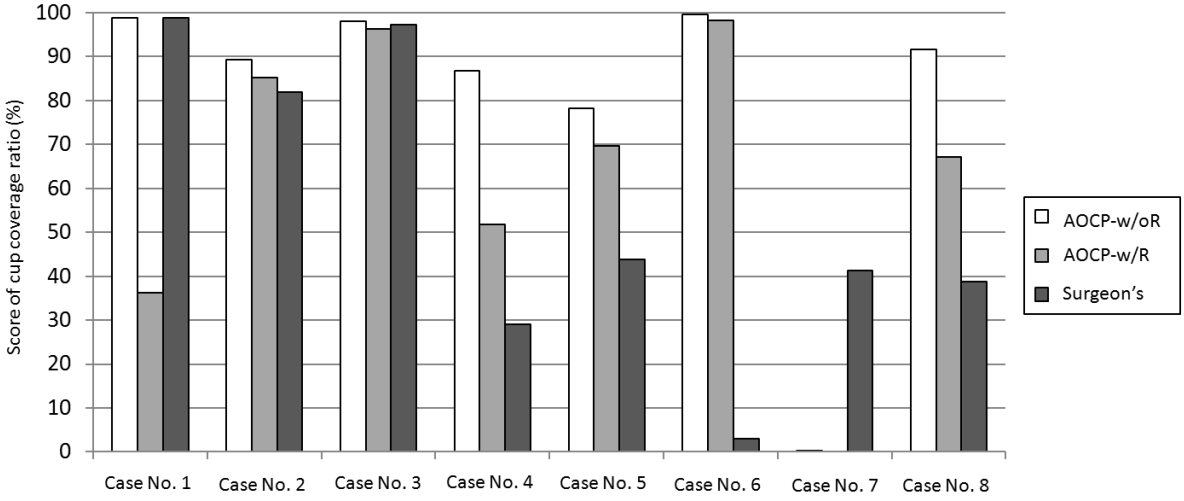

Figure 6.6: Comparison of score of cup coverage ratio in each case.

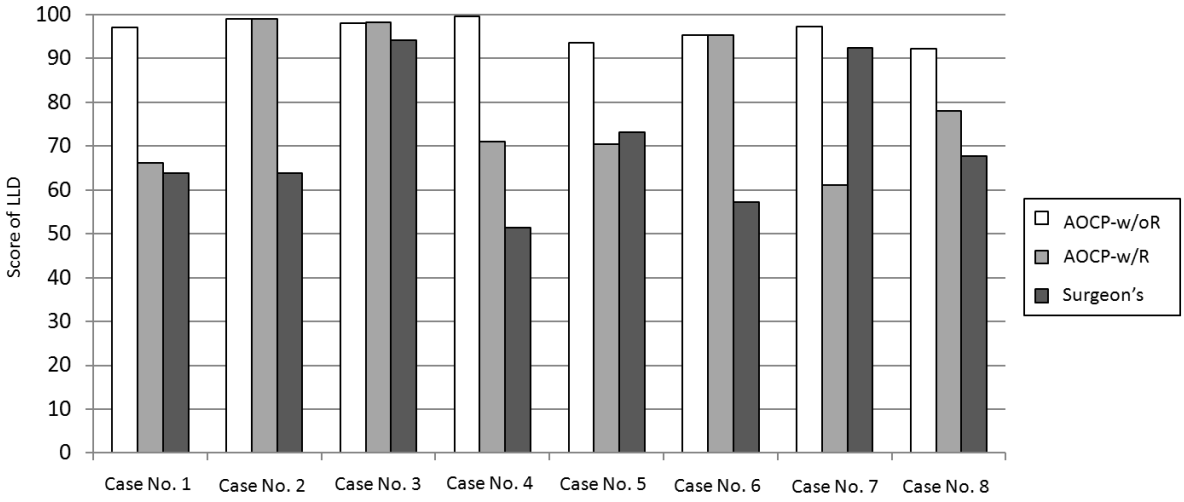

Figure 6.7: Comparison of score of leg length discrepancy in each case.

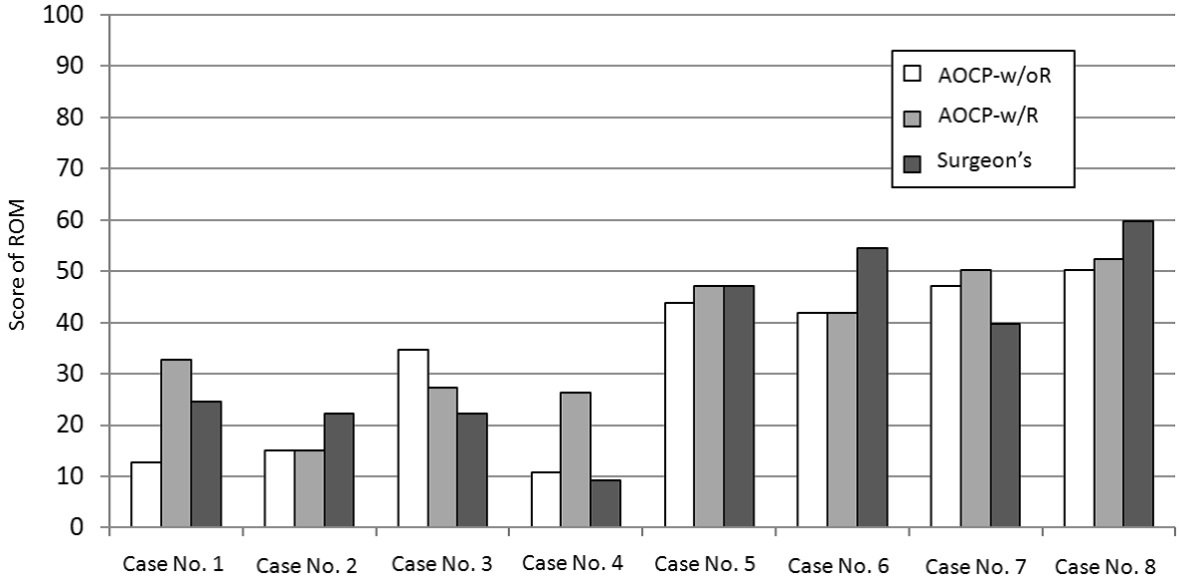

Figure 6.8: Comparison of score of range of motion in each case.

Chapter 7

Conclusion

This study proposes an atlas-based automated 3D surgical planning for total hip arthroplasty (THA). The statistical atlases are constructed from a number of past planning datasets prepared by an experienced surgeon. Since artificial implants of THA consist of femoral implant (stem) and pelvic implant (cup), the automated planning methods for stem and cup are developed independently. Each planning results are obtained by optimizing parameters of the statistical atlases so as to fit the statistical atlases to the patient's femoral surface and pelvis surface. In advance of a development of the atlas-based method, an automated stem planning method based on an user-defined objective function are developed in chapter 2. In this method, the objective function is defined based on interviews of an experienced surgeon. The atlas-based automated stem planning method is then developed in chapter 3. In chapter 4, the atlas-based automated cup planning method is developed. In chapter 5, the usability of the automated cup planning method developed in chapter 4 is expanded. The method in chapter 4 only allows 3D-CT images as input. On the other hand, an automated 3D cup planning using standard 2D X-ray image as input is performed in chapter 5. In chapter 6, an preliminary work for optimization of hip joint functions such as leg length discrepancy and range of motion is introduced.

The achievement of this study is to formulate an atlas-based automated planning as optimization problem. Previous methods proposed in [21] and chapter 2 are based on manually-defined algorithms. These methods consist of several constraints or objective functions and need to be tuned parameter with trial-and-error process. In addition to this problem, these method cannot represent implicit knowledge of surgeons. On the other hand, in the proposed study, explicit and implicit knowledge is modeled all together using the statistical atlases. For these reasons, the proposed study is considered to show one possible direction of quantification of surgeon's expertise in preoperative planning.

Another achievement point is the 2D X-ray image-based automated planning method as shown in chapter 5. Because acquisition of 3D-CT images for THA is not so common in other countries although which is popular in Japan, the usability of the proposed study is limited. In the study as shown in chapter 5, 2D X-ray-based automated cup planning is achieved by utilizing a 2D-3D pelvis reconstruction method [72]. This result is considered to show the possibility that the automated planning can used in not only hospitals in Japan which have 3D-CT but also hospitals in various countries.

One remaining problem of the proposed study is in performance evaluation. The current performance evaluation compares between automated planning results and experienced surgeon's preop-

erative plans and does not compare between automated planning results and actual surgical results. According to a previous study, surgical plans in preoperative stage may be different with surgical results in postoperative stage, even though experienced surgeon prepare the preoperative plans [14]. Therefore, to discuss usefulness of the proposed study, the automated planning results should be compared with the actual surgical results obtained from postoperative 3D-CT images. One problem in obtaining the implant parameters (size, position, and orientation) from postoperative CT images is metal artifact in the images caused by implants. Estimation of implant parameters from such a noisy images is need to be developed. Obtaining the implant parameters from postoperative CT images based on image registration technique between pre- and post-operative CT images have been proposed [76]. By using this method, the performance evaluation procedure of the proposed study may needs to be improved.

Future work will include extensions of the proposed methods to other implant designs and other surgery. In principle, if 3D surface models of a new implant design are available and a sufficient number of planning datasets are prepared using the new implant by an experienced surgeon, the proposed statistical atlases can be constructed and utilized for automated planning. This point need to be confirmed by performance evaluations. As shown in the preliminary work in chapter 6, the research group including the author has been developing an adjustment method by considering LLD and ROM and various evaluation values. This method needs to be evaluated by applying to many cases. Additionally, establishing a performance evaluation procedure using postoperative CT images is needed to discuss clinical usefulness of the proposed study.

Acknowledgment

The author would like to give special thanks to Professor Yukio Tada of Graduate School of System Informatics, Kobe University, for his kind advices, discussions and guidance.

The author would like to give special thanks to Professor Yasuo Ariki, and Professor Toshiya Kaihara for their efforts for reviewing this doctoral dissertation.

The author also would like to give special thanks to Associate Professor Yoshinobu Sato, Assistant Professor Masahiko Nakamoto, Postdoctoral Fellow Toshiyuki Okada of the Image Analysis Group, Division of Diagnostic and Interventional Radiology, Department of Radiology, Graduate School of Medicine, Osaka University for their precious advices and instructions about this study.

The author would like to thank to Associate Professor Kazuyuki Hanahara, Assistant Professor Takateru Urakubo of Graduate School of System Informatics, Kobe University for their guidance and instructions.

The author would like to thank to Professor Nobuhiko Sugano of the Department of Orthopaedic Medical Engineering, Graduate School of Medicine, Osaka University and Assistant Professor Masaki Takao of the Department of Organ Regulation Medicine, Graduate School of Medicine, Osaka University for their support, discussion from clinical aspects and providing clinical hip CT images.

The author would like to thank to Assistant Professor Yoshiyuki Kagiyama of the Interdisciplinary Graduate School of Medicine and Engineering, Yamanashi University for his precious advices, discussions and encouragements about this study.

The author would like to thank to Dr. Guoyan Zheng of the Institute for Surgical Technology & Biomechanics, University of Bern, Switzerland for collaborative research and his precious advice for utilization of 2D Xray image for this study.

The author would like to thank to Mr. Futoshi Yokota, Mr. Kazuto Kobayashi of Graduate School of Engineering, Kobe University and Ms. Mika Takaya and Ms. Yuki Nakanishi of Faculty of Engineering, Kobe University for their cooperative activity and encouragements about this study.

Tha author thanks to all the members of CS-22 Tada Laboratory of the Graduate School of System Informatics, Kobe University and the Image Analysis Group, Division of Diagnostic and Interventional Radiology, Department of Radiology, Graduate School of Medicine, Osaka University.

Finally, I would like to thank to my family, and all of my friends for ungrudging support for my academic life.

Bibliography

[1] R. H. Taylor and D. Stoianovici, “Medical Robotics in Computer-Integrated Surgery”, *IEEE Transactions on Robotics and Automation*, 19(5), 765–781, (2003)

[2] R. H. Taylor, B. Mittelstadt, H. Paul, W. Hanson, P. Kazanzides, J. Zuhars, B. Williamson, B. Musits, E. Glassman, and W. Bargar, “An Image-directed Robotic System For Precise Orthopaedic Surgery”, *IEEE Transactions on Robotics and Automation*, 10(3), 261–275, (1994)

[3] M. A. Hafez and A. M. DiGioia, “Computer-assisted total hip arthroplasty: the present and the future”, *Future Rheumatology*, 1(1), 121–131, (2006)

[4] A. M. DiGioia, B. Jaramaz, M. Blackwell, D. A. Simon, F. Morgan, J. E. Moody, C. Nikou, B. D. Colgan, C. A. Aston, R. S. Labarca, E. Kischell, and T. Kanade, “Image Guided Navigation System to Measure Intraoperatively Acetabular Implant Alignment”, *Clinical Orthopaedics and Related Research*, 355, 8–22, (1998)

[5] A. M. Digioia, B. Jaramaz, C. Nikou, R. S. Labarca, J. E. Moody, and B. D. Colgan, “Surgical navigation for total hip replacement with the use of hipnav”, *Operative Techniques in Orthopaedics*, 10(1), 3–8, (2000)

[6] W. L. Bargar, A. Bauer, and M. Borner, “Primary and Revision Total Hip Replacement using the Robodoc System”, *Clinical Orthopaedics & Related Research*, 354, 82–91, (1998)

[7] K. Cleary and C. Nguyen, “State of the art in surgical robotics: Clinical applications and technology challenges”, *Computer Aided Surgery*, 6(6), 312–328, (2001)

[8] N. Sugano, “Computer-assisted Orthopedic Surgery”, *Journal of Orthopaedic Science*, 8(3), 442–448, (2003)

[9] P. Gomes, “Surgical robotics: Reviewing the past, analysing the present, imagining the future”, *Robotics and Computer-Integrated Manufacturing*, 27(2), 261–266, (2011)

[10] M. Honl, O. Dierk, C. Gauck, V. Carrero, F. Lampe, S. Dries, M. Quante, K. Schwieger, E. Hille, and M. Morlock, “Comparison of robotic-assisted and manual implantation of a primary total hip replacement: A prospective study”, *Journal of Bone and Joint Surgery - Series A*, 85(8), 1470–1478, (2003)

[11] N. Sugano, T. Nishii, H. Miki, H. Yoshikawa, Y. Sato, and S. Tamura, “Mid-term results of cementless total hip replacement using a ceramic-on-ceramic bearing with and without computer navigation.”, *The Journal of bone and joint surgery. British volume*, 89(4), 455–460, (2007)

[12] C. Nikou, B. Jaramaz, A. M. DiGioia, M. Blackwell, M. E. Romesberg, and M. M. Green. “POP: Preoperative Planning and Simulation Software for Total Hip Replacement Surgery”. In *Medical Image Computing and Computer-Assisted Intervention -MICCAI ’99*, volume 1679 of *Lecture Notes in Computer Science*, 868–875. Springer-Verlag Berlin Heidelberg, (1999)

[13] R. Lattanzi, M. Viceconti, C. Zannoni, P. Quadrani, and A. Toni, “Hip-Op: An Innovative Software to Plan Total Hip Replacement Surgery”, *Medical Informatics and the Internet in Medicine*, 27(2), 71–83, (2002)

[14] M. Viceconti, R. Lattanzi, B. Antonietti, S. Paderni, R. Olmi, A. Sudanese, and A. Toni, “CT-based surgical planning software improves the accuracy of total hip replacement preoperative planning”, *Medical Engineering & Physics*, 25(5), 371–377, (2003)

[15] H. Laine, T. J. S. Puolakka, T. Moilanen, K. J. Pajamaki, J. Wirta, and M. U. K. Lehto, “The effects of cementless femoral stem shape and proximal surface texture on “fit-and-fill” characteristics and on bone remodeling”, *International Orthopaedics*, 24(4), 184–190, (2000)

[16] D. Testi, M. Simeoni, C. Zannoni, and M. Viceconti, “Validation of two algorithms to evaluate the interface between bone and orthopaedic implants”, *Computer Methods and Programs in Biomedicine*, 74(2), 143–150, (2004)

[17] B. Reggiani, L. Cristofolini, E. Varini, and M. Viceconti, “Predicting the subject-specific primary stability of cementless implantsduring pre-operative planning: Preliminary validation of subject-specific finite-element models”, *Journal of Biomechanics*, 40(11), 2552–2558, (2007)

[18] E. Schileo, F. Taddei, L. Cristofolini, and M. Viceconti, “Subject-specific finite element models implementing a maximum principal strain criterion are able to estimate failure risk and fracture location on human femurs tested in vitro”, *Journal of Biomechanics*, 41(2), 356–367, (2008)

[19] M. T. Bah, P. B. Nair, and M. Browne, “Mesh morphing for finite element analysis of implant positioning in cementless total hip replacements”, *Medical Engineering & Physics*, 31(10), 1235–1243, (2009)

[20] R. Lattanzi, E. Grazi, D. Testi, M. Viceconti, A. Cappello, and A. Toni, “Accuracy and repeatability of cementless total hip replacement surgery in patients with deformed anatomies”, *Medical Informatics & The Internet in Medicine*, 28(1), 59–71, (2003)

[21] Y. Kagiyama, N. Sugano, M. Takao, M. Nakamoto, Y. Sato, H. Yoshikawa, K. Akazawa, and Y. Tada, “Automated Preoperative Planning Procedure for Acetabular Cup Based on 3D Pelvic Bone Structure in Total Hip Replacement”, *Japan Society for Medical and Biological Engineering*, 46(4), 437–450, (2008)

[22] M. Viceconti, D. Testi, M. Simeoni, and C. Zannoni, “An Automated Method to Position Prosthetic Components within Multiple Anatomical Spaces”, *Computer Methods and Programs in Biomedicine*, 70(2), 121–127, (2003)

[23] R. H. Taylor, A. Menciassi, G. Fichtinger, and P. Dario, “Medical Robotics and Computer-Integrated Surgery”, *Splinger Handbook of Robotics*, 1199–1222, (2008)

[24] T. F. Cootes, C. J. Taylor, D. H. Cooper, and J. Graha, “Active Shape Models - Their Training and Application”, *Computer Vision and Image Understanding*, 61(1), 38–59, (1995)

[25] T. Heimann and H.-P. Meinzer, “Statistical shape models for 3D medical image segmentation: A review”, *Medical Image Analysis*, 13(4), 543–563, (2009)

[26] D. Rueckert, A. F. Frangi, and J. A. Schnabel, “Automatic Construction of 3-D Statistical Deformation Models of the Brain Using Nonrigid Registration”, *IEEE Transactions on Medical Imaging*, 22(8), 1014–1025, (2003)

[27] P. M. Thompson and A. W. Toga, “Detection, visualization and animation of abnormal anatomic structure with a deformable probabilistic brain atlas based on random vector field transformations”, *Medical Image Analysis*, 1(4), 271–294, (1997)

[28] H. Park, P. H. Bland, and C. R. Meyer, “Construction of an Abdominal Probabilistic Atlas and its Application in Segmentation”, *IEEE Transactions on Medical Imaging*, 22(4), 483 – 492, (2003)

[29] M. Fleute and S. Lavallée. “Nonrigid 3-D/2-D Registration of Images Using Statistical Models”. In *Proc. Medical Image Computing and Computer-Assisted Intervention*, volume 1679 of *Lecture Notes in Computer Science*, 138–147. Springer-Verlag Berlin Heidelberg, (1999)

[30] G. Zheng, X. Dong, K. T. Rajamani, X. Zhang, M. Styner, R. U. Thoranaghatte, L.-P. Nolte, and M. A. G. Ballester, “Accurate and Robust Reconstruction of a Surface Model of the Proximal Femur From Sparse-Point Data and a Dense-Point Distribution Model for Surgical Navigation”, *IEEE Transactions on Biomedical Engineering*, 54(12), 2109–2122, (2007)

[31] D. Shen, Z. Lao, J. Zeng, W. Zhang, I. A. Sesterhenn, L. Sun, J. W. Moul, E. H. Herskovits, G. Fichtinger, and C. Davatzikos, “Optimized prostate biopsy via a statistical atlas of cancer spatial distribution”, *Medical Image Analysis*, 8(2), 139–150, (2004)

[32] Y. Zhan, D. Shen, J. Zeng, L. Sun, G. Fichtinger, J. Moul, and C. Davatzikos, “Targeted Prostate Biopsy Using Statistical Image Analysis”, *IEEE Transactions on Medical Imaging*, 26(6), 779–788, (2007)

[33] N. Kozic, S. Weber, P. Büchler, C. Lutz, N. Reimers, M. A. G. Ballester, and M. Reyes, “Optimisation of orthopaedic implant design using statistical shape space analysis based on level sets”, *Medical Image Analysis*, 14(3), 265–275, (2010)

[34] M. Kazhdan, P. Simari, T. McNutt, B. Wu, R. Jacques, M. Chuang, and R. Taylor. “A Shape Relationship Descriptor for Radiation Therapy Planning”. In G.-Z. Yang, D. Hawkes, D. Rueckert,

A. Noble, and C. Taylor, editors, *Medical Image Computing and Computer-Assisted Intervention -MICCAI 2009*, volume 5762 of *Lecture Notes in Computer Science*, 100–108. Springer-Verlag Berlin Heidelberg, (2009)

[35] K. Haraguchi, N. Sugano, T. Nishi, T. Koyama, S. Nishihara, H. Yoshikawa, and T. Ochi, "Comparison of fit and fill between anatomic stem and straight tapered stem using virtual implantation on the ORTHODOC workstation", *Computer aided surgery*, 6(5), 290–296, (2001)

[36] S. Nishihara, N. Sugano, T. Nishii, H. Miki, N. Nakamura, and H. Yoshikawa, "Comparison Between Hand Rasping and Robotic Milling for Stem Implantation in Cementless Total Hip Arthroplasty", *The Journal of Arthroplasty*, 21(7), 957–966, (2006)

[37] T. M. Ecker, M. Tannast, and S. B. Murphy, "Computed tomography-based surgical navigation for hip arthroplasty", *Clinical Orthopaedics and Related Research*, 465, 100 –105, (2007)

[38] M. Nakamoto, Y. Sato, N. Sugano, T. Sasama, T. Nishii, P. S. Pak, K. Akazawa, Y. Tada, H. Yoshikawa, and S. Tamura, "Automated CT-based 3D surgical planning for total hip replacement: a pilot study", *International Congress Series*, 1256, 389–394, (2003)

[39] Y. Kagiyama, M. Nakamoto, M. Takao, Y. Sato, N. Sugano, and Y. Tada. "Automated preoperative 3D planning for multi-component implants based on leg length evaluation in total hip arthroplasty using CT data: pilot study". In *Proc. CAOS-International*, 204–206, (2005)

[40] I. Otomaru, M. Takao, M. Nakamoto, N. Sugano, Y. Kagiyama, and Y. Sato. "Automated Preoperative Planning System of Total Hip Arthroplasty Using Anatomical Femoral Components". In *Proc. of 6th Annual Meeting of CAOS-International*, 419–423, (2006)

[41] Y. Kagiyama, M. Takao, M. Nakamoto, Y. Sato, N. Sugano, H. Yoshikawa, K. Akazawa, S. Tamura, and Y. Tada, "Automated planning of multi-component implants for THA using multiple criteria including limb length and range of motion", *International Journal of Computer Assisted Radiology and Surgery*, 1, 232–234, (2006)

[42] W. L. Bargar, "Shape the Implant to the Patient. A Rationale for the Use of Custom-Fit Cementless Total Hip Implants", *Clinical orthopaedics and related research*, 249, 73–78, (1989)

[43] A. Bo, S. Imura, H. Omori, Y. Okumura, M. Ando, H. Baba, P. White, and A. Zarnowski, "Fit and fill analysis of a newly designed femoral stem in cementless total hip arthroplasty for patients with secondary osteoarthritis", *Journal of Orthopaedic Science*, 2(5), 301–312, (1997)

[44] S. Nishihara, N. Sugano, T. Nishii, H. Tanaka, H. Yoshikawa, and T. Ochi, "Comparison of the fit and fill between the Anatomic Hip femoral component and the VerSys Taper femoral component using virtual implantation on the ORTHODOC workstation", *Journal of Orthopaedic Science*, 8(3), 352–360, (2003)

[45] J. L. Howard, A. J. Hui, R. B. Bourne, R. W. McCalden, S. J. MacDonald, and C. H. Rorabeck, "A quantitative analysis of bone support comparing cementless tapered and distal fixation total hip replacements", *The Journal of Arthroplasty*, 19(3), 266–273, (2004)

[46] H.-J. Laine, J. K. Pajamaki, T. Moilanen, and M. U. Lehto, "The femoral canal fill of two different cementless stem designs The accuracy of radiographs compared to computed tomographic scanning", *International Orthopaedics*, 25(4), 209–213, (2001)

[47] N. Sugano, P. C. Noble, and E. Kamaric, "Predicting the Position of the Femoral Head Center", *The Journal of Arthroplasty*, 14(1), 102–107, (1999)

[48] N. Sugano, P. C. Noble, and E. Kamaric, "A comparison of alternative methods of measuring femoral anteversion", *Journal of Computer Assisted Tomography*, 22(4), 610–614, (1998)

[49] T. Okada, R. Shimada, Y. Sato, M. Hori, K. Yokota, M. Nakamoto, Y.-W. Chen, H. Nakamura, and S. Tamura. "Automated Segmentation of the Liver from 3D CT Images Using Probabilistic Atlas and Multi-level Statistical Shape Model". In *Medical Image Computing and Computer-Assisted Intervention - MICCAI 2007*, volume 4791 of *Lecture Notes in Computer Science*, 86 – 93. Springer-Verlag Berlin Heidelberg, (2007)

[50] M. Nakamoto, I. Otomaru, M. Takao, N. Sugano, Y. Kagiyama, H. Yoshikawa, Y. Tada, and Y. Sato. "Construction of a Statistical Surgical Plan Atlas for Automated 3D Planning of Femoral Component in Total Hip Arthroplasty". In D. Metaxas, L. Axel, G. Fichtinger, and G. Székely, editors, *Medical Image Computing and Computer-Assisted Intervention -MICCAI 2008*, volume 5242 of *Lecture Notes in Computer Science*, 718 – 725. Springer-Verlag Berlin Heidelberg, (2008)

[51] I. Otomaru, K. Kobayashi, T. Okada, M. Nakamoto, Y. Kagiyama, M. Takao, N. Sugano, Y. Tada, and Y. Sato. “Expertise Modeling for Automated Planning of Acetabular Cup in Total Hip Arthroplasty Using Combined Bone and Implant Statistical Atlases”. In *Medical Image Computing and Computer-Assisted Intervention -MICCAI 2009*, volume 5762 of *Lecture Notes in Computer Science*, 532–539. Springer-Verlag Berlin Heidelberg, (2009)

[52] I. Otomaru, M. Nakamoto, M. Takao, N. Sugano, Y. Kagiyama, H. Yoshikawa, Y. Tada, and Y. Sato, “Automated Preoperative Planning of Femoral Component for Total Hip Arthroplasty (THA) from 3D CT Images”, *Journal of Biomechanical Science and Engineering*, 3(4), 478 – 489, (2008)

[53] F. Yokota, T. Okada, M. Takao, N. Sugano, Y. Tada, and Y. Sato. “Automated Segmentation of the Femur and Pelvis from 3D CT Data of Diseased Hip Using Hierarchical Statistical Shape Model of Joint Structure”. In *Proc. Medical Image Computing and Computer-Assisted Intervention*, volume 5762, 811–818. Springer-Verlag Berlin Heidelberg, (2009)

[54] F. Yokota. “Automated segmentation of the femur and pelvis from 3D CT image of diseased hip joint using hip joint statistical shape and motion model”. Master’s thesis, Graduate School of Engineering, Kobe University, (2009)

[55] H. Chui and A. Rangarajan, “A New Point Matching Algorithm for Non-rigid Registration”, *Computer Vision and Image Understanding*, 89(2 - 3), 114–141, (2003)

[56] R. P. Brent. *Algorithms for Minimization without Derivatives*. Prentice-Hall, Inc., Englewood Cliffs, New Jersey, USA, (1973)

[57] H. J. A. Crooijmans, A. M. R. P. Laumen, C. v. Pul, and J. B. A. v. Mourik, “A new digital preoperative planning method for total hip arthroplasties.”, *Clinical orthopaedics and related research*, 467(4), 909–916, (2009)

[58] J. Kwon, H. Naito, I. Otomaru, M. Takao, Y. Sato, T. Matsumoto, and M. Tanaka. “Biomechanical index for evaluation of stem size and position planning in THR surgery”. In *Proceedings of KSME-JSME Joint Symposium 2010 on Computational Mechanics and Computer-Aided Engineering*, 68–69, (2010)

[59] C. J. Twining, T. Cootes, S. Marsland, V. Petrovic, R. Schestowitz, and C. J. Taylor. “A unified information-theoretic approach to groupwise non-rigid registration and model building.”. In *Proc. Information processing in medical imaging*, volume 19, 1–14, (2005)

[60] B. T. T. Yeo, M. R. Sabuncu, T. Vercauteren, N. Ayache, B. Fischl, and P. Golland, “Spherical demons: fast diffeomorphic landmark-free surface registration.”, *IEEE Transactions on Medical Imaging*, 29(3), 650–668, (2010)

[61] S. Joshi, B. Davis, M. Jomier, and G. Gerig, “Unbiased diffeomorphic atlas construction for computational anatomy.”, *NeuroImage*, 23 Suppl 1, S151–S160, (2004)

[62] P. Aljabar, R. A. Heckemann, A. Hammers, J. V. Hajnal, and D. Rueckert, “Multi-atlas based segmentation of brain images: atlas selection and its effect on accuracy.”, *NeuroImage*, 46(3), 726–38, (2009)

[63] R. A. Heckemann, J. V. Hajnal, P. Aljabar, D. Rueckert, and A. Hammers, “Automatic anatomical brain MRI segmentation combining label propagation and decision fusion”, *NeuroImage*, 33(1), 115–26, (2006)

[64] R. Wolz, P. Aljabar, J. V. Hajnal, A. Hammers, and D. Rueckert, “LEAP: learning embeddings for atlas propagation.”, *NeuroImage*, 49(2), 1316–1325, (2010)

[65] D. J. Blezek and J. V. Miller, “Atlas stratification”, *Medical image analysis*, 11(5), 443–57, (2007)

[66] I. Otomaru, M. Nakamoto, M. Takao, N. Sugano, Y. Kagiyama, H. Yoshikawa, Y. Tada, and Y. Sato, “Evaluation of automated 3D planning of femoral component in total hip arthroplasty based on statistical surgical plan atlas”, *Journal of Computer Aided Surgery*, 10, 369–370, (2008)

[67] T. F. Cootes, A. Hill, C. J. Taylor, and J. Haslam. “The Use of Active Shape Models for Locating Structures in Medical Images”. In *Lecture Nots in Computer Science*, volume 687, 33–47, (1993)

[68] Y. Kagiyama, M. Nakamoto, M. Takao, Y. Sato, N. Sugano, H. Yoshikawa, and S. Tamura. “Automated Preoperative 3D Planning of Acetabular Cup Positioning and Size Selection in Total Hip Arthroplasty using CT Data”. In *Proc. CAOS-International*, 312 – 313, (2004)

[69] I. Otomaru, K. Kobayashi, T. Okada, M. Nakamoto, M. Takao, N. Sugano, Y. Tada, and Y. Sato. “CT-based Automated Preoperative Planning of Acetabular Cup Size and Position using Pelvis-cup Integrated Statistical Shape Model”. In *CAOS 2009*, 185 – 188, (2009)

[70] T. Okada, R. Shimada, M. Hori, M. Nakamoto, Y.-W. Chen, H. Nakamura, and Y. Sato, “Automated Segmentation of the Liver from 3D CT Images Using Probabilistic Atlas and Multilevel Statistical Shape Model”, *Academic Radiology*, 15(11), 1390–1403, (2008)

[71] D. Bongini, M. Carfagni, and L. Governi, “Hippin: a semiautomatic computer program for selecting hip prosthesis femoral components”, *Computer Methods and Programs in Biomedicine*, 63(2), 105–115, (2000)

[72] G. Zheng. “Statistically deformable 2D/3D registration for accurate determinationof post-operative cup orientation from single standard X-ray radiograph”. In *Medical Image Computing and Computer-Assisted Intervention - MICCAI 2009*, volume 5761 of *Lecture Notes in Computer Science*, 820–827. Springer-Verlag Berlin Heidelberg, (2009)

[73] J. F. Crowe, J. Mani, and C. S. Ranawat, “Total hip replacement in congenital dislocation and dysplasia of the hip”, *The Journal of Bone and Joint Surgery American Volume*, 61, 15–23, (1979)

[74] H. Handels, J. Ehrhardt, W. Plotz, and S. J. Poppl, “Three-dimensional planning and simulation of hip operations and computer-assisted construction of endoprostheses in bone tumor surgery”, *Computer aided surgery : official journal of the International Society for Computer Aided Surgery*, 6(2), 65–76, (2001)

[75] P. Noble, N. Sugano, J. Johnston, M. Thompson, M. Conditt, C. Engh, and K. Mathis, “Computer simulation: how can it help the surgeon optimize implant position?”, *Clinical orthopaedics and related research*, 417, 242–252, (2003)

[76] Y. Watanabe. “Development of quantification system for position of artificial hip joint based on image registration of pre- and post-operative CT images”. Master’s thesis, Graduate School of Information Science and Technology, Osaka University, (2004)

[77] Y. Kagiyama, I. Otomaru, F. Yokota, T. Okada, M. Nakamoto, M. Takao, N. Sugano, Y. Tada, N. Tomiyama, and Y. Sato. “Optimization of implant compatibility and hip joint function based on statistical atlas for automated 3D surgical planning of total hip arthroplasty”. In *9th World Congress on Structural and Multidisciplinary Optimization*, (2011)